Dissertation

Influences of G-protein activated inwardly rectifying potassium channel subunit 1 on vital parameters of breast cancer cells

submitted by

Simin REZANIA

for the Academic Degree of

Doctor of Medical Science

(Dr. scient. med.)

at the

Medical University of Graz

Institute of Biophysics

under the supervision of

Prof.Wolfgang SCHREIBMAYER

2016

Eidesstattliche Erklärung
Ich erkläre ehrenwörtlich, dass ich die vorliegende Arbeit selbstständig angefertigt und abgefasst, und jene Personen und Institutionen, die am Zustandekommen der Forschungsdaten beteiligt waren, namentlich genannt habe. Andere als die angegebenen Quellen habe ich nicht verwendet und die den benutzten Quellen wörtlich oder inhaltlich entnommenen Stellen habe ich als solche kenntlich gemacht. Die Arbeit an der Dissertation und daraus entstandener Publikationen wurde gemäß den Regeln der „Good Scientific Practice“ durchgeführt.

Graz, am 27.09.2016 *Simin Rezania*

Declaration
I hereby declare that this thesis is my own original work and that I have fully acknowledged by name all of those individuals and organizations that have contributed to the research for this thesis. Due acknowledgement has been made in the text to all other material used. Throughout this thesis and in all related publications I followed the guidelines of “Good Scientific Practice”.

Date: 27.09.2016 *SiminRezania*

Acknowledgments:

First and foremost, I would like to thank my thesis supervisor professor Wolfgang Schreibmayer for allowing me to become a part of his lab. I would additionally like to thank him for the excellent guidance, knowledge and support that he provide during my time as a PhD student.

My sincere thanks also go to my committee members, professor Thomas Bauernhofer and professor Amir Hassan Zarnani for their insightful comments, support and encouragement through my research studies.

I greatly appreciate the members of the “Ion Channels and Cancer Biology research unit”, including Astrid Gorischek, Dr. Sarah Kammerer, Dr. Bibiane Steinecker-Frohnwieser and Dr. Trevor Devaney for their valuable contribution, helpful ideas and making my time productive and enjoyable.

There are several collaborators who made invaluable contributions to this thesis, including Dr.Nassim Ghaffari Tabrizi-Wizsy and Christina Passegger for the CAM assay method, Dr. Stephan Jahn for all the pathology related discussions and professor Ernst Malle his for his assistance with western blot.

Special thanks go to my talented friend, Dr. Chintan Koyani for all his support, suggestions and being always available!

This last word of acknowledgment I have saved for my husband, Kamyar, who has been with me all these years, without him this thesis would never have been written.

Table of Contents:

1. List of Abbreviations:

a. dest.	aqua destillata
ATCC	American Type Culture Collection
BSA	bovine serum albumin
CAM	chorioallantoic membrane
C-T	carboxy terminus
DAB	diaminobenzidine
DMEM	Dulbecco's Modified Eagle Medium high glucose
DNA	deoxyribonucleic acid
eCFP	enhanced cyan fluorescence protein
ECL	enhanced chemiluminescence
ER	endoplasmic reticulum
ESR1	estrogen receptor 1 (gene)
eYFP	enhanced yellow fluorescence protein
FBS	fetal bovine serum
GIRK1	G-protein activated inwardly rectifying K^+ channel, subunit 1
GIRK1a	Splice variants *a* of the G-protein activated inwardly rectifying K^+ channel, subunit 1
GIRK1b	Splice variants *b* of the G-protein activated inwardly rectifying K^+ channel, subunit 1
GIRK1c	Splice variants *c* of the G-protein activated inwardly rectifying K^+ channel, subunit 1
GIRK1d	Splice variants *d* of the G-protein activated inwardly rectifying K^+ channel, subunit 1
GIRK4	G-protein activated inwardly rectifying K^+ channel, subunit 4
GPCR	G-protein coupled receptor
GpI	glycosylphosphatidylinositol
Gβ1	G-protein β1 subunit
Gγ2	G-protein γ2 subunit
HEK	human embryonic kidney
IHC	immunohistochemistry

KCNJ3	Gene encoding G-protein activated inwardly rectifying K^+ channel, subunit 1
KCNJ9	Gene encoding G-protein activated inwardly rectifying K^+ channel, subunit 4
MC	cellular motility coefficient
MCF-7	Michigan Cancer Foundation cell line 7
MCS	multiple cloning site
MEC	mammary epithelial cell
MEM	minimum essential medium
MVS	macroscopic vascularization score
N-T	amino terminus
PBS	phosphate-buffered saline
Pen/Strep	penicillin and streptomycin
qPCR	quantitative polymerase chain reaction
RIPA	radio immunoprecipitation assay
RNA	ribonucleic acid
SDS	sodium dodecyl sulfate
SDS-PAGE	sodium dodecyl sulfate-polyacrylamide gel electrophoresis
Srß	signal recognition particle receptor ß-subunit
wt	wildtype

2. List of Figures:

2. List of Tables:

4. Zusammenfassung:

Überexpression von mRNA und/oder Protein von G protein- activated Inwardly rectifying potassium (K+) channel subunit 1 (Girk1 /Kir3.1) im primären Brusttumor korreliert positiv mit Lymphknotenmetastasierung und negativ mit Prognose.

Um die funktionelle Rolle der GIRK1 Überexpression auszutesten wurden, basierend auf der MCF-7 Zelllinie, Zelllinien produziert, welche stabil die KCNJ3 Gen Splicevarianten GIRK1a, GIRK1c und GIRK1d überexprimieren. Expressionslevels wurden mittels Real Time PCR und Immunocytochemie vermessen. Ausgesuchte Neoplasie assoziierte vitale Parameter wie Invasion, Adhäsion, Wundheilung, Proliferation, Motilität, zelluläre Geschwindigkeit und Angiogenesie der Zelllinien wurden analysiert und verglichen.

Überexpression von GIRK1a und GIRK1c verstärkte signifikant Invasion, Motilitätskoeffizienten, Geschwindigkeit und Wundheilung, während Überexpression von GIRK1d das Gegenteil bewirkte. Darüberhinaus behinderte Überexpression von GIRK1d die Angiogenese und verlängerte die G_0/G_1 Phase des Zellzyklus. Überexpression sämtlicher GIRK1 Varianten hatte keinen Einfluss auf die Proliferation und die Adhäsion an Fibronectin beschichtete Oberflächen.

Wir folgern daraus, daß die Überexpression von GIRK1a und GIRK1c die Aktivität von endogenen GIRK Komplexen verstärkt, während die Überexpression von GIRK1d funktionelle GIRK Komplexe zerstört. Durch den Vergleich der Primärstruktur der GIRK1 Varianten wird offenkundig, daß Aminosäuren 235-307 wichtig für die canzerogene Aktivität sind. Unsere Ergebnisse zeigen, daß die Expression von GIRK1 Varianten als neuer prognostischer Biomarker und GIRK1 Proteine als mögliche pharmazeutische Angriffsziele zur Behandlung von Brustkrebs dienen könnten.

5. Abstract:

Previous studies have shown that overexpression of mRNA or protein of G protein- activated Inwardly rectifying potassium (K^+) channel subunit 1 (Girk1 /Kir3.1) are associated with increased lymph node metastasis and poor prognosis in breast cancer.

In order to test whether GIRK1 overexpression has impact on tumorigenicity, breast cancer cell line derived from MCF-7 stably overexpressing different KCNJ3 splice variants (GIRK1a, GIRK1c and GIRK1d) were produced. Expression levels were quantified by real time PCR and immunocytochemistry. Selected cardinal neoplasia associated vital parameters such as invasion, adhesion, wound healing, proliferation, motility, velocity and angiogenesis were evaluated.

Our finding revealed that, overexpression of GIRK1a and GIRK1c significantly increased the invasion, motility coefficient, velocity and wound healing of the cells while overexpression of GIRK1d resulted quite the contrary. In addition, GIRK1d also affected the angiogenesis and increased the G0/G1 phase of cell cycle. Overexpression played no influence on proliferation (S phase) and adhesion to fibronectin-coated surface.

To conclude, these results have shown that overexpression of GIRK1a and GIRK1c increased the activity of endogenous GIRK complexes, while GIRK1d acts as a dominant negative parts of functional GIRK channel. According to structure of GIRK channel, exon 2 which consist of amino acids 235-307 is important for the cancerogenic action since this fragment is exist in GIRK1a and GIRK1c but missing in GIRK1d splice variant. These results suggest that expression of GIRK1 and shorter splice variants might be a new prognostic biomarkers as well as putative pharmaceutical target for breast cancer but more studies on the mechanism and signaling of GIRK1 channels are required.

6. Introduction:

Potassium (K^+) channels are the largest family of ion channels in the human genome. This family is comprised of nearly 80 different gene products. The family of K^+ channels comprises three subfamilies, with the subdivisions made on the basis of the channel structure. These subfamilies are: the voltage- and Ca^{2+}-dependent K^+ channels (K_v and K_{Ca}), the inward rectifying K^+ channels (K_{ir}) and the two pore K^+ channel (K_{2P}) (1).

K^+ channels known as G protein activated inwardly rectifying K^+ channels (GIRK) are members of a large family (Kir1-Kir7) of inwardly rectifying K^+ channels. These can be functionally dividing into 4 different groups: The first group (group 1) includes the K^+ transporter channels Kir1.1 (KCNJ1), Kir7.1 (KCNJ13), Kir4.2 (KCNJ15) and Kir5.1 (KCNJ 16). The second group (group 2) includes the classical Kir channel, Kir2.1 (KCNJ2), Kir2.4 (KCNJ14), Kir 2.2 (KCNj12) and Kir2.3 (KCNJ4), members of which are always active. The third group (group 3) includes G protein gated K^+ channels. Kir3 is the only member of this group, and these channels are regulated by G proteins. The sub families are: Kir 3.1 (KCNJ3), Kir3.3 (KCNJ9), Kir3.4 (KCNJ5) and Kir3.2 (KCNJ6). The last group (group 4) is the ATP-sensitive K^+ channel, represented by Kir6. These channels are strongly involved in cell metabolism and include Kir6.1 (KCNJ8) and Kir6.2 (KCNJ11) (2) (See the Kir channel phylogenetic tree in Inwardly rectifying potassium channels: their structure, function, and physiological roles by Hibino H et al. Physiological reviews. 2010;90(1):291-366).

The Kir3 family (group 3) consists of the Kir3.1, Kir3.2, Kir3.3, and Kir3.4 subunits (GIRK1-4)(3). The first functional Kir subunit identified was Kir3.1/GIRK1/KCNJ3 (4). Five different isoforms (splice variants) of Kir 3.1 have been identified. These are referred to as GIRK1a, GIRK1b, GIRK1c, GIRK1d and GIRK1e. It is not yet known whether all isoforms exist in humans (5). KCNJ3 (Kir3.1) is located on chromosome 2 (2q24.1)(6). The protein encoded by this gene consists of two transmembrane domains (TM1 and TM2) and a pore-forming loop (H5), in addition to cytoplasmic amino- and carboxy-terminal domains (Figure. 6.2). The H5 pore is responsible for the ionic selectivity (GYG) (7).

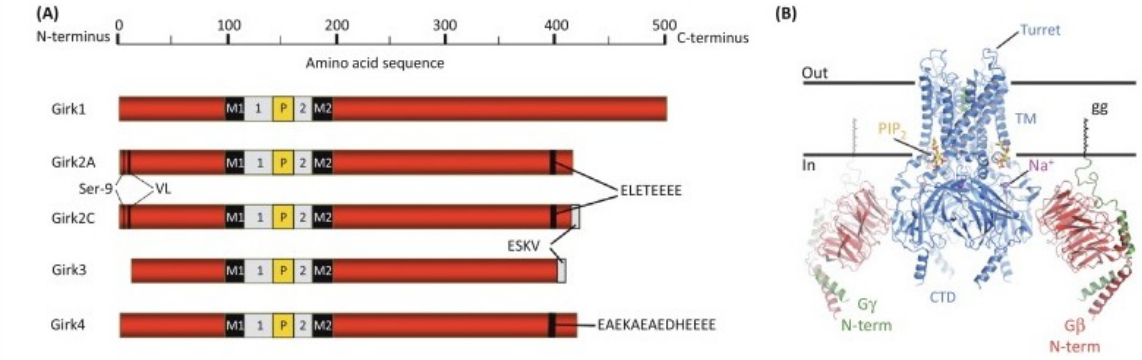

Figure 6.1: Structure of Kir channels. 6.2.A: Linear depiction of Girk channel subunits. 6.2.B: Structure of the Girk-Gβγ complex. (From New insights into the therapeutic potential of Girk channels; Luján R. et al. 2014, with permission).

GIRK subunits can form homo- or heterotetrameric channels. In order to form functional channels through the plasma membrane, heterotetrameric assemblies of GIRK1/3 or GIRK2/3 subunits are necessary (8). In contrast, GIRK2 subunits can form either active homo- or heterotetrameric channels in the plasma membrane(9, 10)(Figure 6.3).

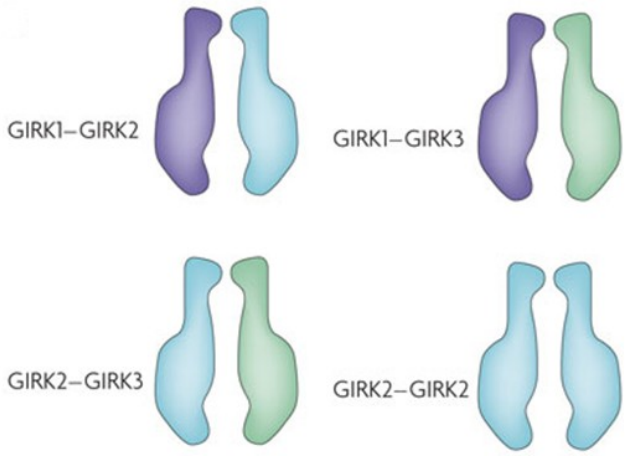

Figure 6.2: Formation of GIRK channel subunits. heterotetramers (GIRK2-GIRK3, GIRK1-GIRK2, and GIRK1-GIRK3) and homotetramers (GIRK2-GIRK2) (from: Emerging roles for G protein-gated inwardly rectifying potassium (GIRK) channels in health and disease. Lüscher C. et al. 2010, with permission).

These channels conduct K^+ currents more strongly in the inward direction than in the outward direction, and they are important for the establishment of the resting

potential. Different types of neurotransmitters, such as dopamine, somatostatin, acetylcholine, opioid, serotonin, adenosine and γ-amino-butyric-acid (GABA) neurotransmitters, activate these channels by stimulating their cognate G protein coupled receptors (GPCRs). These cognate GPCRs, in turn, couple specifically to pertussis toxin (PTX) sensitive heterotrimeric G proteins that activate GIRK channels(10, 11) (Figure.6.4).

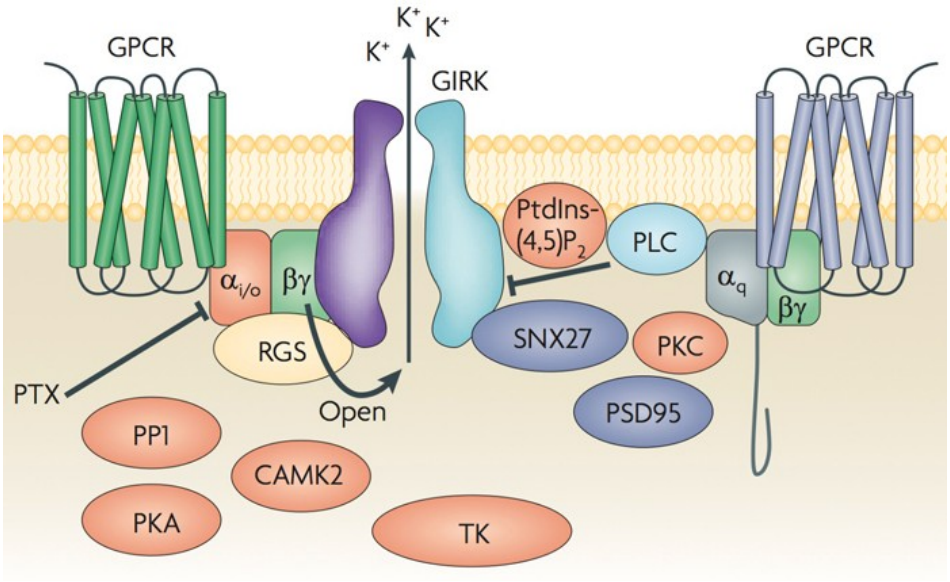

Figure 6.3: Activation mechanism of GIRK channel. (From: Emerging roles for G protein-gated inwardly rectifying potassium channels in health and disease. Lüscher C. 2010, with permission).

The roles of GIRKs in neuronal cells and in the regulation of the heartbeat has been thoroughly studied (12). The accumulated evidence indicates that GIRKs also play roles in the regulation of other cellular activities. These activities include insulin secretion in the pancreas (13), blood platelet aggregation (14) and the regulation of lipid metabolism in fat cells (15). Moreover, abnormal GIRK function has been demonstrated to alter neuronal excitability and lead to cell death. These findings indicate that GIRKs may be important in the pathophysiology of certain human diseases (channelopathies) such as epilepsy(16), Down's syndrome(17), Parkinson's disease(18) and drug addiction (10).

During recent years, a steadily increasing number of studies have shown that yet another disease can be ascribed, at least in part, to GIRK channel malfunction: **cancer** (19).

In 2001, Stringer et al. showed that the mRNA levels encoding the GIRK1 subunit were much higher in primary breast carcinomas than in healthy breast tissue. This significant increase in mRNA levels in primary tumor tissue could be correlated with an increased incidence in lymph node metastases(20). Three years later, in 2004, Takanami *et al.* identified a positive correlation between the mRNA levels encoding GIRK1 and the progression of non-small cell lung cancer (21). The results of a study conducted by Plummer et al. and published in 2004 indicated that the β-adrenergic receptors and G protein inwardly rectifying potassium channels subunit 1 were involved in the regulation of breast cancer in humans (22). In 2005, Plummer et al. (23) published the results of an investigation on the expression of G protein inwardly rectifying potassium channels in lung cancer cell lines. Their findings showed stimulation of GIRK1 or GIRK2 channels may be involved in the progression of lung cancer. They concluded that the stimulation of GIRK channels along with β-adrenergic signaling could potentially activate similar signaling pathways in both small cell lung cancer (SCLC) and breast cancer.
Using immunohistochemical analyses, Brevet *et al*. investigated the expression of GIRK1 in both normal and cancerous breast tissues. During this study, they observed that GIRK1 K^+ channels were expressed more strongly and significantly in cancerous breast tissue than in normal breast tissue. (24). A retrospective study conducted by Kammerer *et al.*, which was based on data collected from 905 invasive breast cancer patients and derived from The Cancer Genome Atlas (TCGA), confirmed that a correlation existed between KCNJ3 expression and breast cancer progression(25).

Breast cancer is the leading cause of death associated with cancer in women (26). This type of cancer most commonly metastasizes in the bones, and 70% of patients who develop bone metastases die (27). For these reasons, it is important to study *KCNJ3* expression in invasive breast carcinomas and evaluate whether this expression can be validated as a new prognostic biomarker (early biomarker) for this disease.

Thus, considering all documented evidence on connection between GIRK expression and cancer development, we aimed to test:

1) The expression of GIRK1a and shorter splice variants of GIRK1 in benign and malignant breast cell lines

2) The potential effects of overexpression and silencing of GIRK1a, c and d on vital parameters that are associated with cardinal neoplasia such as invasion, adhesion, wound healing, proliferation, motility and angiogenesis.

7. Material and Methods:

7.1. Cell lines:

Here is a short description of the cell lines, which were used in this thesis:

MCF-7 (Kindly provided by Prof. Bauernhofer. Passage number: 35)

Organism: Homo sapiens, human
Cell type: Epithelial
Tissue: Mammary gland, breast; derived from metastatic site: Pleural effusion
Disease: Adenocarcinoma
Receptor expression: Estrogen receptor positive
Complete growth medium: The base medium is Eagle's Minimum Essential Medium, (Gibco, #31095_029), fetal bovine serum to a final concentration of 10% (Sigma, #F2442), Sodium Pyruvate 1mM (Sigma, #S8636).
Freeze medium: Complete growth medium supplemented with 5% (v/v) DMSO (Sigma, #D2438).

MCF10A (Kindly provided by Prof. Bauernhofer. P: 2)

Organism: Homo sapiens, human
Cell type: Epithelial
Tissue: Mammary gland, breast
Disease: Fibrocystic disease (non-tumorigenic epithelial cell line)
Complete growth medium: The base medium is MEGM, (Lonza, #CC-3150). To make the complete growth medium, 100 ng/mL cholera toxin, (Sigma, #C8052) should be added.
Freeze medium: Complete growth medium supplemented with 5% (v/v) DMSO (Sigma, #D2438).

MDA-MB-231 (Kindly provided by Prof. Bauernhofer. P: 6)

Organism: Homo sapiens, human
Cell Type: Epithelial

Disease: Adenocarcinoma
Complete growth medium: The base medium is DMEM Low Glucose (Sigma, #D6046). To make the complete growth medium, FBS (Sigma, #F2442) is added to the final concentration of 10%.
Freeze medium: Complete growth medium supplemented with 5% (v/v) DMSO.

MCF-12A (Kindly provided by Prof. Bauernhofer. P: 8)

Organism: Homo sapiens, human
Cell Type: Epithelial
Tissue: Mammary gland; Breast
Complete growth medium: 1:1 mixture of Dulbecco's modified Eagle's medium and Ham's F12 medium (ATCC, #30-2006), 20 ng/mL Epidermal growth factor (Sigma, # E4127), 100 ng/mL cholera toxin, 0.01 mg/mL insulin (Sigma, #I2643), 500 ng/mL hydrocortisone (Sigma, #H0396) and horse serum, 5% (ATCC, #30-2040).
Freeze medium: Complete growth medium 95%; DMSO, 5%.

T-47D (Kindly provided by Prof. Bauernhofer. P: 3)

Organism: Homo sapiens, human
Cell Type: Epithelial
Tissue: Mammary gland; derived from metastatic site: Pleural effusion
Disease: Ductal carcinoma
Receptor expression: Androgen, estrogen, progesterone, prolactin receptors positive.
Complete growth medium: The base medium is RPMI1640 and 10% FBS (PAA, #E15-840).
Freeze medium: Complete growth medium supplemented with 5% (v/v) DMSO.

SK-BR-3 (Kindly provided by Prof. Bauernhofer. P: 17)

Organism: Homo sapiens, human
Tissue: Mammary gland/breast; derived from metastatic site: Pleural effusion
Disease: Adenocarcinoma

Complete growth medium: The base medium is RPMI1640 and 10% FBS.
Freeze medium: Complete growth medium supplemented with 5% (v/v) DMSO.

DU4475 (From ZMF, Cell Culture Facility, P:5)

Organism: Homo sapiens, human
Tissue: Mammary gland/breast
Comments: This line grows in floating clusters.
Complete growth medium: The base medium is RPMI1640 and 10% FBS.
Freeze medium: Complete growth medium supplemented with 5% (v/v) DMSO.

MDA-MB-175-VIII (Kindly provided by Prof. Zarnani. P: 6)

Organism: Homo sapiens, human
Cell type: Epithelial
Tissue: Mammary gland; Breast/Duct; derived from metastatic site: Pleural effusion
Disease: Ductal carcinoma
Complete growth medium: The base medium is RPMI1640 and 10% FBS.
Freeze medium: Complete growth medium supplemented with 5% (v/v) DMSO.

SUM 159PT (Kindly provided by Prof. Bauernhofer. P: 7)

Organism: Homo sapiens, human
Cell type: Epithelial
Tissue: Mammary gland; Breast
Disease: Anaplastic carcinoma
Complete growth medium: Ham's F-12 (PAA, #E15-817) with 5% Fetal bovine serum, Insulin (Sigma, #I2643), 5 ug/mL , Hydrocortisone (Sigma, #H0396) 1ug/mL and HEPES 10mM (PAA, #511-001).
Freeze medium: Complete growth medium supplemented with 5% (v/v) DMSO.

KPL-1 (From ZMF, Cell Culture Facility, P: 5)

Organism: Homo sapiens, human
Tissue: Mammary gland; breast
Disease: Breast carcinoma (derivative of MCF-7)
Comment: Estrogen receptor positive. however, DNA fingerprinting analysis showed cross-contamination with MCF-7 (DSMZ data).
Complete growth medium: The base medium is DMEM high glucose (Sigma, #D0572). To make the complete growth medium, add FBS to a final concentration of 10%.
Freeze medium: Complete growth medium supplemented with 10% (v/v) DMSO and 20% (v/v) FBS.

CAL-85-1 (From ZMF, Cell Culture Facility, P: 5)

Organism: Homo sapiens, human
Tissue: Mammary gland; breast
Disease: Breast Adenocarcinoma
Complete growth medium: The base medium is DMEM Low Glucose (Sigma, #D6046). To make the complete growth medium, add fetal bovine serum to a final concentration of 10%.
Freeze medium: Complete growth medium supplemented with 10% (v/v) DMSO and 20% (v/v) FBS.

HEK-293 (Kindly provided by Prof. Malle. P: 6)

Organism: Homo sapiens, human
Cell type: Embryonic
Tissue: Embryonic kidney
Complete growth medium: The base medium for this cell line is DMEM high Glucose (Sigma, #D0572). Additives are: 200 mM L-glutamine (Sigma, #G7513) and 1M HEPES (PAA, #511-001).To make the complete growth medium, fetal bovine serum is added to a final concentration of 10%.
Freeze medium: Complete growth medium supplemented with 5% (v/v) DMSO.

HL-1 (Kindly provided by Prof. Groschner. P: 79)

Cardiac murine atrial myocyte by Dr. W. Claycomb
Complete growth medium: The base medium is Claycomb (Sigma, #51800 C). Additives are: 2 mM L-glutamine (Sigma, #G7513), 0.1 mM Norepinephrine (Sigma, #A0937) and 10% fetal bovine serum (Sigma, #F2442).
Freeze medium: Complete growth medium supplemented with 5% (v/v) DMSO (Sigma, #D2438).

7.2. Generation of constructs:

7.2.1. Overexpression:

The first step of overexpressing the cells, is to subclone the insert encoding the ion channel subunits human GIRK1a, human GIRK1c into a plasmid expression vector to yield a C-terminal fusion (pEYFPN1 clontech, #6006-1) and human GIRK1a and human GIRK1d in N-terminal fusion with eYFP (pEYFPC1 clontech, #6005-1) . In addition, we subcloned the insert encoding human GIRK1a in eGFP vector (PIRES2 –eGFP clontech, #6029-1).

7.2.1.1: GIRK1a: Homo sapiens potassium channel, inwardly rectifying subfamily J, member 3 (KCNJ3), transcript variant 1

This variant represents the longest transcript and encodes the longest isoform (also known as GIRK1a).

NCBI Reference Sequence: NM_002239.3 (from NCBI data base)
https://www.ncbi.nlm.nih.gov/nuccore/386781835/

mRNA:

CDS: 196..1701

```
1 ctccgtccca ggggagaagg agaggcgtct gcaggggca gagaccgcag ctacctgccg
61 ggtgcgcccc ccacccagga gcgctcgctt cgccccttt cctcccccgc ccccacctcc
121 ttattggtgc tagtttgcag cgcccagctc ctgcgccttc gcttcgcgtt tgaatctggc
181 tcgccccttc gtattatgtc tgcactccga aggaaatttg gggacgatta tcaggtagtg
241 accacatcgt ccagcggctc gggcttgcag ccccaggggc caggccagga ccctcagcag
```

301 cagcttgtgc ccaagaagaa gcggcagcgg ttcgtggaca agaacggccg gtgcaatgta
361 cagcacggca acctgggcag cgagacaagc cgctacctct cggacctctt caccacgctg
421 gtggacctca agtggcgctg gaacctcttc atcttcattc tcacctacac cgtggcctgg
481 cttttcatgg cgtccatgtg gtgggtgatc gcctacactc ggggcgacct gaacaaagcc
541 cacgtcggta actacacgcc ttgcgtggcc aatgtctata acttcccttc tgccttcctc
601 ttcttcatcg agacggaggc caccatcggc tatggctacc gatacatcac agacaagtgc
661 cccgagggca tcatcctctt cctcttccag tccatcctgg gctccatcgt ggacgccttc
721 ctcatcggct gcatgttcat caagatgtcc cagcccaaga agcgcgccga gaccctcatg
781 ttcagcgagc acgcggtgat ctccatgagg gacggaaaac tcacgcttat gttccgggtg
841 ggcaacctgc gcaacagcca catggtctcc gcgcagattc gctgcaagct gctcaaatct
901 cggcagacac ctgagggtga gttccttccc cttgaccaac ttgaactgga tgtaggtttt
961 agtacagggg cagatcaact ttttcttgtg tccccccctca caatttgcca cgtgatcgat
1021 gccaaaagcc ccttttatga cctatcccag cgaagcatgc aaactgaaca gttcgagatt
1081 gtcgtcatcc tagaaggcat tgtggaaaca actgggatga cttgtcaagc tcgaacatca
1141 tatactgaag atgaagttct ttggggtcat cgtttttttc ctgtaatttc cttagaagag
1201 ggattcttta aagttgatta ctcccagttc catgcaacat ttgaagtccc caccccacct
1261 tacagtgtga aagagcagga ggaaatgctt ctcatgtcgt ccccttttaat agcaccagcc
1321 ataactaaca gcaaagaaag acataattct gtggaatgct tagatggact agatgatatt
1381 actacaaaac taccatctaa gctgcagaaa attactggaa gagaagactt tcccaaaaaa
1441 ctcttgagga tgagttctac aacttcagaa aaagcctaca gcttgggaga cttgcccatg
1501 aaacttcaac gaataagttc agttccgggc aactcagaag aaaaactggt atctaaaacc
1561 accaagatgt tatctgatcc catgagccag tctgtggctg atttgccacc aaagcttcaa
1621 aagatggctg gaggagcagc taggatggaa gggaaccttc cagccaaatt aagaaaaatg
1681 aactctgatc gcttcacata acaaagcact cccttaggca ttatttaatg tttgatttag
1741 taatagtcca atatttggcg atgaggtaat tctccctaag gaatctgaaa gtatattttc
1801 ctcccagttc tacaagcata tttgagaacc cttccttttcc caagtattgc gaatgtgcag
1861 aaagcaacag ttacggaggg aggacatcat aaggaagtta ttaacgggca tgtattatca
1921 catcaagcat gcaataatgt gcaaattttg catttagttt tatggcatga tttatatatg
1981 gcatatttat attgtatatt ctggaaaaaa aatatatata tatatttaaa ggggagatac
2041 tctccctgac atttctaaca tatgtattaa gccaaacatg agtgaatagc tttcagggcg
2101 ataaaactaa atatatgtct gtgtgtgtgt gtgtatgtat acacacatat acatatatat
2161 atacacatac atacacatac atacatacat acatatatat ctgataaaat tgtgatgttt
2221 tgttcaaagt tgtagttctt gtgcatgttt actttattag agtaggaagg ctactggcat
2281 taattattaa taccaaatat tttagcctta aatttttgtc attttaaaat ctgatttaat
2341 gttttctgct gtttaaggtc ttgggaggct ttcaattgta ttttatatga gagaatcaca
2401 caagtttgtg ctatctatgg ccctgcaaaa atataaccat tacatgttta aattgtaaat
2461 tttagagcat accagtactc agtatagcat tgaacatttc ttatgatttt taaaagttgc
2521 tagtactggg gagaaataat tgttgattaa tttgagaatt attccttttcc tagactaatt
2581 aaaatctgga aatctgtttt gtatatgatc taatacaaag atgagctctg aacaaacact
2641 gaatcatgtt aatagacagt agccaagtta tattgaatat atcagaatct gtgtgaagtt
2701 acacaattaa ttgtccctgt ttcaaactga gtaaattgga aacattttct ttctttttct
2761 ggaaattttg tccatttttaa aaaccaatca ttttaagaag acatgacaat gcaatgaaac
2821 agatgataaa tatttatgct taaaatatgt atgtctaatt gagtctcttt tttattctgt
2881 tttcttgttt atggcatttg ttgtaacagg atagacttttt tcctcaccta ggaaacctat
2941 cccatgcctg tcacttatag ttcaggagga agtttttgca cagaccagag agaaattaaa
3001 attagatgat aaattgaaga tatcttacac acagtttttt ggtgaacact gattttattg
3061 gtgtcttaga tccctagtct acccaaataa ttttaacagt actgtttttt ctaatcctga
3121 agtctgatat ttatgactca ttagcaggaa tcaaaactag tgatcagtag aacactttca
3181 aaataaaaat ttggaatgca gacttttatg aaaatttaaa agtgctcctt aacagaatat
3241 catgggtttt cctataaaac ttctttaagt attgtaattc cagtctgccc caactttaaa
3301 aaaaattctt attaatatgt cagtcattaa ttgctagttt gggctctcat tatttcctgt
3361 tttttaacaa ttttgtgata attttattat tggcaaatta atacatcaac acttaaatca
3421 ttgactataa taataccttc tggctacctc tgtatcaacc aaattctgta ggtgcaaaca
3481 tataccaggg aattcttact ggcaaaatga tcaatctgga gtgtgcatcc actgtgaatg
3541 gagcaaattg ccctataccc attgataacc tagctttctt agtttgtaga tgtaggaaac
3601 aaaatagtga cagagagaga agggggtcca cagggcatgg tatatttatc agcagtggaa
3661 aaaaagtgca tagatcattt agtccaagaa cttaaaacta aatagagcca taatttactt
3721 tggagagtca ttttaatttg tctttggtac caaggagaag acggaaccaa aaacaaactc
3781 tccaagtata ttcacacatt caacaaaatt tttgcatgcc ttctatgtcg taggcatttt
3841 tagttcctgg ggatttggac atggctaagt cagagaaggc cattgctcac catgaacact
3901 gtataccaga aggagagtgg ggaggagaca aaaaacaaat aagaccactt cagacaatca

```
3961 aagtatcagt taagagaatg aaaacaggcc tgactcagtg gctcacgcct gtaatcccag
4021 tactttggga ggcggaggtt gggggatcac ctgaggtcag gagatcgaga ccagcctgga
4081 caacatggtg aaaacccgtc tctactaaaa atacaaaaat taactgggca tggtggcagg
4141 cacctgtaat cccagctact ggggaagctg aggcaggaga atcgtttgaa cctgggaggc
4201 ggaggttgca gtgagccaag attctgccac tgcactccag cctgggtgac agtgcgagac
4261 tccatctcaa catcaaaaaa aaaaaaaaaa aaaaaaaaaa aaaaaaaaaa aaaaagaata
4321 aaaacagggt aacataatgc aaagtaactg tgtggaataa aaattgatta ttttagaaaa
4381 tgtgactggc ttaggacggg gataatatgt gaacagaaat ctatctcatg agaaagtgct
4441 actgttgtca aaattacctt atctgagtga atggtatttt ttttatcttt tccacacatg
4501 cgtgggaaag gtatgatttc tgcatgtaat tgcagtttaa ccctttatttc taggttgatc
4561 ataggtccca gtttacccag gaaaattcca gtttatacct gttgtacctg tgtaattatt
4621 ggtagcactc cctttcactc ttacaatgtc ttggtttgga tgatatatgg tgaagttttt
4681 gttgaaacta aattatgaag tctgatatat ttggataaaa ataaagaatt gcttttcttc
```

Translation:

"MSALRRKFGDDYQVVTTSSSGSGLQPQGPGQDPQQQLVPKKKRQ

RFVDKNGRCNVQHGNLGSETSRYLSDLFTTLVDLKWRWNLFIFILTYTVAWLFMASMW

WVIAYTRGDLNKAHVGNYTPCVANVYNFPSAFLFFIETEATIGYGYRYITDKCPEGII

LFLFQSILGSIVDAFLIGCMFIKMSQPKKRAETLMFSEHAVISMRDGKLTLMFRVGNL

RNSHMVSAQIRCKLLKSRQTPEGEFLPLDQLELDVGFSTGADQLFLVSPLTICHVIDA

KSPFYDLSQRSMQTEQFEIVVILEGIVETTGMTCQARTSYTEDEVLWGHRFFPVISLE

EGFFKVDYSQFHATFEVPTPPYSVKEQEEMLLMSSPLIAPAITNSKERHNSVECLDGL

DDITTKLPSKLQKITGREDFPKKLLRMSSTTSEKAYSLGDLPMKLQRISSVPGNSEEK

LVSKTTKMLSDPMSQSVADLPPKLQKMAGGAARMEGNLPAKLRKMNSDRFT"

7.2.1.2. GIRK1d: Homo sapiens potassium channel, inwardly rectifying subfamily J, member 3 (KCNJ3), transcript variant 2.

Compared to variant 1, this splice variant lacks an exon in the coding region. This difference results in a frameshift and a protein (isoform 2; also known as GIRK1d) with a truncated C-terminus.

NCBI Reference Sequence: NM_001260508.1 (From NCBI data base https://www.ncbi.nlm.nih.gov/nuccore/NM_001260508.1)

mRNA:

CDS: 196..903

```
1 ctccgtccca ggggagaagg agaggcgtct gcaggggca gagaccgcag ctacctgccg
61 ggtgcgcccc ccacccagga gcgctcgctt cgccccttt cctcccccgc ccccacctcc
121 ttattggtgc tagtttgcag cgcccagctc ctgcgccttc gcttcgcgtt tgaatctggc
```

181 tcgccccttc gtattatgtc tgcactccga aggaaatttg gggacgatta tcaggtagtg
241 accacatcgt ccagcggctc gggcttgcag ccccaggggc caggccagga ccctcagcag
301 cagcttgtgc ccaagaagaa gcggcagcgg ttcgtggaca agaacggccg gtgcaatgta
361 cagcacggca acctgggcag cgagacaagc cgctacctct cggacctctt caccacgctg
421 gtggacctca agtggcgctg gaacctcttc atcttcattc tcacctacac cgtggcctgg
481 cttttcatgg cgtccatgtg gtgggtgatc gcctacactc ggggcgacct gaacaaagcc
541 cacgtcggta actacacgcc ttgcgtggcc aatgtctata acttcccttc tgccttcctc
601 ttcttcatcg agacggaggc caccatcggc tatggctacc gatacatcac agacaagtgc
661 cccgagggca tcatcctctt cctcttccag tccatcctgg gctccatcgt ggacgccttc
721 ctcatcggct gcatgttcat caagatgtcc cagcccaaga agcgcgccga gaccctcatg
781 ttcagcgagc acgcggtgat ctccatgagg gacggaaaac tcacgcttat gttccgggtg
841 ggcaacctgc gcaacagcca catggtctcc gcgcagattc gctgcaagct gctcaaagga
901 tgacttgtca agctcgaaca tcatatactg aagatgaagt tctttggggt catcgttttt
961 ttcctgtaat ttccttagaa gagggattct ttaaagttga ttactcccag ttccatgcaa
1021 catttgaagt ccccacccca ccttacagtg tgaaagagca ggaggaaatg cttctcatgt
1081 cgtccccttt aatagcacca gccataacta acagcaaaga aagacataat tctgtggaat
1141 gcttagatgg actagatgat attactacaa aactaccatc taagctgcag aaaattactg
1201 gaagagaaga ctttcccaaa aaactcttga ggatgagttc tacaacttca gaaaaagcct
1261 acagcttggg agacttgccc atgaaacttc aacgaataag ttcagttccg ggcaactcag
1321 aagaaaaact ggtatctaaa accaccaaga tgttatctga tcccatgagc cagtctgtgg
1381 ctgatttgcc accaaagctt caaaagatgg ctggaggagc agctaggatg gaagggaacc
1441 ttccagccaa attaagaaaa atgaactctg atcgcttcac ataacaaagc actcccttag
1501 gcattattta atgtttgatt tagtaatagt ccaatatttg gcgatgaggt aattctccct
1561 aaggaatctg aaagtatatt ttcctcccag ttctacaagc atatttgaga acccttcctt
1621 tcccaagtat tgcgaatgtg cagaaagcaa cagttacgga gggaggacat cataaggaag
1681 ttattaacgg gcatgtatta tcacatcaag catgcaataa tgtgcaaatt ttgcatttag
1741 ttttatggca tgatttatat atggcatatt tatattgtat attctggaaa aaaaatatat
1801 atatatattt aaaggggaga tactctccct gacatttcta acatatgtat taagccaaac
1861 atgagtgaat agctttcagg gcgataaaac taaatatatg tctgtgtgtg tgtgtgtatg
1921 tatacacaca tatacatata tatatacaca tacatacaca tacatacata catacatata
1981 tatctgataa aattgtgatg ttttgttcaa agttgtagtt cttgtgcatg tttacttttat
2041 tagagtagga aggctactgg cattaattat taataccaaa tattttagcc ttaaattttt
2101 gtcattttaa aatctgattt aatgttttct gctgtttaag gtcttgggag gctttcaatt
2161 gtattttata tgagagaatc acacaagttt gtgctatcta tggccctgca aaaatataac
2221 cattacatgt ttaaattgta aattttagag cataccagta ctcagtatag cattgaacat
2281 ttcttatgat ttttaaaagt tgctagtact ggggagaaat aattgttgat taatttgaga
2341 attattcctt tcctagacta attaaaatct ggaaatctgt tttgtatatg atctaataca
2401 aagatgagct ctgaacaaac actgaatcat gttaatagac agtagccaag ttatattgaa
2461 tatatcagaa tctgtgtgaa gttacacaat taattgtccc tgtttcaaac tgagtaaatt
2521 ggaaacattt tctttctttt tctggaaatt ttgtccattt taaaaaccaa tcattttaag
2581 aagacatgac aatgcaatga aacagatgat aaatatttat gcttaaaata tgtatgtcta
2641 attgagtctc ttttttattc tgttttcttg tttatggcat ttgttgtaac aggatagact
2701 ttttcctcac ctaggaaacc tatcccatgc ctgtcactta tagttcagga ggaagttttt
2761 gcacagacca gagagaaatt aaaattagat gataaattga agatatctta cacacagttt
2821 tttggtgaac actgatttta ttggtgtctt agatccctag tctacccaaa taattttaac
2881 agtactgttt tttctaatcc tgaagtctga tatttatgac tcattagcag gaatcaaaac
2941 tagtgatcag tagaacactt tcaaaataaa aatttggaat gcagactttt atgaaaattt
3001 aaaagtgctc cttaacagaa tatcatgggt tttcctataa aacttcttta agtattgtaa
3061 ttccagtctg ccccaacttt aaaaaaaatt cttattaata tgtcagtcat taattgctag
3121 tttgggctct cattatttcc tgtttttaa caattttgtg ataattttat tattggcaaa
3181 ttaatacatc aacacttaaa tcattgacta taataatacc ttctggctac ctctgtatca
3241 accaaattct gtaggtgcaa acatatacca gggaattctt actggcaaaa tgatcaatct
3301 ggagtgtgca tccactgtga atggagcaaa ttgccctata cccattgata acctagcttt
3361 cttagtttgt agatgtagga aacaaaatag tgacagagag agaaggggt ccacagggca
3421 tggtatattt atcagcagtg gaaaaaaagt gcatagatca tttagtccaa gaacttaaaa
3481 ctaaatagag ccataattta ctttggagag tcattttaat ttgtctttgg taccaaggag
3541 aagacggaac caaaaacaaa ctctccaagt atattcacac attcaacaaa atttttgcat
3601 gccttctatg tcgtaggcat ttttagttcc tggggatttg gacatggcta agtcagagaa
3661 ggccattgct caccatgaac actgtatacc agaaggagag tggggaggag acaaaaaaca
3721 aataagacca cttcagacaa tcaaagtatc agttaagaga atgaaaacag gcctgactca
3781 gtggctcacg cctgtaatcc cagtactttg ggaggcggag gttgggggat cacctgaggt

```
3841 caggagatcg agaccagcct ggacaacatg gtgaaaaccc gtctctacta aaaatacaaa
3901 aattaactgg gcatggtggc aggcacctgt aatcccagct actggggaag ctgaggcagg
3961 agaatcgttt gaacctggga ggcggaggtt gcagtgagcc aagattctgc cactgcactc
4021 cagcctgggt gacagtgcga gactccatct caacatcaaa aaaaaaaaaa aaaaaaaaaa
4081 aaaaaaaaaa aaaaaaaaga ataaaaacag ggtaacataa tgcaaagtaa ctgtgtggaa
4141 taaaaattga ttattttaga aaatgtgact ggcttaggac ggggataata tgtgaacaga
4201 aatctatctc atgagaaagt gctactgttg tcaaaattac cttatctgag tgaatggtat
4261 ttttttttatc ttttccacac atgcgtggga aaggtatgat ttctgcatgt aattgcagtt
4321 taacccttat ttctaggttg atcataggtc ccagtttacc caggaaaatt ccagtttata
4381 cctgttgtac ctgtgtaatt attggtagca ctccctttca ctcttacaat gtcttggttt
4441 ggatgatata tggtgaagtt tttgttgaaa ctaaattatg aagtctgata tatttggata
4501 aaaataaaga attgctttc ttc

translation="MSALRRKFGDDYQVVTTSSSGSGLQPQGPGQDPQQQLVPKKKRQ

RFVDKNGRCNVQHGNLGSETSRYLSDLFTTLVDLKWRWNLFIFILTYTVAWLFMASMW

WVIAYTRGDLNKAHVGNYTPCVANVYNFPSAFLFFIETEATIGYGYRYITDKCPEGII

LFLFQSILGSIVDAFLIGCMFIKMSQPKKRAETLMFSEHAVISMRDGKLTLMFRVGNL

RNSHMVSAQIRCKLLKG"
```

7.2.1.3. hGIRK1c: Homo sapiens potassium channel, inwardly rectifying subfamily J, member 3 (KCNJ3), transcript variant 3.

NCBI Reference Sequence: NM_001260509.1 (From NCBI data base https://www.ncbi.nlm.nih.gov/nuccore/NM_001260509.1)

This splice variant lacks the 3' terminal exon and uses an alternate splice site in the upstream coding region, when compared to variant 1. These differences result in a protein (isoform 3; GIRK1c) with a truncated C-terminus, compared to isoform 1.

mRNA:

```
CDS :196..1122

1 ctccgtccca ggggagaagg agaggcgtct gcaggggca gagaccgcag ctacctgccg
61 ggtgcgcccc ccacccagga gcgctcgctt cgccccctt cctcccccgc ccccacctcc
121 ttattggtgc tagtttgcag cgcccagctc ctgcgccttc gcttcgcgtt tgaatctggc
181 tcgccccttc gtattatgtc tgcactccga aggaaatttg gggacgatta tcaggtagtg
241 accacatcgt ccagcggctc gggcttgcag ccccaggggc caggccagga ccctcagcag
301 cagcttgtgc ccaagaagaa gcggcagcgg ttcgtggaca agaacggccg gtgcaatgta
361 cagcacggca acctgggcag cgagacaagc cgctacctct cggacctctt caccacgctg
421 gtggacctca agtggcgctg gaacctcttc atcttcattc tcacctacac cgtggcctgg
481 cttttcatgg cgtccatgtg gtgggtgatc gcctacactc ggggcgacct gaacaaagcc
541 cacgtcggta actacacgcc ttgcgtggcc aatgtctata acttcccttc tgccttcctc
601 ttcttcatcg agacggaggc caccatcggc tatggctacc gatacatcac agacaagtgc
661 cccgagggca tcatcctctt cctcttccag tccatcctgg gctccatcgt ggacgccttc
```

```
721 ctcatcggct gcatgttcat caagatgtcc cagcccaaga agcgcgccga gaccctcatg
781 ttcagcgagc acgcggtgat ctccatgagg gacggaaaac tcacgcttat gttccgggtg
841 ggcaacctgc gcaacagcca catggtctcc gcgcagattc gctgcaagct gctcaaatct
901 cggcagacac ctgagggtga gttccttccc cttgaccaac ttgaactgga tgtaggtttt
961 agtacagggg cagatcaact ttttcttgtg tccccccctca caatttgcca cgtgatcgat
1021 gccaaaagcc ccttttatga cctatcccag cgaagcatgc aaactgaaca gttcgagatt
1081 gtcgtcatcc tagaaggcat tgtggaaaca actggtgagt aaaaacagat atgccataaa
1141 gtttc

translation="MSALRRKFGDDYQVVTTSSSGSGLQPQGPGQDPQQQLVPKKKRQ

RFVDKNGRCNVQHGNLGSETSRYLSDLFTTLVDLKWRWNLFIFILTYTVAWLFMASMW

WVIAYTRGDLNKAHVGNYTPCVANVYNFPSAFLFFIETEATIGYGYRYITDKCPEGII

LFLFQSILGSIVDAFLIGCMFIKMSQPKKRAETLMFSEHAVISMRDGKLTLMFRVGNL

RNSHMVSAQIRCKLLKSRQTPEGEFLPLDQLELDVGFSTGADQLFLVSPLTICHVIDA

KSPFYDLSQRSMQTEQFEIVVILEGIVETTGE"
```

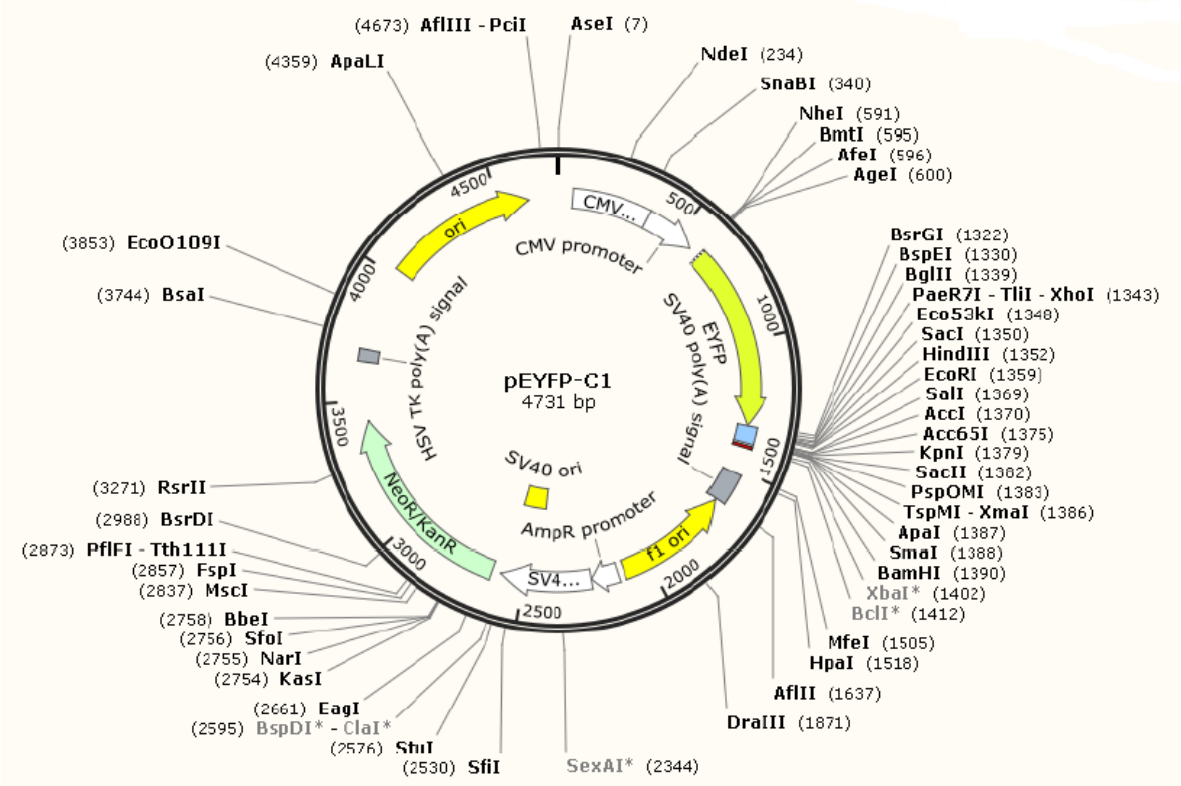

Figure 7.1: Map of pEYFP-C1 vector. All the restriction enzymes in the map are 6 unique and sticky ends cutters. Grey restriction enzymes: blocked by Dcm methylation. (Created by snap gene program).

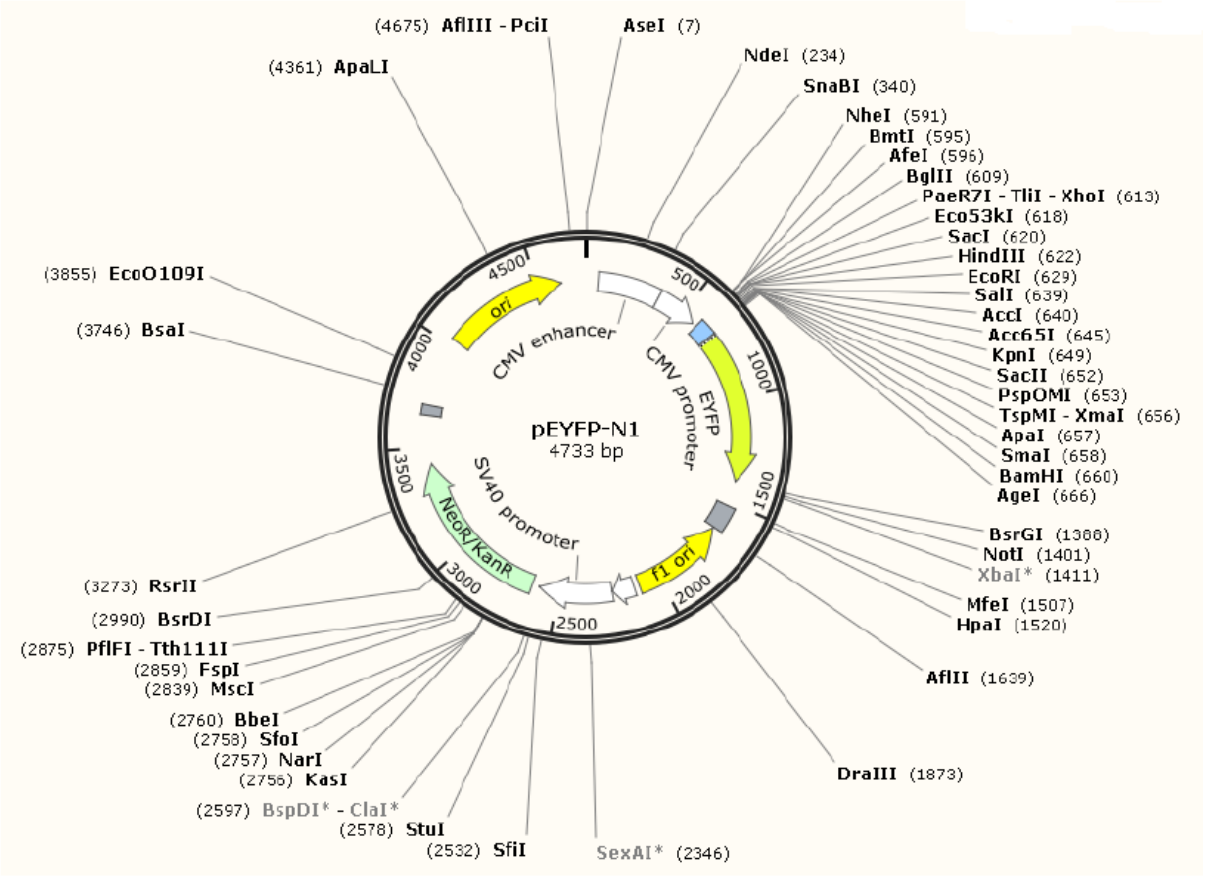

Figure 7.2: Map of pEYFP-N1 vector. All the restriction enzymes in the map are 6 unique and sticky ends cutters. Grey restriction enzymes: blocked by Dcm methylation. (Created by snap gene program).

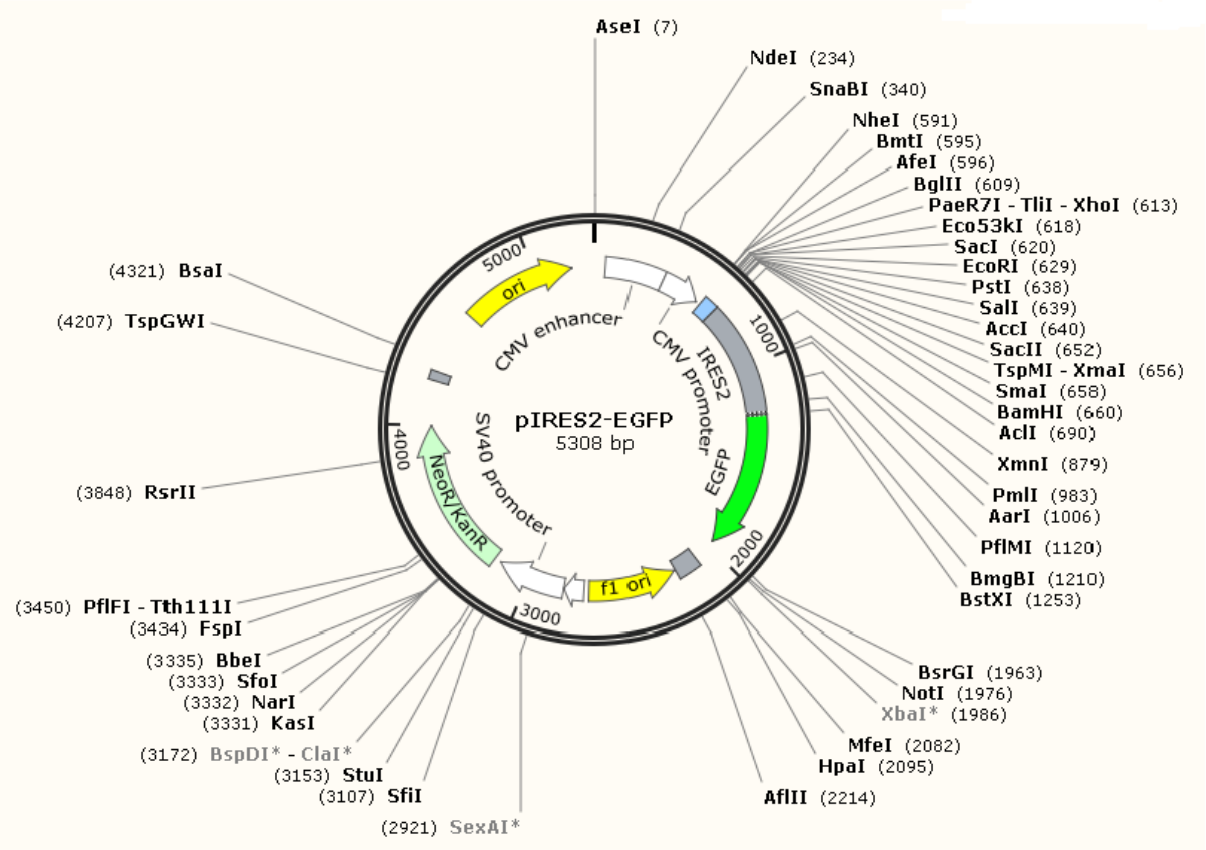

Figure 7.3: Map of pIRES2-EGFP vector. All the restriction enzymes in the map are 6 unique and sticky ends cutters. Grey restriction enzymes: blocked by Dcm methylation. (Created by snap gene program).

7.2.1.4. Designing the Primers:

Primer for human GIRK1a, d in pEYFPC1 vector:
XhoI (Promega, #R6161) and EcoRI (Promega, #R60111) were used for digestion.

Forward primer: 5´-TTACTCGAGCTATGTCTGCACTCCGAAGGAAATTT G-3´
Reverse primer: 5´-TTAGAATTCGTGTGAAGCGGTCAGAGTTCATTTTTC-3´

Primer for human GIRK1c in pEYFPN1 vector:
XhoI and EcoRI were used for digestion.

Forward primer 5´-TTACTCGAGCTATGTCTGCACTCCGAAGGAAATTTG-3´
Reverse primer: 5´-TTAGAATTCGCTCACCAGTTGTTTCCACAATGCC-3´

Primer for human GIRK1a in PIRES2-EGFP vector:
NheI (Promega, #R6501) and BamHI (Promega, #R6021) were used for digestion.

Forward primer: 5´-TTAGCTAGCATGTCTGCACTCCGAAGGAAATTT G-3´
Reverse primer: 5´-TTAGGATCCTTATGTGAAGCGATCAGAGTT C-3´

Next step was finding out the best annealing temperature by using a temperature gradient PCR. For preparing PCR reactions, the following protocol was used:

Pfu-buffer (10X)	5 µL
dNTP (10 mM each) (Sigma, #DNTP100)	1 µL
a. dest	41.5 µL
Template plasmid (1ng/µL)	1.5 µL

The vials were vortexed and picufuged and the following reagents were added to them:

Forward primer (100ng/ µL)	0.3 µL
Reverse primer (100ng/ µL)	0.3 µL
Pfu polymerase (Promega, #M7741) (2.5U/ µL)	0.5 µL

The vials were vortexed and picufuged and subdivided 8 µL in 6 PCR tubes and 3 µL of mineral oil were added to each eppendorf tubes and all were put in Thermocyclere (Eppendorf Master Gradient).

Program in the thermocycler (gradient):

1. 2 min at 95°C
2. 1 min at 95°C
3. 1 min at 50-68°C
4. 4 min at 73°C

5. 35 cycles between 2 and 4.
6. 5 min at 73°C
7. Infinite time at 14°C

1.5% analytical agarose (ROTH, #2267.2) gel was prepared and electrophorase was done in TAE buffer to find out the best temperature for PCR products.

After observing the best temperature for PCR, large scale PCR was done to obtain sufficient inset DNA, then the PCR products were cleaned by Wizard sv Gel and PCR clean up system (Promega, #A9281).

7.2.1.4. Digestion of PCR product:

PCR products were restricted with XhoI and EcoRI in case of pEYFPC1 and pEYFPN1 vector and NheI and BamHI in case of PIRES2-EGFP vector.

Protocol for digesting the PCR products by restriction enzymes:

To each DNA sample the following materials were added:

a. dest	22 µL
Appropriate 10X buffer	10 µL
BSA (10X) (Promega, #R396E)	10 µL
Restriction enzyme #1	4 µL
Restriction enzyme #2	4 µL

They were mixed, picofuged and put in the 37°C incubator for overnight.

7.2.1.5. Digestion of vector:

This step was done simultaneously with the digestion of PCR products. The following materials were mixed in eppendorf tube:

Appropriate 10X Buffer	10 µL
a. dest	52 µL
BSA (10X)	10 µL

Plasmid DNA	20µg
Restriction enzyme#1	4 µL
Restriction enzyme#2	4 µL

They were mixed, picofuged and put in the 37°C incubator overnight.The completeness of digestion was checked on 1.5% analytical DNA gel and uncut plasmid was used as a control and DNA Ladder 1kb (Promega, #G5711) was applied to check the size of the plasmid.

7.2.1.7. Eluting the DNA from the gel:

1% pereparative gel was prepared and DNAs were loaded in the gel and were run for 1 hour at 80 v. The bands were cut out under UV illumination and were put in pre-weighted eppendorfs. Samples were cleaned up by wizards sv gel clean up system and the concentrations were measured by nanodrop (Peqlab 2000C).

7.2.1.8. Ligation:

The following materials were mixed on ice:

Digested vector	95 *f*mole
Insert	195 *f*mole
a. dest	final Volume of 20 µL

The weight was calculated according to the relation (weight/bp): 660 pg of double stranded DNA (1 bp) corresponding to 1 pmole.
Vials were put at 45°C for 5 minutes and back on ice afterward, then the following materials were added to them:

T4 buffer (10X) (NEB, # B0202S)	2 µL
T4 ligase (NEB, #M020S)	0.3 µL

The vials were incubated overnight at 12°C.

7.2.1.9. Preparing ligation mixture for electroporation:

To each ligation mixture 23 µL of 10M NH4COO (MERCK) and 300 µL of 95% ethanol (MERC) were added and put them in -20°C for 2 hours. Eppendorfs were centrifuged and at 13000 rpm for 30 min, then supernants were removed and the pellets were washed with 80% Ethanol for 20 min. The pellets were air dried and resuspend in 5 µL nuclease free water (ROTH, #T143).

7.2.1.10. Electroporation:

XL1-Blue E. Coli (Stratagene, #200228) was used, mixed the whole aliquots with 5 µL of ligation mixture and put in electroporation cuvet (Bioenzyme, #748020) and electroporated (BioRad). Immediately after electroporation 500 µL of SOC medium was added to each cuvet and put in pre warmed shaker incubator 250 rpm 37°C for 1 hour. After that 150 µL of the mixture were cultured on LB Agar medium with kanamycine (10µg/mL) (Sigma, #K4378) and put it in 37°C incubator overnight.

7.2.1.11. Colony counting and doing minipreps for restriction analysis:

Number of colonies were counted and 5 of them were selected for miniprep. In sterile 15 mL falcon (Greiner, # 82050-276) 5mL LB broth medium were put and one colony of bacteria was cultured in each tube and put in the shaker incubator in 37°C 250 rpm overnight.

Day after, tubes were taken from the incubator and miniprep were done according to manufacturer's protocol (Promega, # A1460).

For checking the size of the construct, restriction analysis was done as following:

Restriction enzyme#1	0.5 µL
Restriction enzyme#2	0.5 µL
Appropriate Buffer	2 µL
BSA (10X)	2 µL

DNA from miniprep	5 µL
Nuclease free water	10 µL

The eppendorf tubes were picofuged and were put in 37°C overnight. The day after, an analytical gel was run to check the DNAs size. Uncut DNA was loaded as control as well as DNA Ladder. To get the higher amount of DNA, Midiprep (Qiagen, #12143) was done according to manufactures protocols.

7.2.1.12. Primer for sequencing:

pEGFPC1, forward primer: 5´ - GATCACTCTCGGCATGGAC-3´

pEGFPC1, reverse primer: 5´ - CATTTTATGCAGGTTCAGGG-3´

7.2.1.13. Linearization of midiPrep plasmid DNA:

A circular plasmid DNA molecule was cut in order to transfect to mammalian cells for having stable transfected cells.

Linearization master mix:

Circular plasmid DNA (1 µg/ µL)	20µL
Appropriate buffer	20 µL
BSA (1/10 diluted)	20 µL
AseI (NEB, #R0526S)	6 µL
RNAse free water	134 µL

The eppendorf tubes were picofuged and were put in 37°C overnight. To ensure that the plasmid DNA is cut properly, an agarose gel was run. 5µL of DNA with 5µL 1X loading buffer were mixed and loaded in the 1.5% agarose gel and were looked for clean cuts. Uncut DNA was loaded as control.

Before transfecting to the cells, DNAs were cleaned up by Wizard sv Gel and PCR clean up system (Promega, # A9281) according to manufactures protocols.

7.2.1.14. Transfecting to mammalian cells:

24 hours before transfection, exponentially growing MCF-7cells were harvested by trypsinization and replated in 6-well tissue culture dishes and 2 mL growth medium was added to each well and were incubated for 24 hours. The cells should be 75% confluent at the time of transfection. For each 6 well plate of culture cells, 3 µg of plasmid DNA, 9 µL of transfast (Promega, # 2431) and 700 µL of opti MEM medium (Gibco, #11058021) were mixed in test tube and were incubated for 10-15 minutes in room temperature before adding to the cells. The cells were incubated for 1 hour in 37°C and after that 700 µL of growth medium was added to them and incubated for 18-20 hours. After the cells have been exposed to the DNA for appropriate time, they were washed with serum-free medium and observed under laser scanning microscope. After the cells had been incubated for 48-72 hours in complete medium, they were trypsinized and replated in the appropriate selective medium according to kill curve. This medium was changed every 2 days for 2-3 weeks to remove the debris of dead cells. After having around $5.0\times10^{6,}$ they were trypsinized and washed twice with PBS (Life technology, #10010-023) and resuspended in 3 mL PBS and were sorted by cell sorting machine (FACS Aria ,BD Biosciences). Cells were sorted and put each single cells in each well of 96 well plate filled with 100 µL growth medium with appropriate selective antibiotic G418 (Life technology, #11811031) and Zeocin (Invivogen, #ant-zn-1). The medium was changes 2-3 times per week. After the cells reached to 90% of confluency, they were trypsinized and put in a 12-well plate and later on in T-25 flask.

7.2.1.15. Kill Curve:

To generate a fully transfected population of cells it is essential to find out the optimal concentration of antibiotic required to eliminate non-transfected cells over specific days. Cells were plated with the density of 40% per 12 well plates and were incubated in the incubator overnight. Medium were replaced with different concentration of antibiotic and one well with normal media as a control. Cells were observed every day for 5 days in case of G418 and 15 days in case of Zeocin. The

minimum antibiotic concentration to use, is the lowest concentration that kills 100% of the cells.

7.2.2. Knockout construct:

7.2.2.1. DS red construct:

Preparation of plasmids: 6 pairs of oligos were designed in order to knockout GIRK1 splice variants specifically (shG1c, shG1d, shG1e) or generally GIRK1 and containing a unique ClaI restriction site for detection and cloned into the pSIREN_Retro Q_DsRed Express vector (Clontech, #632487).

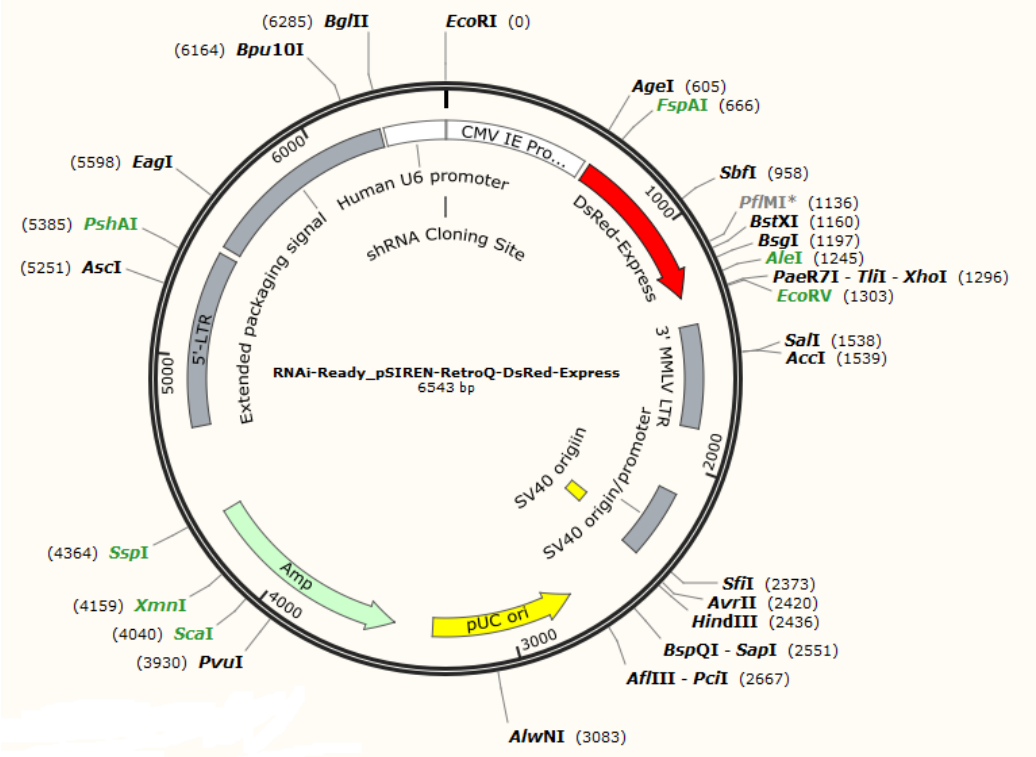

Figure 7.4: Map of RNAi-Ready_pSIREN-RetroQ-DsRed-Express vector. All the restriction enzymes in the map are 6 unique. Green restriction enzymes: Blunt end cutters. Black restriction enzymes: Sticky ends cutters. Grey restriction enzymes: blocked by Dcm methylation. (Created by snap gene program).

7.2.2.2. Knock out oligo sequence:

Sh-G1c#1 (from 3´UTR of exon 2 and we expect to knockout G1c specifically):

F:GATCCGACAGATATGCCATAAAGTTTTCAAGGAGAACTTTATGGCATCTGTTTTTTTATCGATG

R:AATTCATCGATAAAAAAACAGATATGCCATAAAGTTCTCCTTGAAAACTTTATGGCATATCTGTCG

Sh-G1e#1 (from 3´UTR of Exon 1):

F:GATCCGCTTCCCCACCGGGAGACCTTTTTCAAGAGAAGGTCTCCCGGTGGGGAAGTTTTTTATCGATG

R:TTAAGATCGATAAAAAACTTCCCCACCGGGAGACCTTCTCTTGAAAGGTCTCCCGGTGGGGAAGCG

Sh-G1a#1 (Exon 1):

F:GATCCGGATACATCACAGACAAGTGTTCAAGAGACACTTGTCTGTGATGTATCTTTTTTTATCGATG

R:TTAAGATCGATAAAAAAGATACATCACAGACAAGTGTCTCTTGAACACTTGTCTGTGATGTATCG

Sh-G1a#2: (exon1/ exon2 Interface):

F:GATCCGGCTCAAATCTCGGCAGACACTTCAAGAGAGTGTCTGCCGAGATTTGAGCTTTTTTTTATCGATG

R:TTAAGATCGATAAAAAAGCTCAAATCTCGGCAGACACTCTCTTGAAGTGTCTGCCGAGATTTGAGC

Sh-G1a#3 (exon 2/ exon 3 Interface):

F:GATCCGAACAACTGGGATGACTTGTTTCAAGAGAACAAGTCATCCCAGTTG TTTTTTTTATCGATG

R:TTAAGATCGATAAAAAAAACAACTGGGATGACTTGTTCTCTTGAAACAAGTC ATCCCAGTTGTTCG

Sh-G1d#1(Exon1/ Exon 3):

F:GATCCGCTGCTCAAAGGATGACTTTTCAAGAGAAAGTCATCCTTTGAGCAG CTTTTTTATCGATG

R:TTAAGATCGATAAAAAAGCTGCTCAAAGGATGACTTTCTCTTGAAAAGTCAT CCTTTGAGCAGCG

ShG1a #4:

F: GATCC G TCT GCA CTC CGA AGG AAA TTT TTCAAGAGA AGA CGT GAG GCT TCC TTT AAA TTTTTT ATCGAT G

R: AATTC ATCGAT AAAAAA TTT AAA GGA AGC CTC ACG TCT T CTC TTG AA AAATTT CCT TCG GAG TGC AGA CG

shG1a#5:

F: GATCC GGG GAC GAT TAT CAG GTA GTG A TTCAAGAGA CCC CTG CTA ATA GTC CAT CAC T TTTTTT ATCGAT G

R: AATTC ATCGAT AAAAAA AGTG ATG GAC TAT TAG CAG GGG TCTCTTGAA T CAC TAC CTG ATA ATC GTC CCC G

shG1a#6:

F: GATCC GTC GGT AAC TAC ACG CCT T TTCAAGAGA CAG CCA TTG ATG TGC GGA A TTTTTT ATCGAT G

R: AATTC ATCGAT AAAAAA TTCC GCA CAT CAA TGG CTG TCTCTTGAA AAGGCGT GTA GTT ACC GAC G

shG1a#1Sc:

F: GATCCG ATC CGGTAT AAG AGCACA A TTCAAGAGA TAG GCC ATA TTC TCG TGT T TTTTTT ATCGAT G

R: AATTC ATCGAT AAAAAA AACACGAGAATATGGCCTA TCTCTTGAA TTGT GCT CTTATA CCG GAT CG

7.2.2.3. Ligation, Transfection:

After ligation of oligos with the vector and transfecting into XL1-Blue E. Coli (as describe before), several clones were picked up and analyzed by restriction with ClaI. Midipreps were performed and sent for sequencing (using U6 forward sequencing primer: from the region 6188–6206 5'-GGGCAGGAAGAGGGCCTAT-3'. The construct with the correct sequences were transfected into MCF-7 wt and MCF-7 stably overexpressing hG1a, hG1d, hG1c, hG1e, MCF-7vec#9 (cell line expressing eYFP only). MCF-7 wt was used as control and for calibrating for quantification. Untransfected MCF-$7^{G1a\#6}$ were also used as control and calibration tool.

7.2.2.4. Confocal laser scanning microscopy:

Images were scanned using the HCX APO L U-V-I 20.0x0.50 W UV objective. Pinhole adjusted to 1 Airy unit for each fluorophore, respectively. 12 bit resolution, image size 512*512 pixel. At the beginning of every experimental day, gain and offset were adjusted and left constant for the entire experiment. eYFP was excited at 514nm (at the beginning at 488 nm, for comparison). Detection 540 nm – 570 nm. DsRed2 was excited at 543 nm and detected at 570 nm – 630 nm. For the determinantion of crosstalk between the two channels, images from MCF-7wt, transfected with the corresponding shRNA plasmid (=DsRed2 only) and from the non-transfected MCF-$7^{G1a\#6}$ cell line (=eYFP only) were obtained. The fluorecence

was measured in both channels using ImageJ (20 fluorescent cells and 5 background values per image) and correlated.

7.2.2.5. Bicistronic Knockout vector:

The second hG1a knochout vector was psiRNA-DUO Dual RNA PolIII Cassette Vector for the Expression of two shRNAs (invivogen, # ksirna4-gz3).This vector has EGFP sequence and in order to check the eYFP cells with LSM, eGFP was changed to eCFP by point mutation.

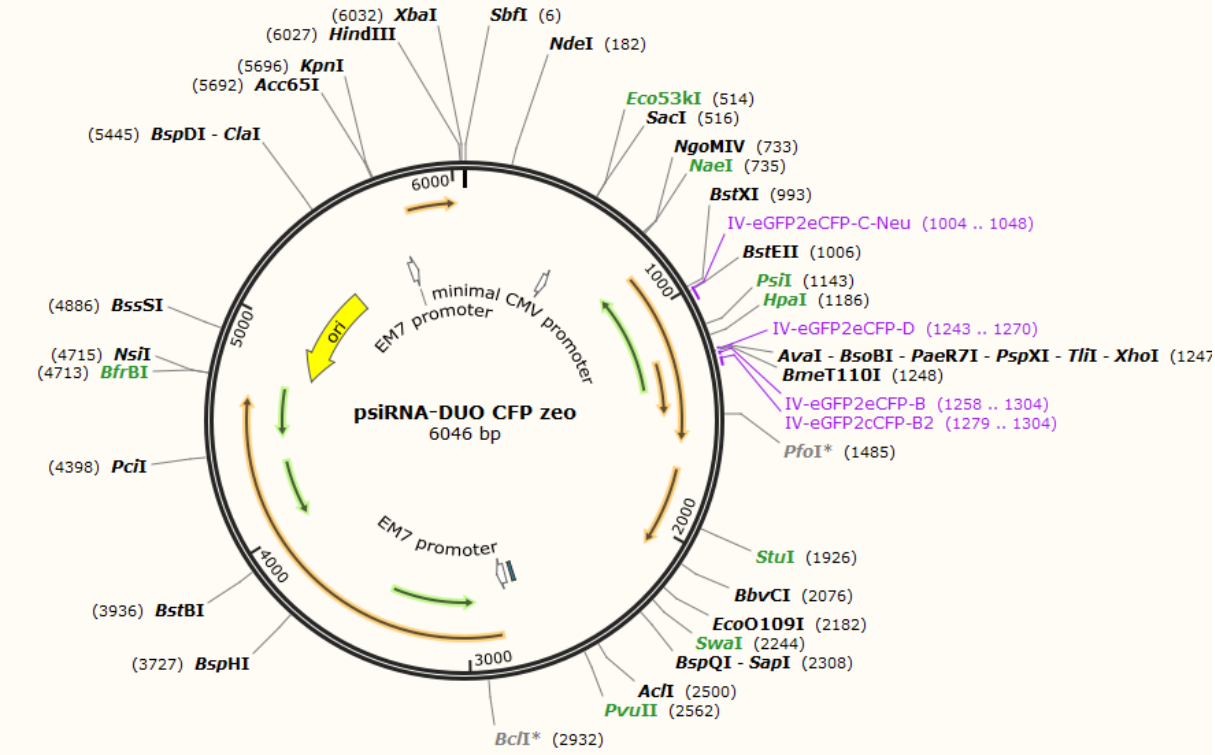

Figure 7.5: Map of DUO-CFPzeo vector. All the restriction enzymes in the map are 6 unique. Green restriction enzymes: Blunt end cutters. Black restriction enzymes: Sticky ends cutters. Grey restriction enzymes: blocked by Dcm methylation. Purple: position of primers for converting the GFP to CFP (Created by snap gene program).

7.2.2.6. Point Mutation primers (CFP to GFP):

IV-eGFP2eCFP-C-Neu-f:
CTGGTGACCACCCTGACTTGGGGGGTCCAATGTTTCAGCAGATAC

IV-eGFP2eCFP-C-Neu-r:
GTATCTGCTGAAACATTGGACCCCCCAAGTCAGGGTGGTCACCAG

IV-eGFP2eCFP-D-f:CAAGCTCGAGTACAACTATATTTCTCAC

IV-eGFP2eCFP-D-r:GTGAGAAATATAGTTGTACTCGAGCTTG

IV-eGFP2eCFP-B2-f:CATTACGGCAGATAAGCAGAAGAATG

IV-eGFP2eCFP-B2-r:CATTCTGCTTATCTGCCGTAATG

IV-eGFP2eCFP-B-f:
CTATATTTCTCACAATGTTTACATTAGGGCCGATAAGCAGAAGAATG

IV-eGFP2eCFPB-
r:CATTCTTCTGCTTATGGGCCGTAATGTAAACAT,TGTGAGAAATATAG

7.2.2.7. Primers for sequencing:

IV-eGFP2eCFP-C-Neu-f:
CTGGTGACCACCCTGACTTGGGGGGTCCAATGTTTCAGCAGATAC

IV-eGFP2eCFP-B-
r:CATTCTTCTGCTTATGGGCCGTAATGTAAACAT,TGTGAGAAATATAG

7.2.2.8. Sequence of the knockout oligoes for psiRNA-DUO Dual eCFP zeo:

P^{SI}_hG1A

ShG1a #1

F: GTACC GAT ACA TCA CAG ACA AGT G TTC AAG AGA CAC TTG TCT GTG ATG TAT CTT TTT T GTCGAC A

R: AGCTT GTCGAC A AAA AAG ATA CAT CAC AGA CAA GTG TCT CTT GAA CAC TTG TCT GTG ATG TATC G

shG1a #5

F: ACCTGGG GAC GAT TAT CAG GTA GTG A TTCAAGAGA T CAC TAC CTG ATA ATC GTC CCC TTTTTT GTCGAC

R: CAAA GTCGAC AAAAAA GGG GAC GAT TAT CAG GTA GTG A TCTCTTGAA T CAC TAC CTG ATA ATC GTC CCC

P^{SI}_hG1scA

shG1a#1Sc

F: GTACC G ATC CGG TAT AAG AGC ACA A TTCAAGAGA TTG TGC TCT TAT ACC GGA T TTTTTT GTCGAC A

R: : AGCTT GTCGAC AAAAAA ATC CGG TAT AAG AGC ACA A TCTCTTGAA TTG TGC TCT TAT ACC GGA T C G

shG1a #2sc

F: ACCT G CAC CAG CTT CAA TGA GGA CC TTCAAGAGA GG TCC TCA TTG AAG CTG GTG TTTTTT GTCGAC

R: CAAA GTCGAC AAAAAA CAC CAG CTT CAA TGA GGA CC TCTCTTGAA GG TCC TCA TTG AAG CTG GTG C

After electroporation to XL1 bacteria and doing midipreps, constructs were sent for sequencing and then transfected to MCF-7 cells with appropriate amount of Zeocin. Cells were sorted and several colons were selected and frozen for further analyzing.

7.3. Characterization of the cell lines:

7.3.1 Confocal laser scanning microscopy:

Cells were cultured on 15mm glass plates (ROTH, #004710281) and scanned after 48 hours in MEM medium using a Leica inverted microscope with a laser-scanning module attached (DMIRE2 and TCS SL2; Leica Microsystems, Heidelberg, Germany). Cells were observed by the 20X and 63 X water immersion objectives and 12-bit resolution. Filter settings for eCFP excitation and detection were 458 nm and 477-500nm, and for eYFP were 514 nm and 540-570nm respectively.

7.3.2. Real time PCR:

7.3.2.1. Harvesting of cell pellets:

Cells were cultures in 6 well plates, As soon as they reached to 80% confluency, cells were trypsinzed and washed twice with PBS and were shock frozen in liquid nitrogen. Cell pellets were kept in -70°C for further experiments.

7.3.2.2. RNA isolation:

For purification of total RNA from the cells, the QIA shredder spin column (Qiagen, #79645) and RNeasy Mini Kit (Qiagen, #74104) were used. extracting the RNA was done according to manufacturers protocol. Concentration of the extracted RNA was measured by Nanodrop and 1µg of RNA were converted to cDNA.

7.3.2.3. Converting the RNA to cDNA:

For having cDNA ,QuantiTect Rev. Transcription kit (Qiagen , #205311) was used and 1µg of RNA was converted to cDNA according to manufacturers protocol. This cDNA was diluted 1:25 and was used for Real time PCR.

7.3.2.4. Primers for qPCR:

For qPCR QuantiTect SYBR® Green PCR Kits (Qiagen, #204143) was used.

GAPDH, f: 5′-ATGGGGAAGGTGAAGGTCG-3′;
GAPDH, r: 5′-GGGGTCATTGATGGCAACAATA-3′

GIRK1a ,f: 5′-GTGGAAACAACTGGGATGAC-3′
GIRK1a ,r 5′-GTTGCATGGAACTGGGAGTA-3′

GIRK1c, f: 5′- CAAGCTGCTCAAATCTCGGC-3′
GIRK1c, r: 5′-AGTTGATCTGCCCCTGTACT-3′

GIRK1d, f: 5′-CAAGCTGCTCAAAGGATGAC-3′
GIRK1d, r: 5′-GTTGCATGGAACTGGGAGTA-3′

7.3.2.5. Protocol for qPCR:

CYBR green	5µL
Forward primer 10pmol/mL	1µL
Reverse primer 10pmol/mL	1µL
cDNA 1/25	3 µL

The above materials were mixed in Light Cycler 480 Multiwell plates 96 white (Roche, #04729692001), covered and centrifuged shortly. To control for possible contamination of the PCR reagents, negative control PCRs for each primer pairs

were prepared whereby the first strand cDNA template was replaced with nuclease-free water. PCR reactions were carried out on a LightCycler 480 system (40 cycles; Roche Diagnostics GmbH)(28). Relative mRNA expression levels of G1a, G1c and G1d gene compared to the housekeeping gene (GAPDH) were calculated using $2^{\Delta\,\Delta Ct}$ (29).

7.3.3. Western blot:

7.3.3. 1.Preparation of cell lysate:

For preparation of protein lysate from cell lines, adherent cells were trypsinzed and were washed three times with PBS. The PBS was aspirated and 100-400 µL (volume depends on pellet size) ice cold Ripa buffer (Thermo scientific, #89901) and protease inhibitor cocktail (sigma, #P8340)(1µL per 100 µL lysis buffer) was added to the cell pellet. Cell pellets were put on ice for 20 minutes and vortexed. The lysates were sonicated (2 cycles, 10 seconds on and 30 seconds off, amplitude 20%) on ice and centrifuged in a pre-cooled Eppendorf centrifuge (13000 rpm, 4°C, 20 minutes) to remove the debris. Supernatants were stored at -20°C until use. Protein concentrations were determined by BCA assay according to manufactures protocol. (Thermo scientific, # 23225). Lysis buffer was considered as blank.

7.3.3. 2. Electrophoresis and Blotting :

50 µg of protein were mixed 1:5 with 5X Laemmli sample buffer containing 10% SDS (Promega, #H5113), 300 mM Tris-HCl (pH: 6.8), 25% glycerol (Sigma, #G5516), traces of bromphenol blue (Merck, #1081220005) and 5% β-mercaptoethanol (Sigma, #M3148). The samples were boiled for 5 minutes and then separated on 8% resolving gel with a 4% stacking gel under reducing condition at 80V for 20 minutes and then 120V. The gels were transferred to the nitrocellulose membranes (Amersham GE healthcare, # RPN203D) for 1.5 hours (150mA, on ice). The membranes were stained with Ponceau S solution (Sigma, #P7170) to check the protein transfer and blocked 1 hours with with PBST (PBS 0.05% Tween, Merck, #8221840500) containing 5% non-fat dry milk (Bio-Rad,

#170-6404) in room temperature on shaker. After washing once with PBST, membranes were probed with anti GIRK1 antibody (abcam, #119246) at the dilutions of 1/1000 in PBST containing 1% non-fat dry milk overnight at 4°C on a shaker. The membranes were then washed 3 times with PBST each 10 minutes. Membranes were consequently incubated with peroxidase-conjugated sheep anti-mouse (Kindly provided by Dr.AH.Zarnani) at a dilution of 1:4000 for 1 hour at room temperature on a shaker. The membranes were then washed 3 times with PBST with 10 minutes intervals. The resulting signal was visualized using ECL select Detection kit (Amrsham GE healthcare, #RPN2235) according to the manufacturer's instruction.

7.3.4. Immunohistochemistry:

Cells were fixed in NBF, embedded in agarose gel (7%) and then processed for paraffin embedding. Target retrieval solution (pH: 9.0; Dako, #S236884) heated for 40 min at 150 W in a microwave was used for antigen retrieval. Slides were then washed in washing buffer (Dako, #S3006) and incubated with a monoclonal antibody against GIRK1 (Abcam, #119246). For visualization, the EnVision+ dual link reagent (rabbit/mouse horse radish peroxidase, #K406311) was used according to manufacturer's protocols. Signals were developed by incubation of sections with diaminobenzidine (Dako, #K406511) as a chromogenic substrate. Slides were then washed in Dako wash buffer, counterstained with Meyer's hematoxylin, rinsed in tap water, dehydrated and mounted with Entellan.

4.4. Vital parameters:

4.4.1. Invasion assay:

Corning® BioCoat™ Matrigel® Invasion Chambers (Corning, #354480) was taken from -20°C storage and allowed to come to room temperature. Warm (37°C) MEM was added to the interior of the inserts and bottom of wells and allowed to rehydrate for 2 hours in humidified tissue culture incubator, 37°C, 5% CO2 atmosphere. After rehydration, the medium was removed without disturbing the

layer of Matrigel™ Matrix on the membrane. $1.25x10^5$ cells/mL for 6-well chambers were prepared in 2 mL MEM without any FBS and put on the upper compartment of Matrigel and MEM with 5% FBS as chemoattractant to the lower compartment of Matrigel. The Matrigel Invasion Chamber was incubated for 24 hours in a humidified tissue culture incubator, at 37°C, 5% CO2 atmosphere. After incubation, the non-invading cells were removed from the upper surface of the membrane by "scrubbing". Cotton tipped swab was inserted into the Matrigel and applied with gentle but firm pressure while moving the tip over the membrane surface. For staining the cells, membrane beneath the insert was cut carefully using scalpel, fixed with ice cold 100% methanol for 5 min and let them dry for 5 min, then stained with 0.1% crystal violet (Sigma, #C0775) for 5 min and finally washed with distilled water to remove excess stain. The membrane was allowed to air dry and put on a slide and mounted with mounting glue (Sigma, #03989) and cover slipped, Invading cells were then counted under microscope.

4.4.2. Adhesion assay:

Cells were removed by trypsin/ EDTA, 2.5×10^4 cells were plated into each well of Corning® BioCoat™ Fibronectin 96 Well Clear Flat Bottom (Corning, #354409). 150 min later, non adherent cells were removed by washing three times with PBS. Adherent cells were fixed for 30 min with 2% formaldehyde (Merck, #k36542103-637) in PBS, air dried, stained for 30 min with 0.1% crystal violet in PBS, washed three times in water, and cells were air dried. Bound dye was solubilized with 10% acetic acid (Merck, #k31668363-304) and absorbance was measured at 550 nm. Cell-free wells were run with each experiment and served as blanks. All the experiments were performed in triplicates.

4.4.3. Wound healing assay:

Cells were plated into the 24 well plates (BD, #353847) to create a confluent monolayer. The dishes were properly incubated for approximately 24 h at 37°C, allowing the cells to adhere and spread on the substrate completely. The cell monolayer was scratched in a straight line with a p200 pipet tip. Debris were removed by washing the cells with 1 mL of the growth medium and then replaced with 2 mL of medium for the in vitro scratch assay (30). The plate was put in cell

observer (Zeiss Axiovert 200M) and monitored for 72 hours with 1 hour interval. For analyzing the data, ImageJ software and ALGov4 Macro which was written by Dr.Trevor Devaney were used.

4.4.4. Cell Motility assay:

5.10^4 cells per well in 24 well plates (BD, #353847) were seeded and put in cell culture incubator for 24 hours. Subsequently single cell motility properties were studied with the cell observer (Zeiss, Axiovert 200M) by following cell migration for 72 hours with 20 min intervals. For analysis, 5 single cells in each field of microscope were tracked and ImageJ software (v1.47; Wayne Rasband, NIH, http:// imageJ.NIH.gov/) was used (Time interval was 20 min and xy calibration was 1µm)(28, 31).

4.4.5. Proliferation assay (BrdU assay):

2.10^5 cells were plated in 6 well plates and incubated in cell culture incubator. After reaching to 80% confluency (Logarithmic phase) labeling was done by adding 10µL of BrdU solution, 1 mM BrdU in DPBS (Lonza, # BE17-512F) directly to each mL of tissue culture media. The treated MCF-7 cells were then incubated for 3 hours in cell culture incubator and test was done according to manufacturers protocols (APC BrdU flow kit BD, #552598).

4.4.6. Angiogenesis assay (Chick Chorioallantoic Membrane assay:

Fertilized white leghorn chicken eggs were purchased from a local hatchery (Schropper GmbH, Gloggnitz, Austria) and incubated at 37.6°C and 70% humidity. On the third day of chicken embryo development, the eggshell was cracked and the embryo was then decanted in to a sterile dish and incubation was continued as above. On day 10 of cultivation, $1x10^6$ cells in 10 µL PBS mixed with equal volume of Matrigel® (BD Biosciences, #356237) were then carefully applied on vascular branches of the CAM within sterile silicon rings of 5 mm diameter. Tumor was allowed to grow for 4 days followed by excision of tumor with the surrounding CAM. The intensity of the angiogenic response was analyzed under a stereomicroscope(32).

8. Results:

8.1. Overexpression of single fusion proteins:

8.1.1. pEYFPN1 based constructs:

A 6229 bp pEYFPN1-hG1a was constructed by inserting hG1a, using XhoI and EcoRI (Figure 8.1.a).Two bands were shown after cutting the constructs with XhoI and EcoRI (hG1a: 1512 bp) (pEYFPN1 vector 4717bp). A single band (6229 bp) was observed after cutting the construct by AseI for linearization purposes (Figure 8.1.b). In another construct using the same vector, a different insert resulted in 5660 bp pEYFPN1-hG1c (Figure 8.1.c). When construct cut by XhoI and EcoRI, bands of 4714 bp (Vector) and 933 bp (hG1c) were observed. AseI was used for linearization for stable transfection purposes and a single band in 5660 bp was observed (Figure 8.1.d).

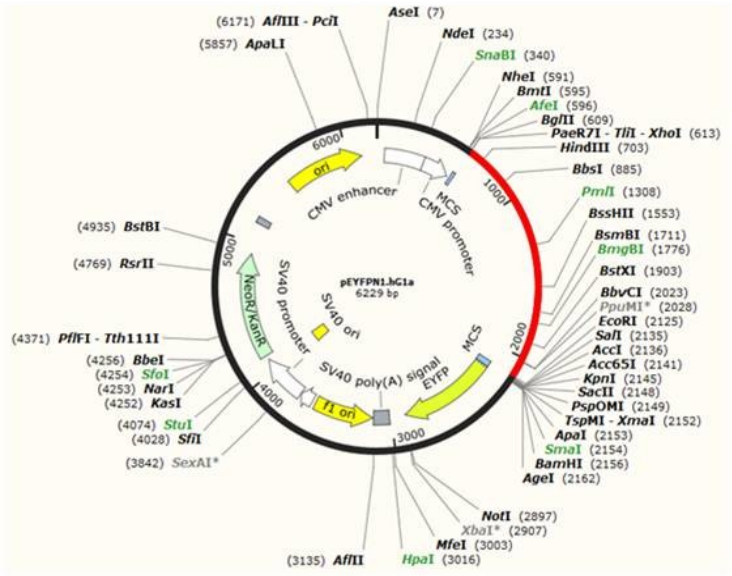

Figure 8.1.a

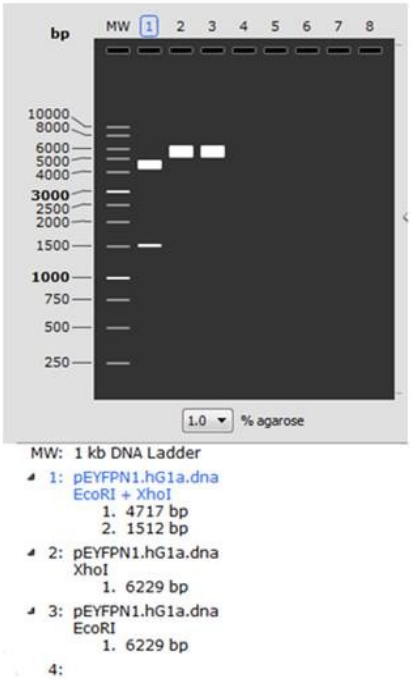

Figure 8.1.b

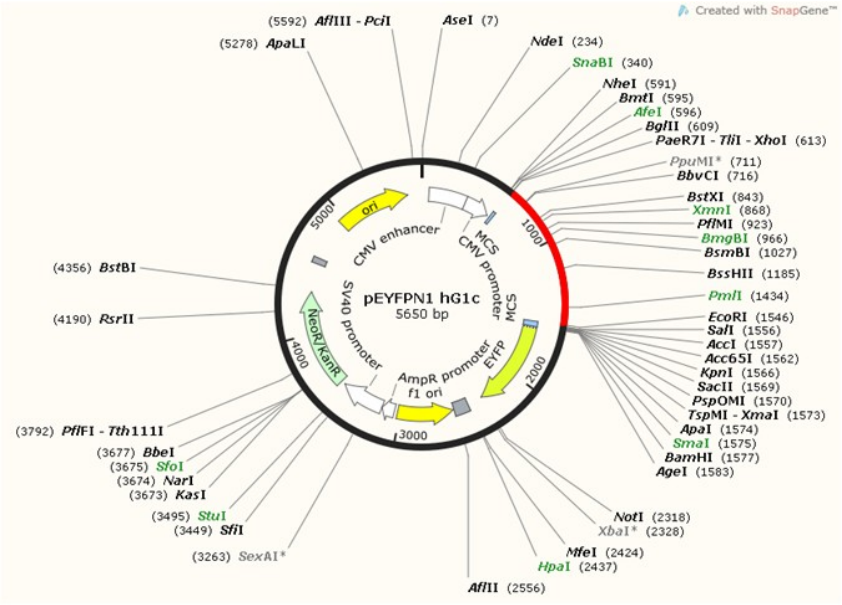

Figure 8.1.c

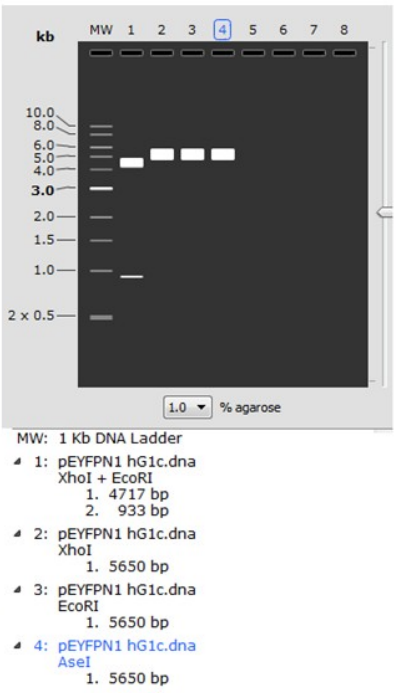

Figure 8.1.d

Figure 8.1: pEYFPN1 constructs. Figure 8.1.a: Map of the pEYFPN1-hG1a construct. all the REs in the map are 6 unique cutters. Green RE: Blunt end cutters . Black RE: Sticky ends cutters. Grey RE: blocked by Dcm methylation. Figure 8.1.b: Schematic bands of DNA construct on 1% Agarose gel. Checked by 1kb DNA Ladder. First lane: pEYFPN1-hG1a DNA was cut with EcoRI and XhoI. Second lane: DNA cut with EcoRI. Third lane: DNA cut with XhoI. Forth lane: DNA cut with AseI for linearization. Figure 8.1.c: Map of the pEYFPN1-hG1c construct. Figure 8.1.d: Schematic bands of DNA construct (pEYFPN1-hG1c) on 1% agarose gel. Checked by 1kb DNA Ladder. First lane: pEYFPN1-hG1c DNA cut with EcoRI and XhoI. Second lane: DNA cut with only EcoRI. Third lane: DNA cut with XhoI. Forth lane: DNA cut with AseI for linearization (created by snap gene program).

8.1.2. pEYFPC1 based constructs:

To create a 6227 bp pEYFPC1-hG1a, G1a was cloned by XhoI and EcoRI. (Figure 8.2.a) The results were a band of 4715bp for the vector and a 1512 bp band for the hG1a while digesting with XhoI and EcoRI. To have a stable transfected cells, AseI restriction enzyme was used (Figure 8.2.b). hG1d was cloned by XhoI and EcoRI and resulted in 5424bp pEYFPC1-hG1d (Figure 8.2.c). When these two REs are digesting the construct, a band of 4717 bp (the cloning vector) and 933 bp (hG1d) was observed. AseI RE was used here as well for linearization (Figure 8.2.d).

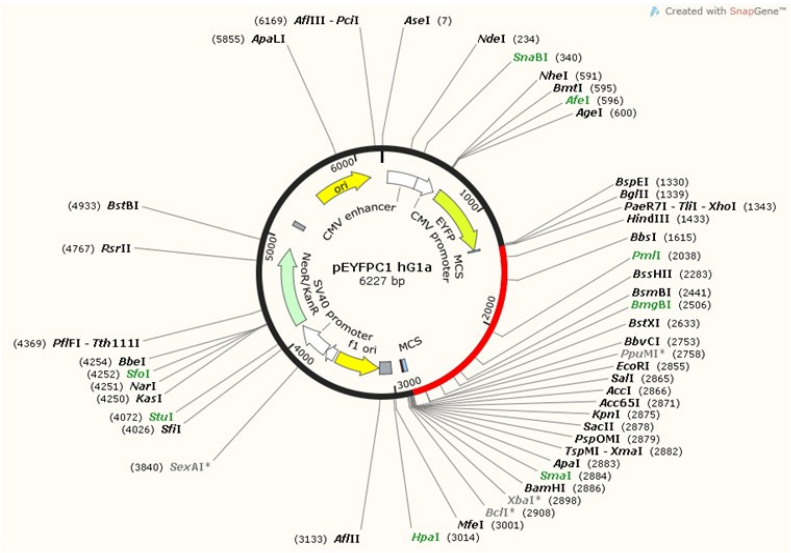

Figure 8.2.a

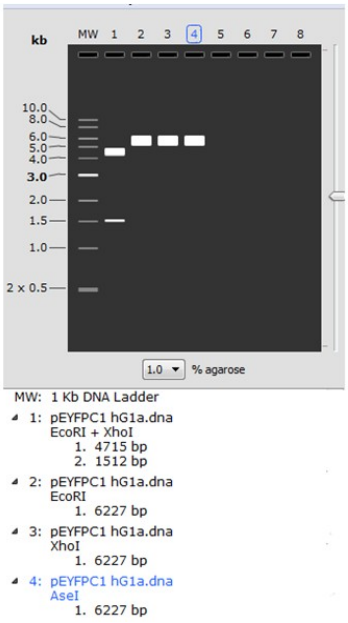

Figure 8.2.b

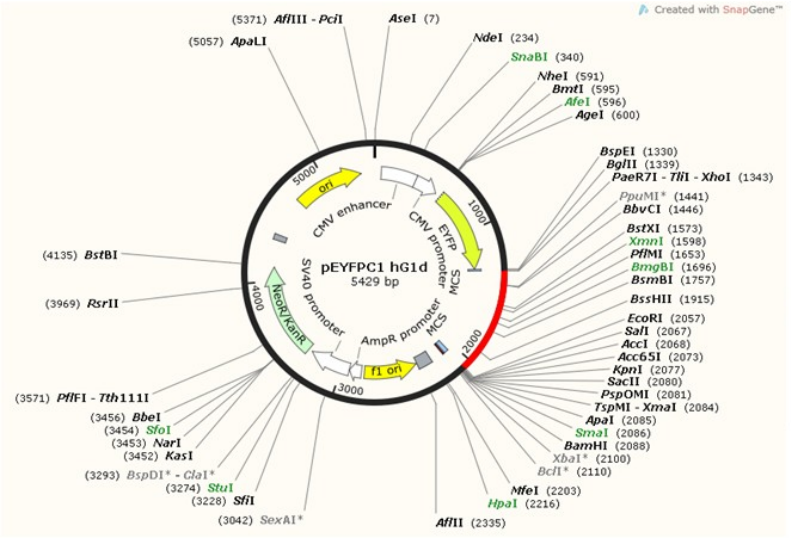

Figure 8.2.c

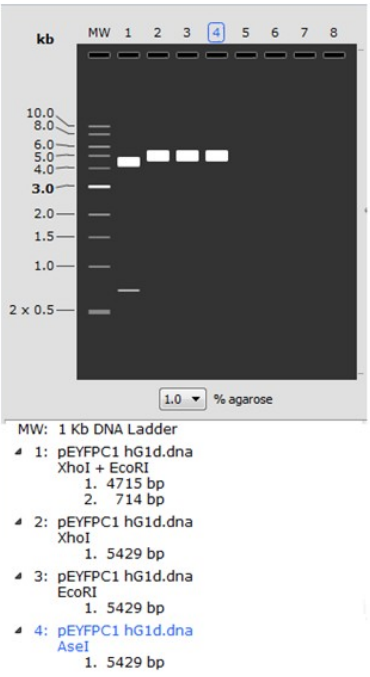

Figure 8.2.d

Figure 8.2: pEYFPC1 constructs. Figure 8.2.a: The map of the pEYFPC1-hG1a construct. all the REs in the map are 6 unique cutters. Green RE: Blunt end cutters. Black RE: Sticky ends cutters. Grey RE: blocked by Dcm methylation. Figure 8.2.b: Schematic bands of DNA construct on 1% agarose gel. Checked by 1kb DNA Ladder. Lane 1: pEYFPC1 hG1a DNA cut with EcoRI and XhoI. lane 2 is DNA cut with EcoRI. lane 3 is DNA cut with XhoI. Lane 4 is DNA cut with AseI for linearization. Figure 8.2.c: The map of the pEYFPC1-hG1d construct. Figure 8.2.d: Schematic bands of DNA construct (pEYFPC1-hG1d) on 1% agarose gel. Checked

by 1kb DNA Ladder. Lane 1: pEYFPC1-hG1d DNA cut with EcoRI and XhoI. Lane 2 is DNA cut with EcoRI. Lane 3 is DNA cut with XhoI. Lane 4 is DNA cut with AseI for linearization. (Created by snap gene program).

8.1.3. PIRES2-EGFP based construct:

A 6779 bp PIRES2-EGFP-hG1a was constructed by inserting hG1a, by using BamHI and NheI (Figure 8.3.a). The bicistronic vector PIRES2 EGFP which digested with BamHI and NheI, ligated to PCR products, which then was transformed into XL1 bacteria. Positive clones were checked and the DNA was sent for sequencing. When PIRES2 EGFP-hG1a digested with BamHI and NheI, a band of 5239 bp for the cloning vector and a band of 1540 bp for the hG1a were observed. AseI RE was used, here as well, for linearization (Figure 8.3.b).

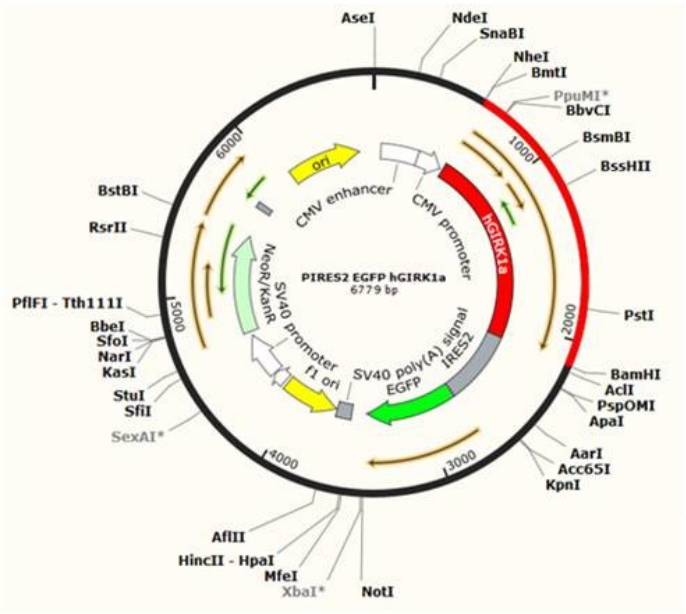

Figure 8.3.a

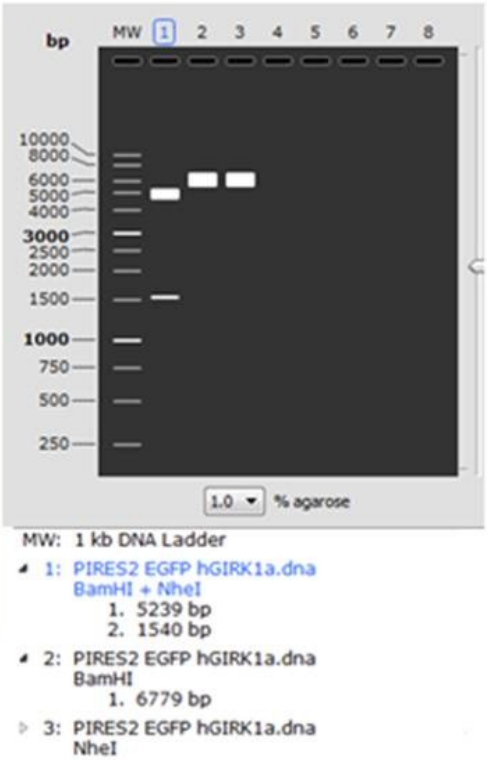

Figure 8.3.b

Figure 8.3: PIRES2 EGFP-hG1a construct: Figure 8.3.a: Map of PIRES2 EGFP hG1a construct. All the REs in the map are 6 unique cutters. Green RE: Blunt end cutters. Black RE: Sticky ends cutters. Grey RE: blocked by Dcm methylation. Figure 8.3.b: Schematic bands of the construct after digesting with REs. Lane

1:PIRES2 EGFP-hG1a cut with BamHI and NheI. Lane 2: PIRES2 EGFP-hG1a cut with BamHI. Lane3: DNA cut with NheI (created by snap gene program

8.2. Knockout constructs:

Nine pairs of oligos were designed to knockout GIRK1 splice variants. They were shG1c, shG1d, shG1e and GIRK1 (shG1a#1_6). For control procedures shG1a#1sc and shG1a#5sc were designed. The oligos, which contained a unique ClaI restriction site for size detection, were cloned into the pSIREN-RetroQ – DsRed Express Vector. shG1a#1, shG1a#4, shG1a#5 and shG1a#6 were selected as Exon1, which had 100% homology with G1a, G1c, G1d and G1e. shG1a#2 was selected from exon 1→exone 2 linker because it has 100% homology with G1a1 and G1c but it has only 54% homology with G1d and G1e. shG1a#3 was selected from exon 2→exone 3 linker because of its specific. The homology percentage with variants: G1a (100%), G1d (53%), G1c (47%) and G1e (21%). The homology percentages of shG1c with variants were as followed: G1a (53%), G1c (53%), G1d (53%) and G1e (53%). shG1d was taken from E1→E3 linker therefore the homology percentage with the variants were: G1d (100%), G1a (53%), G1e (53%) and G1c (53%). Followed the ligation of oligos with the vector and transfection into XL1 Blue Ecoli bacteria, five clones were chosen and analyzed for restriction analyzing with ClaI. Midipreps were performed and selected DNAs were sent for sequencing using U6 primer. All shG1a#1, shG1a#2, shG1a#3, shG1c and shG1d functioned normally (as indicated by DsRed expression) and tested for their efficiency to knockout GIRK1 variants, although shG1e#1 failed to produce detectable DsRed fluorescence.

8.2.1. Quantitative Confocal LSM:

Images were scanned using the HCX APO L U-V-I 20.0x0.50 W UV objective. Pinhole adjusted to 1 Airy unit for each fluorophore, respectively. A 12-bit resolution was set with image size 512*512 pixel. Gain and offset were adjusted but only at the beginning of each experiment. eYFP was excited at 514nm

(although initially set at the at 488 nm, for comparison purposes and detected within 540 nm – 570 nm. DsRed2 was excited at 543 nm and detected at 570 nm – 630 nm. To determine the crosstalk and bleeding through channels, images from MCF-7wt were obtained, transfected with the corresponding shRNA plasmid (=DsRed2 only) and the non-transfected MCF-7G1a#6 cell line (=eYFP only). The fluorescence was measured in both channels using ImageJ (20 fluorescent cells and 5 background values per image) and results were correlated.

8.2.2. Image analysis:

Using ImageJ cursor tool, 10 cells were chosen which express both eYFP and DsRed. Then 10 more cells were picked which expressed eYFP only. Moreover 5 locations were selected which never had any cells in it (for background correction). The fluorescence intensity was measured at all those 25 positions in both DsRed and eYFP channels. After the average background was deducted, the eYFP only cells were calculated and normalized to 100%. The eYFP fluorescence of both the cells expressing exclusively eYFP and the ones expressing eYFP/DsRed were calculated in percentage term and were given ± SEM (Table 8.1) Figures 8.4 and 8.5). Results showed that the most efficient shRNAs were those, which could silence G1a; therefore, shG1a#1 and shG1a#5 were chosen. (Figure 8.6). Bicstronic psiRNA-DUO-CFPzeo vector was used to express 2 shRNAs therefore shG1a#1 and shG1a#5 were cloned in it (p^{SI}_hG1a_A) (Figure 8.7.a). As a control construct, shG1a#1Sc and shG1a#5Sc were cloned into the same vector, p^{SI}_hG1aSc_B (Figure 8.7.b). The efficiencies of these constructs were checked by MCF-7^{GIRK1a} cells .The result showed that the final construct is able to silence the GIRK1a gene as much as 50% (Figure 8.8). We conclude that this efficiency is not good enough to continue. At the moment CRISPR/cas9 knockout model is running for silencing GIRK1a.

Table 8.1: Efficiency of the oligos. Table 8.1.a: Efficiency of the oligos after 24 hours of transfection. According to the results ShG1a#1 was the most effective oligos and ShG1d was the least effective one. Table 8.1.b: Efficiency of the oligos after 48 hours of transfection. The results revealed that after 48 hour of transfection the efficiency of some oligos such as shG1a#1 increased for MCF-7 GIRK1a cells and not for all. Results also showed that most of the oligos could be more efficient after 24h. 7

Table 8.1.a

	ShG1a#1	ShG1a#2	ShG1a#3	ShG1c	ShG1d
G1a#6	24.6	29.1	30.9	34.2	56.8
G1c#4	23.8	27.7	69.3	79.4	57.9
G1d#7	-0.3	6.7	25.7	17.8	20.9
G1e#9	28.5	27.1	51.7	100.1	27.4
Vector#9	82.1		65.6	98.5	74.3

Table 8.1.b

	ShG1a#1	ShG1a#2	ShG1a#3	ShG1c	ShG1d
G1a#6	9.6	32.3	50.3	60.1	53.7
G1c#4	31.6	59.5	73.1	69.3	76.7
G1d#7	6.2	13.7	14.4	42.8	24.9
G1e#9	37.1	22.7	82.5	89.8	68.4
Vector#9	74.3		90.0	111.2	90.0

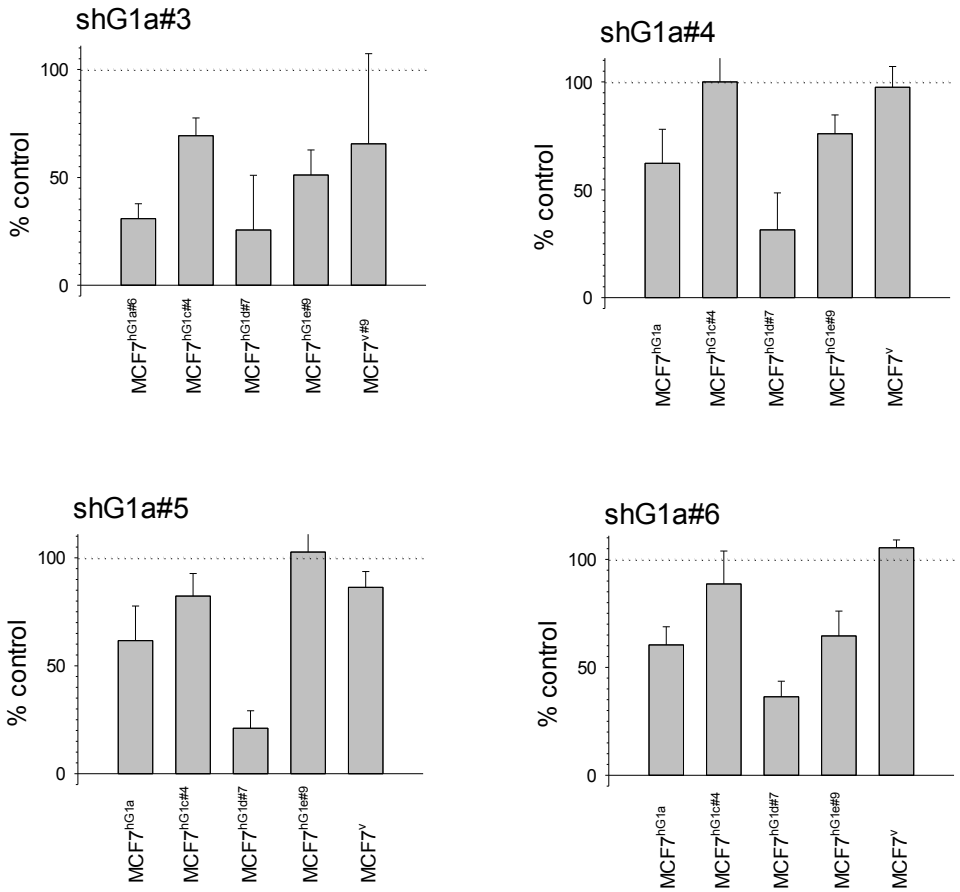

Figure 8.4: Efficiency of the ShG1a oligos tested on MCF-7 cells overexpressing hG1a, vector and splice variants. Figure 8.4.a: Efficiency of ShG1a#1: (24h&48h pooled): G1d (3%), G1a (17%), G1c (28%), G1e (33%), vector (78%) (The most effective oligo). Figure 8.4.b: Efficiency of ShG1a#2: (24h&48h pooled):

G1d (14%), G1e (23%), G1a (33%), G1c (60%) (Data for vector are not available!). Figure 8.4.c: Efficiency of ShG1a#3: (24h&48h pooled G1d (20%), G1a (41%), G1e (67%), G1c (71%), vector (78%). Figure 8.4.d: Efficiency of ShG1a#4: G1d (40%), G1a (60%), G1e (75%), G1c (100%), vector (98%).Figure 8.4.e: Efficiency of ShG1a#5: G1d (20%), G1a (60%), G1e (100%), G1c (85%), vector (90%). Figure 8.4.f: Efficiency of ShG1a#6: G1d (40%), G1a (60%), G1e (65%), G1c (90%), vector (100%).

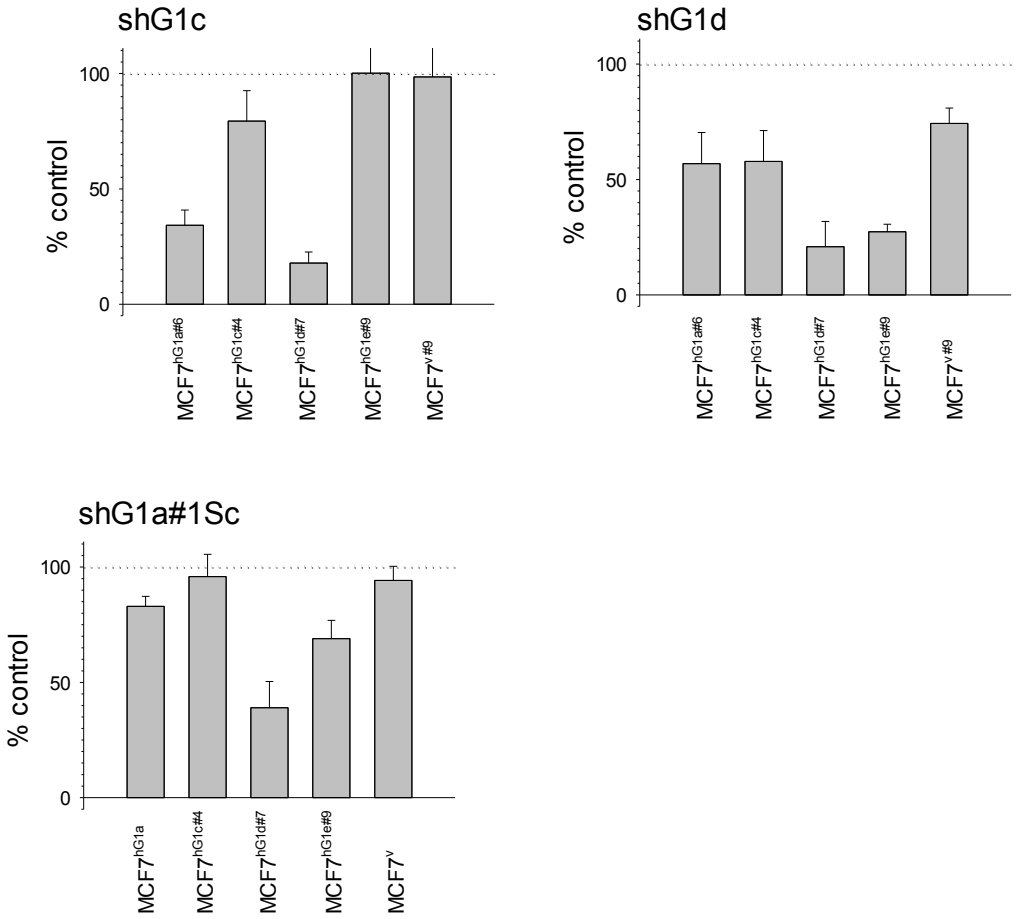

Figure 8.5: Efficiency of the ShG1c, d, and 1Sc oligos tested on MCF-7 cells expressing hG1a, vector and splice variants. Figure 8.5.a: Efficiency of ShG1c: (24h&48h pooled): G1d (30%), G1a (47%), G1c (74%), G1e (95%),vector (105%). Figure 8.5.b: Efficiency of ShG1d: (24h&48h pooled Efficiency (24h&48h pooled): G1d (23%), G1e (47%), G1a (55%), G1c (67%), vector (82%). Figure 8.5.c: Efficiency of ShG1sc: G1d (40 %), G1a (83%), G1e (70%), G1c (96%), vector (94%).

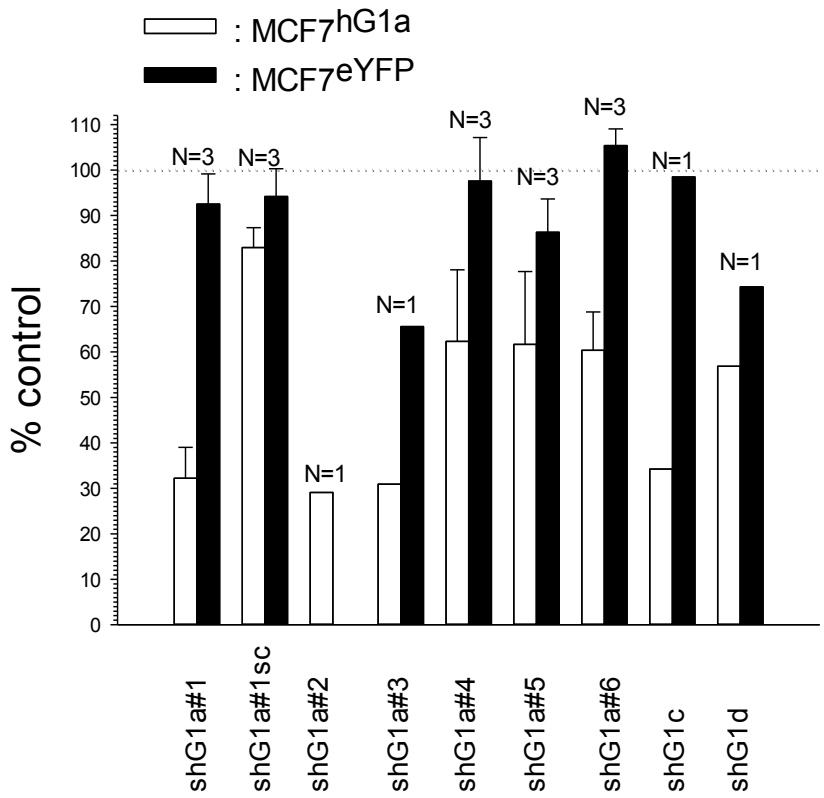

Figure 8.6: Overall efficiency of the oligos. Efficiency of all the oligos tested on MCF-7^{GIRK1a} and MCF-7eYFP (control), the most efficient ones shG1a#1 and shG1a#5 were selected for the Bicstronic psiRNA-DUO-CFPzeo vector.

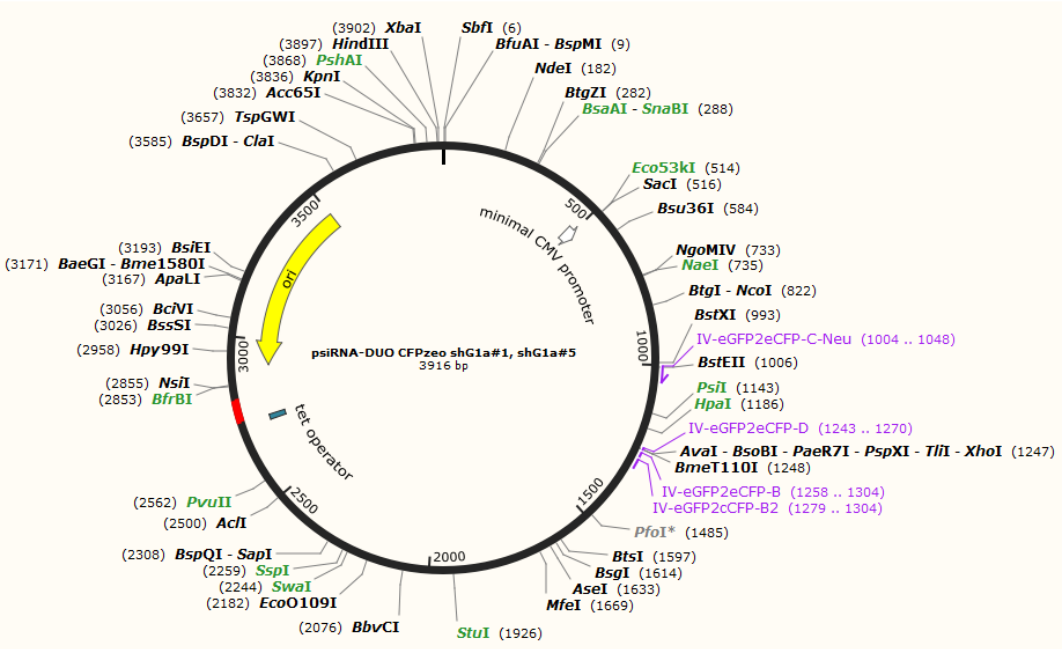

Figure 8.7.a

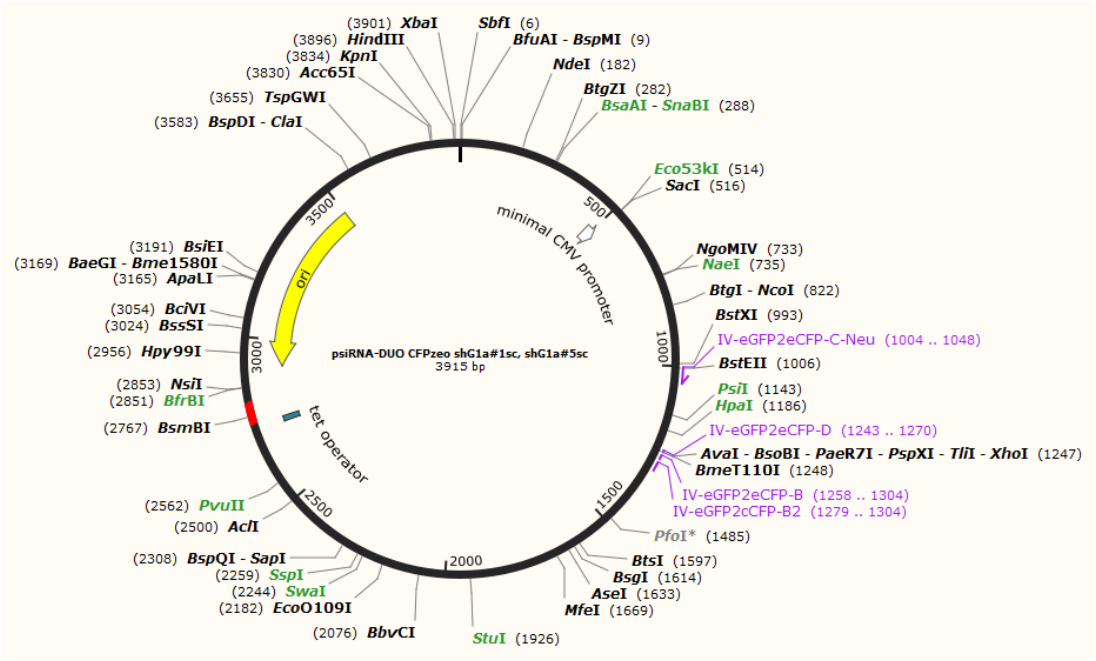

Figure 8.7.b

Figure 8.7: Map of Knockout construct: 8.7.a: map of ko construct psiRNA-DUO-CFP zeo shG1a#1, shG1a#5, it is 3916 bp. 8.7.b: map of control construct psiRNA-DUO-CFP zeo shG1a#1Sc, shG1a#5Sc, it is 3915 bp. all the RE enzymes are unique cutters. Blacks are sticky end cutters and greens are blunt end cutters. Purples are the location of primers for changing the vector from GFP to CFP. (Created by snap gene program).

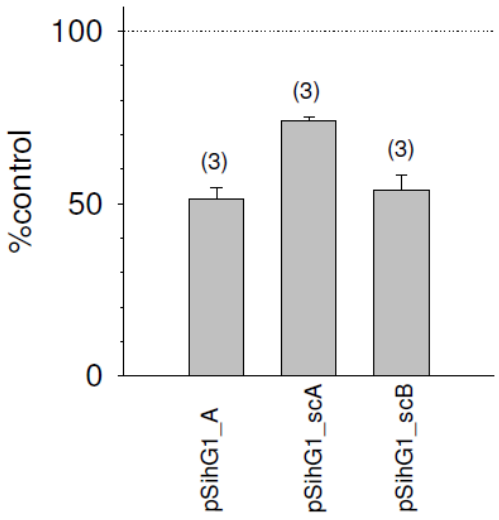

Figure 8.8: Final efficiency of the constructs. pSIhG1a_A could knockout the GIRK for 50%, and as a control pSIhG1a_scA was selected.

8.3. Generation of cell lines

8.3.1. Kill curve test:

The first step to generate stable cell line is to determine the optimal antibiotic concentration level. Therefore, a kill curve test was performed; the MCF-7 cells subjected to gradually increased level of G418 or Zeocin to determine the minimum antibiotic concentration level required killing all cells in 7-15 days. The most effective concentration level of Zeocin to stabilize MCF-7 transfected cells was determine to be 15 µg/µL. The calculated number was obtained on the 15th days (Figure 8.9). Kill curve test of G418 for MCF-7 was performed by Brigit Niesner and Stefanie Furtinger. Their reported number was 3 mg/mL.

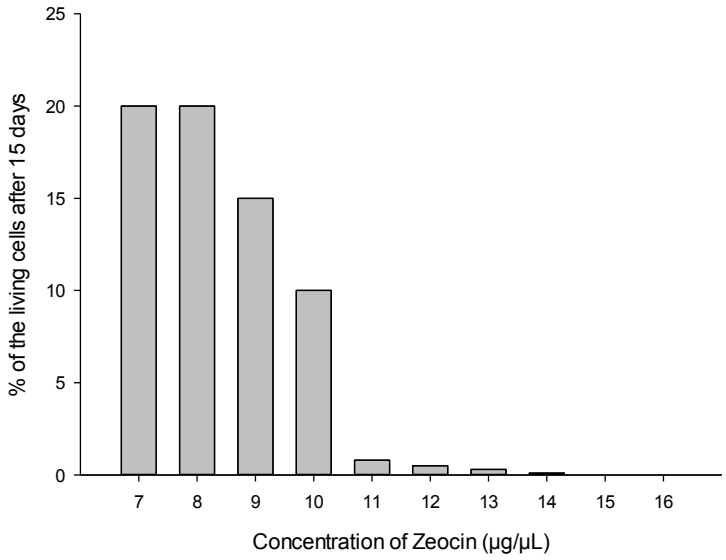

Figure 8.9: Titration for determining the selection concentration. This Figure is showing the different concentration of Zeocin from 7µg/mL to 16 µg/mL over the period of 15 days for MCF-7 cells. The result showed that the minimum concentration of zeocin for killing the cells after 15 days is 15 µg/mL.

8.3.2. Selecting the clones by cLSM:

Transfected cells were taken for single cell sorting and a single cell was put in each well of 96 well plates. 10-14 days later, around 40-50 clones in 96 well plates were checked. Among those 2-4 clones were selected by cLSM based on the fluorescent intensity (Figure 8.10).

The clone numbers for constructs were as followed:

1. MCF-7 pEYFPC1-hG1a: 6, 17, 20, 21

2. MCF-7 pEYFPN1-hG1a: 2, 3, 4, 6

3. MCF-7 pEYFPC1-hG1d: 1, 7

4. MCF-7 pEYFPN1-hG1c: 11, 16, 19

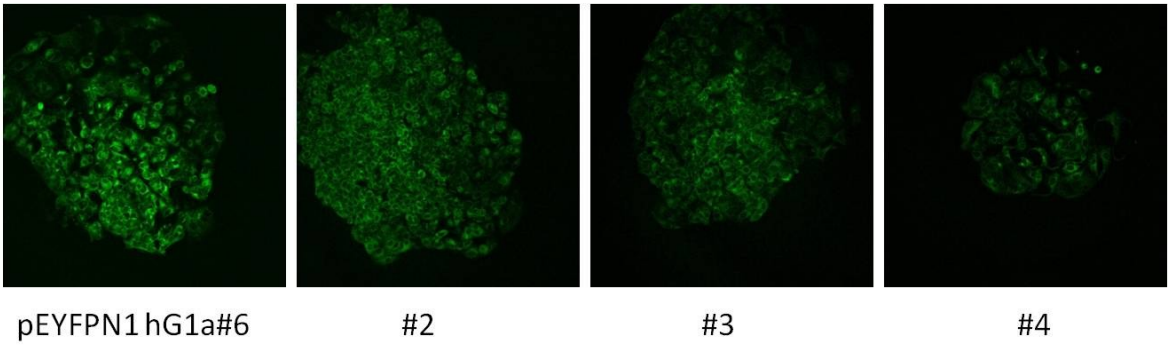

Figure 8.10: different clones of stably transfected cell. Figure 8.10.a: MCF-7 pEYFPN1 hG1a clones. Selected clones are #6, #2, #3, and #4. Clone#6 is strongly fluorescent and clone #4 is weakly fluorescent. Clone #2 and Clone #3 were used in our experiments.

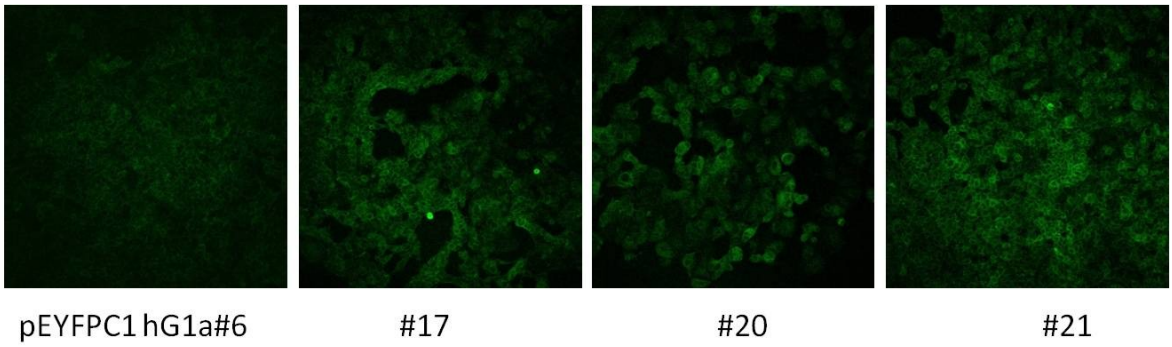

Figure 8.10.b: MCF-7 pEYFPC1 hG1a clones. Selected clones are #6, #17, #20, and #21. Clone #17 and clone #21 are the strong florescent while clone #6 and clone #20 are weak florescent clones. #20 and #21 were used in our experiments.

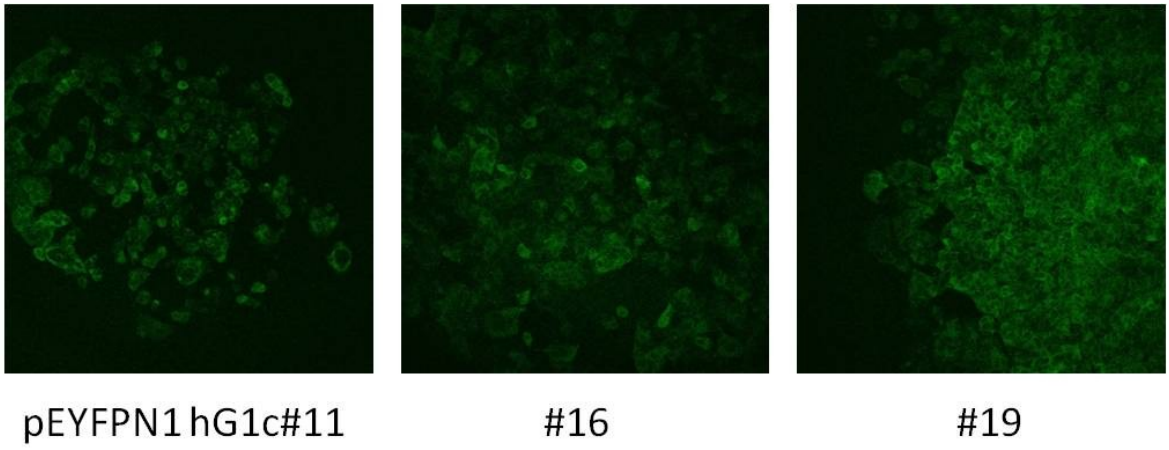

Figure 8.10.c: MCF-7 pEYFPN1 hG1c clones. Selected clones are #11, #16, and #19. Clones #19 is strong florescent clone and clone #11 and clone #16 showed weak florescent. Clone #16 and #19 were used in our experiments.

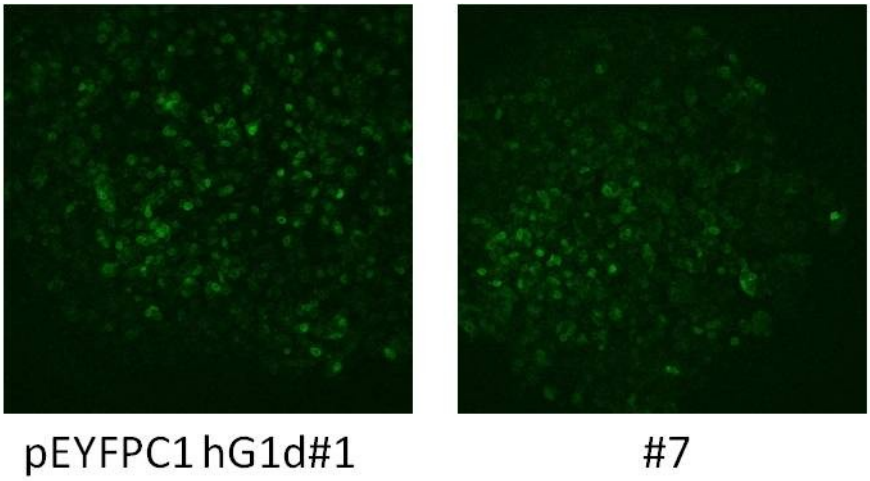

Figure 8.10.d: MCF-7 pEYFPN1 hG1d clones. Selected clones are #1, #7. Both clones show intermediate fluorescents and were used in our experiments.

8.4 Characterization of the cell lines:

8.4.1. Subcellular localization of GIRK1 protein:

To check the subcellular localization of GIRK1 protein, selected clones were tested by confocal laser scanning microscopy. GIRK overexpressed cells were transiently transfected with srß marker (ER marker) and GpI (lipid rafts marker). LSM data showed that GIRK1a is primarily located in endoplasmic reticulum (RE) and very rarely in the plasma membrane (Figure 8.11.a). The same patterns were seen in splice variants (GIRK1c and GIRK1d). The eYFP control cells, however,

showed a different pattern of fluorescence: The eYFP was distributed within the cytosol and nucleus (Figure 8.11.b). In addition, the subcellular distribution of MCF-7 PIRES2 eGFP hG1a (Figure 8.12) as well as MCF-7 GIRK1 knockout cells (Figure 8.13) were observed. An evenly distributed pattern of GFP/ CFP in the cytosol and nucleus was found in both cells.

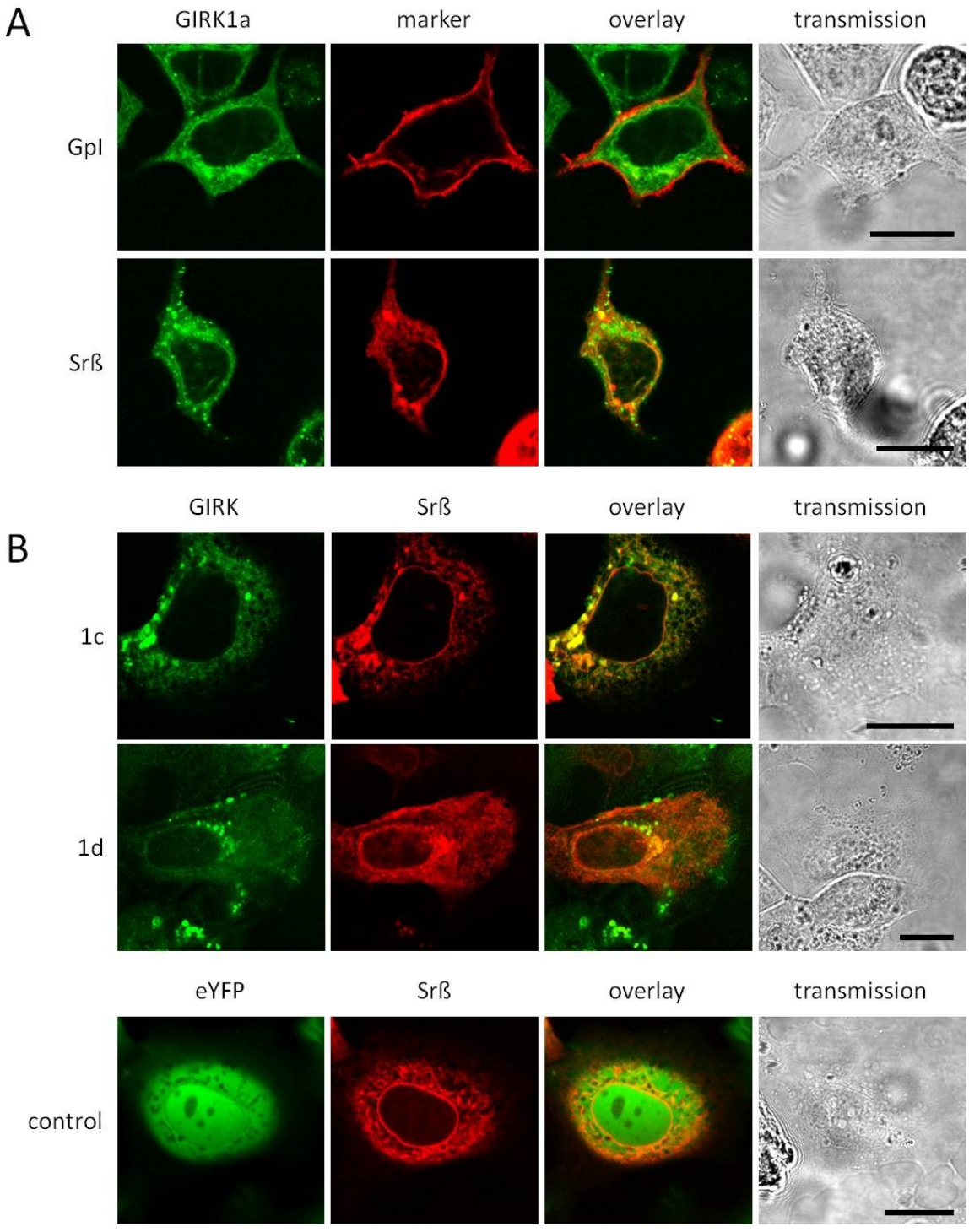

Figure 8.11: Subcellular localization of MCF-7GIRK1 protein. 8.1.a: MCF-7GIRK1a cells transiently transfected with GPI (Marker of lipid drafts) and srß (marker of RE). Left to right: eYFP, srß, overlay and transmission. 8.11.b: MCF-7^{GIRK1c}, MCF-7^{GIRK1d} and MCF-7 ^{eYFP} (control). Transiently transfected with srß. Scale bar is 15 µm.

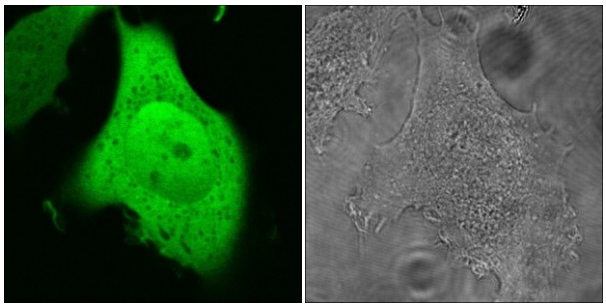

Figure 8.12: Subcellular localization of MCF-7 PIRES2 EGFP hG1a protein. From left to right: eGFP (Green) and transmission (Grey).

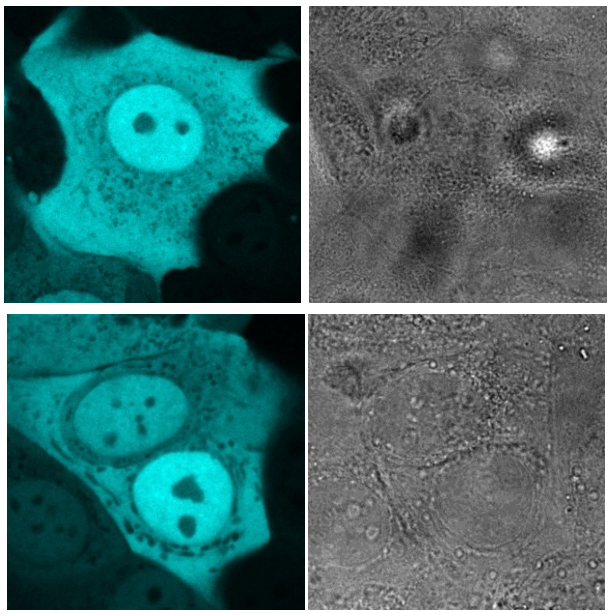

Figure 8.13: Subcellular localization of MCF-7 GIRK1 knockout cells. Upper panel from left to right: MCF-7 PSI_hG1a_A (CFP) and MCF-7 PSI_hG1a_A (transmission). Lower panel from left to right: MCF-7 P^{SI}_hG1a_ScA (CFP) and MCF-7 P^{SI}_hG1a_ScA (transmission).

8.4.2. Real time PCR:

Real time PCR was performed In order to identify GIRK mRNA in wild type breast cell lines and also to confirm the overexpression of GIRK1a and splice variants in

MCF-7 cells. Among wild type breast cell, estrogen receptor positive cells (MCF-7, T-47D and KPL_1) showed higher GIRK1a mRNA. MCF-7 showed substantial levels of mRNA compared to the others (Figure 8.14.a). qPCR also showed more than 300 folds of GIRK1a mRNA in both MCF-7 pEYFPC1-hG1a and pEYFPN1-hG1a cells ($P<0.01$), compared to MCF-7wt and MCF-7 vector control. MCF-7 pEYFPN1-hG1c and pEYFPC1-hG1d also showed higher amount of mRNA when compared to the control group ($P<0.05$ and $P<0.01$ respectively) (Figure 8.14.b and 8.14.c).

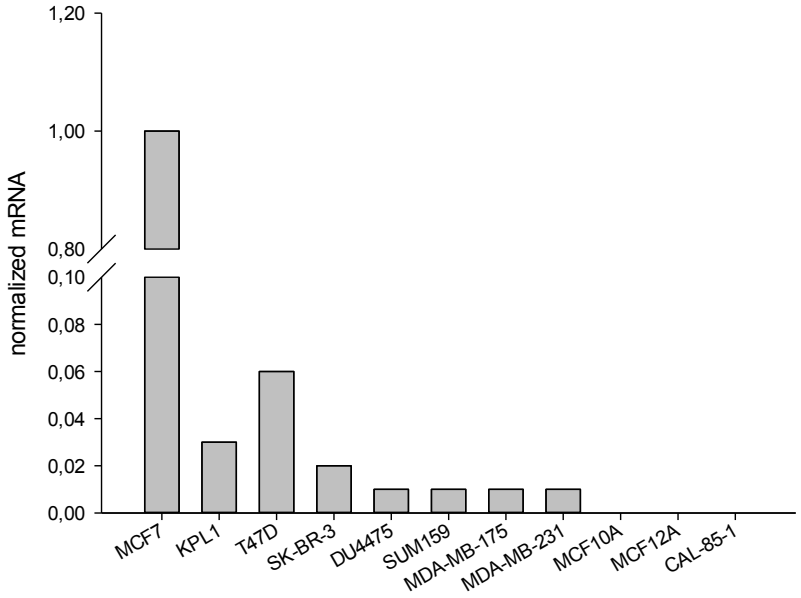

Figure 8.14.a

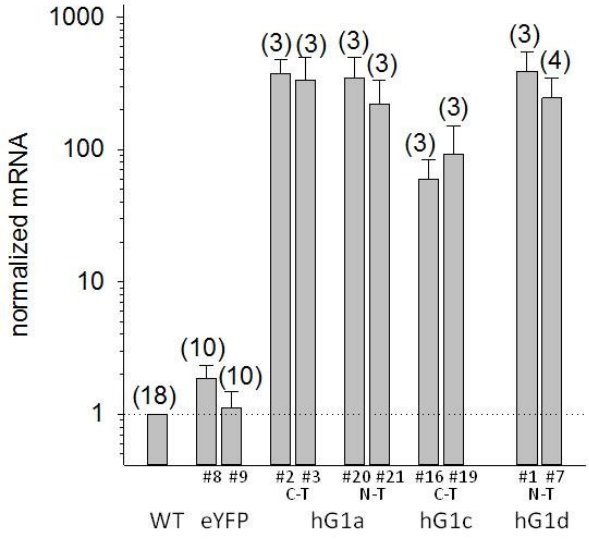

Figure 8.14.b

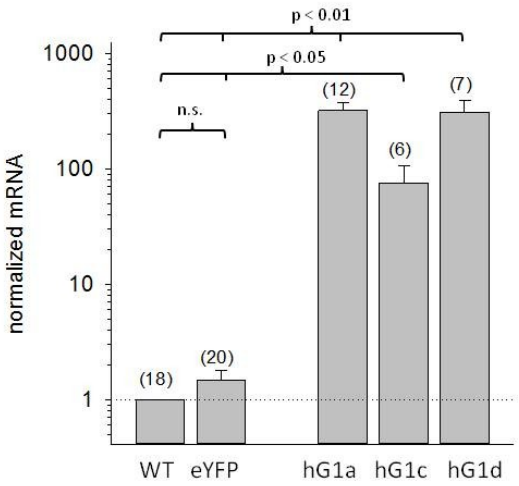

Figure 8.14.c

Figure 8.14. Expression of GIRK1 mRNA. 8.14.a: mRNA expression of hG1a in diferrent breast cell lines. MCF-7, T-47D and KPL-1 cells showed highest amount of GIRK1a. Expression was normalized to the expression level in the MCF-7wt cell line. Figure 8.14.b and 8.14.c: mRNA expression of hG1a, hG1c and hG1d in MCF-7 overexpressed cell line. Data was normalized to MCF-7wt. 2 different clones of each overexpressed cell lines were investigated. Figure 8.14.c: mRNA expression of hG1a, hG1c and hG1d in MCF-7 stably overexpressed cells. Data drived from two cell lines overexpressing eYFP , hG1a (C-T fussion , N-T fussion), hG1c (C-T Fussion) and hG1d (N-t fussion). Mean values ± SEM were plotted (number of experiments is given in parenthesis above each bar). Statistical significances between groups are indicated. hG1a, as well as hG1d differs from both WT, as well as from eYFP, statistically significant at the $p < 0.01$ level. hG1c differs from both WT, as well as from eYFP, statistically significant at the $p < 0.05$ level. Kruskal-Wallis one way analysis on ranks was used for analysis of statistical significance.

8.4.3. Western blot:

In order to detect the protein level of GIRK1 in wild type breast cell lines, western blot was performed. According to our results, no GIRK1 protein was detected in wild type breast cell lines (band size 56.6 /72 KD for glycosylated form) (Figure 8.15.a). In addition, western blot was done for MCF-7 overexpressed cells and only in MCF-7$^{GIRK1a\#20}$ and MCF-7$^{GIRK1a\#21}$, appropriate band of 85 KD was detected (Figure 8.15.b) (Table 8.2). It should mention that the antibody, which used in this study, was able to react with the full length GIRK1a only. For this reason, it was not possible to monitor the expression of the other variants, GIRK1c/d, at the protein level by either IHC or WB.

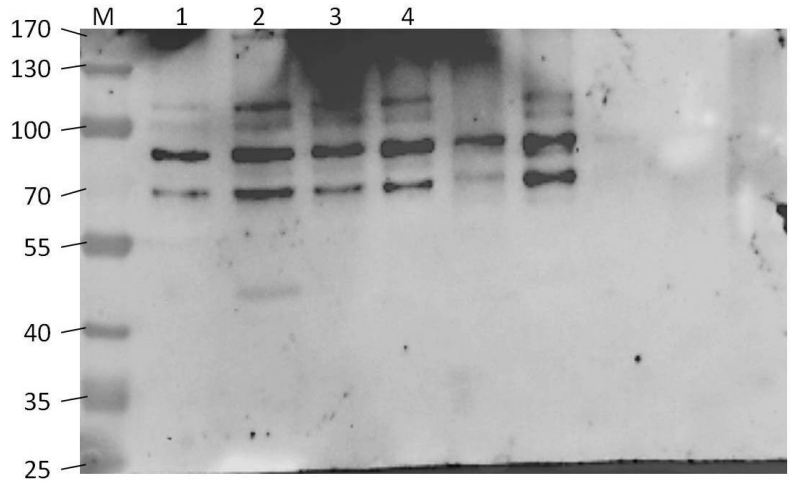

Figure 8.15.a

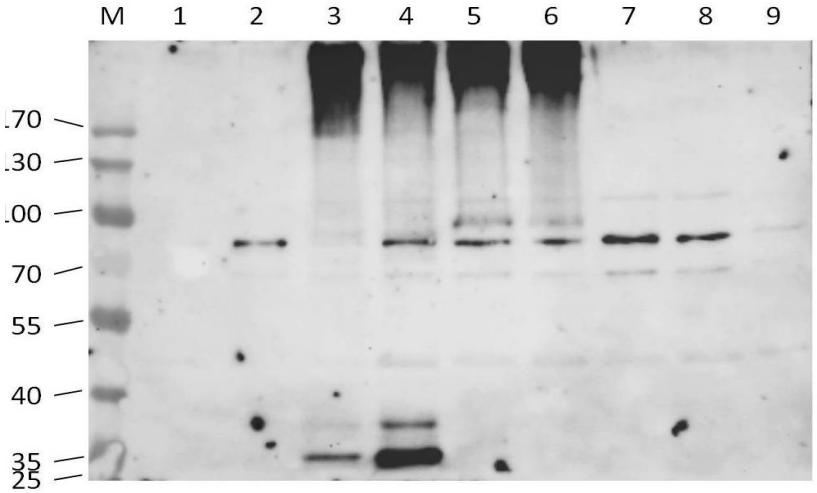

Figure 8.15.b

Figure 8.15: Western blot analysis for detection of GIRK1 protein. Figure 8.15.a: GIRK1 protein detection on wild type breast cell lines. From left to right: first lane is the protein marker. Lane 1: HepG2 (50µg). Lane 2: KPL-1(50µg). Lane 3: CAL-85-1 (50µg). Lane 4: DU-4475 (50µg). Lane 5: HL1 (50µg). Lane 6: MCF-7 (50µg). Lane 7: MCF10A (50µg). Lane 8: native oocytes (20µg)(Negative Control) . Lane 9: oocytes with G1a and G4 (20µg)(Positive control) . Figure 3.14.b: GIRK1 protein detection on MCF-7 overexpressed cell lines. From left to right: first lane is the protein marker. Lane 1: MCF-7^{wt}. Lane 2: MCF-$7^{V\#8}$ .Lane 3: MCF-$7^{GIRK1a\#2}$ .Lane 4: MCF-$7^{GIRK1a\#3}$ .Lane 5: MCF-$7^{GIRK1a\#20}$ .Lane 6: MCF-$7^{GIRK1a\#21}$ .Lane 7: MCF-$7^{GIRK1c\#16}$ .Lane 8: MCF-$7^{GIRK1d\#1}$ .Lane 9: MCF-7^{Gby}. Primary Ab was Anti-GIRK1 (Abcam mouse monoclonal) (1:1000) and secondary Ab was sheep anti mouse HRP (1:4000).

Table 8.2: Protein size of GIRK1 and splice variants. Second column is the actual protein size in KD and third column is the protein size in addition with eYFP (eYFP alone: 29 KD). * is the size of glycosylated form.

Protein	Size (KD)	+YFP (KD)
hG1a	56.6/72*	85.6/101*
hG1c	35	64
hG1d	26.8	55.8
hG1e	28.7	57.7

8.4.4. Immunohistochemistry:

In order to detect the G1a protein in cell lines IHC was done. Like cLSM data, here also hG1a protein was detected mostly in the cytoplasm and fairly in the cell membrane. No GIRK1 protein was detected in MCF-7^{GIRK1c} and MCF-7^{GIRK1d} since the antibody could detect only the full length of G1RK1a. In addition, IHC could not detect any GIRK1a protein in MCF-7 wt cells although we identified high amount of mRNA. HL1 and HEK293 cell lines were considered as positive and negative control respectively.

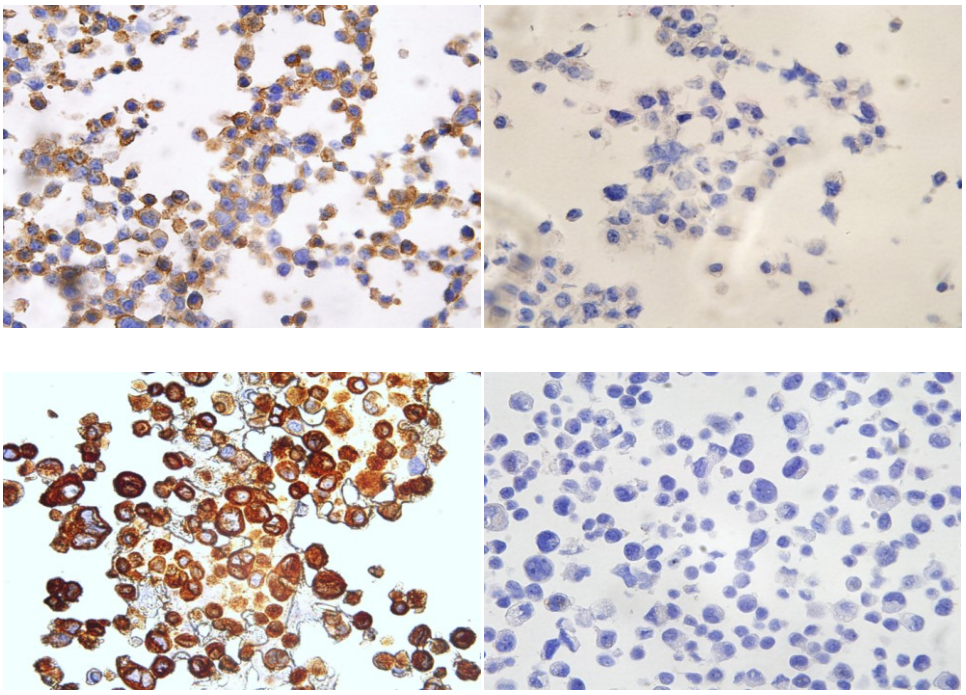

Figure 8.16: Detection of GIRK1a protein in stably transfected cell line. Upper panel left to right: HL1 cells as a positive control and HEK293 as negative control. Lower panel from left to right: MCF-7^{GIRK1a} and MCF-7^{wt}. Brown: Immunoreactivity. Blue: hematoxylin stain.

8.5. Vital Parameters:

8.5.1. Proliferation assay:

Uncontrolled cells proliferation is a hallmark of cancerous cells(33) and so cell proliferation assay was performed with thymidine analog BrdU (5-bromo-2'-deoxyuridine) following its incorporation into newly synthesized DNA to compare the proliferation of MCF-7^{wt} or MCF-7^{eYFP} control with MCF-7^{GIRK1a} MCF-7^{GIRK1c} and MCF-7^{GIRK1d}. Our result showed that proliferation remained unaffected upon overexpression of GIRK1a, GIRK1c and GIRK1d. Only MCF-7^{GIRK1d} showed higher G0/G1 fraction ($p < 0.05$) compared to MCF-7^{GIRK1a}. (Figure 8.17).

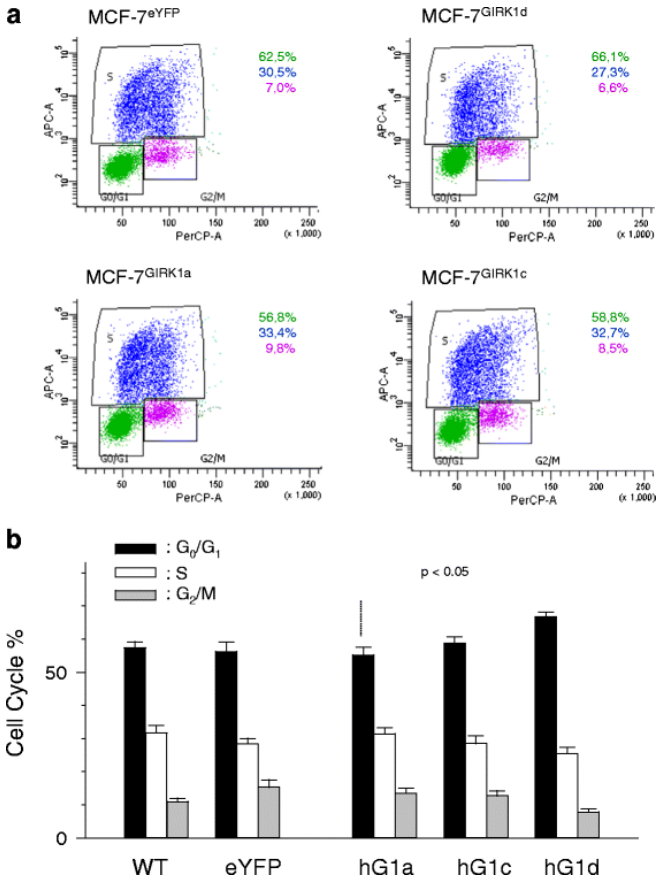

Figure 8.17: Proliferation assay. Figure 8.17.a: Original results from the assessment of cell cycle using gated cell sorting according to fluorescence intensities for PerCP-A (*x-axis*) and APC-A (*y-axis*) for different experimental groups. % of cells for the given experiment is stated in respective colors besides the plot. Figure 8.17.b: *Statistics for the percentage of time spent in the different phases of the cell cycle* Mean values ± SEM were plotted. N was (in parenthesis behind each experimental group): MCF-7WT (8) / MCF-7eYFP (12) / MCF-7GIRK1a (16) / MCF-7GIRK1d (12) / MCF-7GIRK1d (6). G1/G0 fraction of MCF-7GIRK1d differs statistically significant at the $p < 0.05$ level from the one of MCF-7GIRK1a. One way ANOVA was used for analysis of statistical significance.

8.5.2: Cell adhesion assay:

Cell adhesion, the binding of a cell to the extracellular matrix or a specific surface, is essential for the growth and survival of the cell and for communication with other cells(34). In our study, the impact of GIRK1 overexpression on adhesion of MCF-7 cells to extracellular matrix were evaluated. Our results indicate that, GIRK1 overexpressed MCF-7 cells could not affect the adhesion of cells to extracellular matrix (Fibronectin) (Figure 8.18).

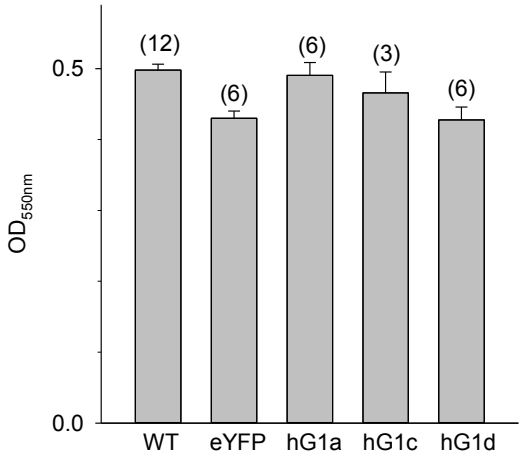

Figure 8.18

Figure 8.18: Quantification of cells adhering to fibronectin-coated substrate via OD550nm. Mean values ± SEM were plotted (number of experiments is given in parenthesis above each bar). The mean values do not differ statistically significantly.

8.5.3: Invasion assay:

Invasion to the surrounding tissue through degradation of extracellular matrix is one of the hallmarks of cancer development (33). In this regard, the invasive potential of GIRK1 overexpressed MCF-7 cells, were investigated. Our results indicate that the ability of invasion was increased when MCF-7 cells were overexpressing GIRK1a or GIRK1c compared to MCF-7 ^{GIRK1d}. Furthermore, MCF-7^{GIRK1d} showed a significant reduction of invasion compared to the MCF-7^{eYFP} (Figure 8.19).

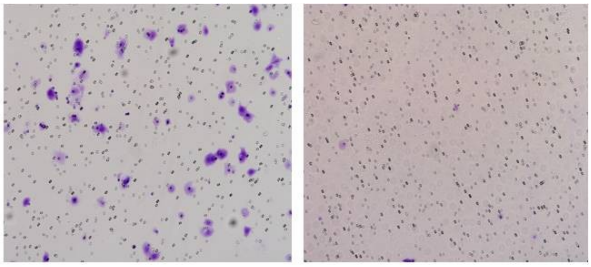

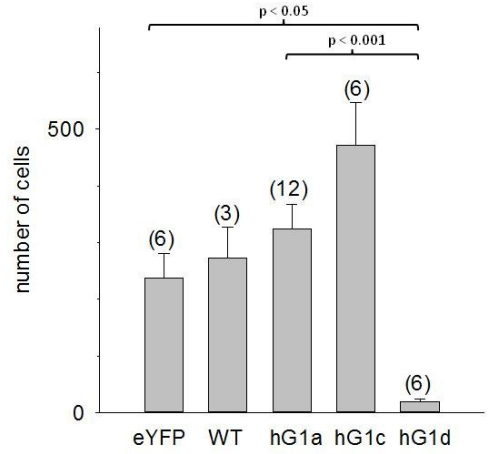

Figure 8.19.a and Figure 8.19.b

Figure 8.19. Effects of GIRK1 overexpression on invasion. Figure 8.19.a: View of the invaded cells through the Matrigel, stained with crystal violet, From left to right: MCF-7^{GIRK1a}, MCF-7^{GIRK1d} (10X magnification). Figure 8.19.b: Quantification of the number of invasive cells after 24h. Mean values ± SEM were plotted (number of experiments is given in parenthesis above each bar). Statistical significant differences between groups are indicated. hG1d differs from eYFP statistically significant at the $p < 0.05$ level. hG1a differs from hG1d statistically significant at the $p < 0.001$ level. Kruskal-Wallis one way analysis on ranks was used for analysis of statistical significance.

8.5.4: Wound healing assay:

This method mimics cell migration during wound healing *in vivo*. This assay was performed to study the influence of GIRK1 overexpression on capacity of breast cancer cells to heal the wound. Results showed that GIRK1 overexpression affects wound healing rate in a differential manners, depending on the variant tested. MCF-7^{GIRK1a} showed a significant increase of wound healing compare to the control group (MCF-7^{eYFP}). In contrast, it was observed that MCF-7 ^{GIRK1d} showed a major reduction of wound healing compared to MCF-7^{GIRK1a} and MCF-7^{GIRK1c} (Figure 8.20).

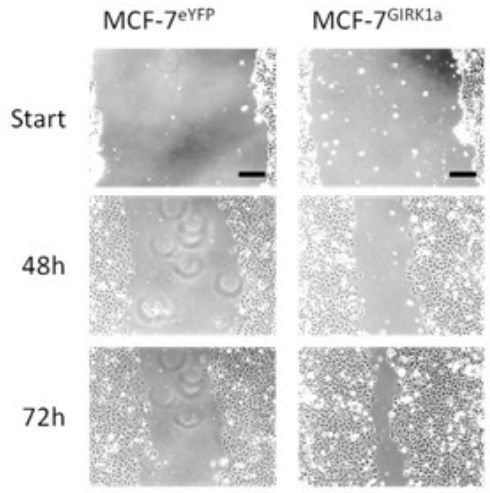

Figure 8.20.a

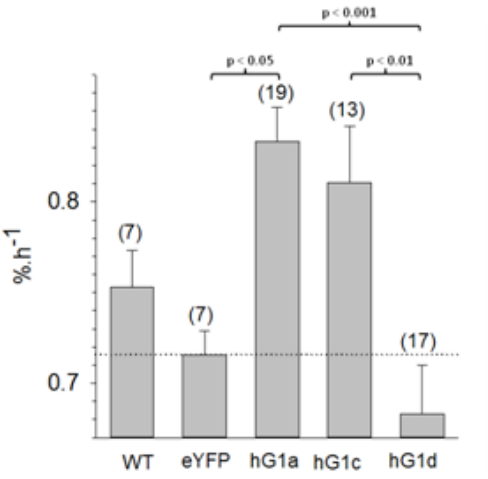

Figure 8.20.b

Figure 8.20. Wound healing assay. Figure 8.20.a: a single view of cell monolayers at different time intervals after scratching (48h and 72h). Scale bars correspond to 200 μm. Left: control; right GIRK1a overexpressors. Figure 8.20.b: Wound healing rates (in percentage healing per h). Mean values ± SEM were plotted (number of experiments is given in parenthesis above each bar). Statistical significances between groups are indicated. hG1a differs from eYFP statistically significant at the $p < 0.05$ level. hG1a differs from hG1d statistically significant at the $p < 0.001$ level. hG1c differs from hG1d statistically significant at the $p < 0.01$ level. Kruskal-Wallis one way analysis on ranks was used for analysis of statistical significance.

8.5.5: Cellular motility and velocity assay:

Motility and enhanced velocity of the cancer cells is a prerequisite step for cancer metastasis. In this context, the effect of GIRK1 overexpression on the motility of the MCF-7 cells was tested. Our findings indicate that there is a significant increase of velocity in MCF-7^{GIRK1a} and MCF-7^{GIRK1c} cells compared to the other

groups (Figure 8.21.a and 8.21.b). In addition MCF-7^{GIRK1d} showed a significant reduction of velocity compared to MCF-7^{GIRK1a}. Similar results were obtained from motility coefficient test (Figure 8.22.a and 8.22.b).

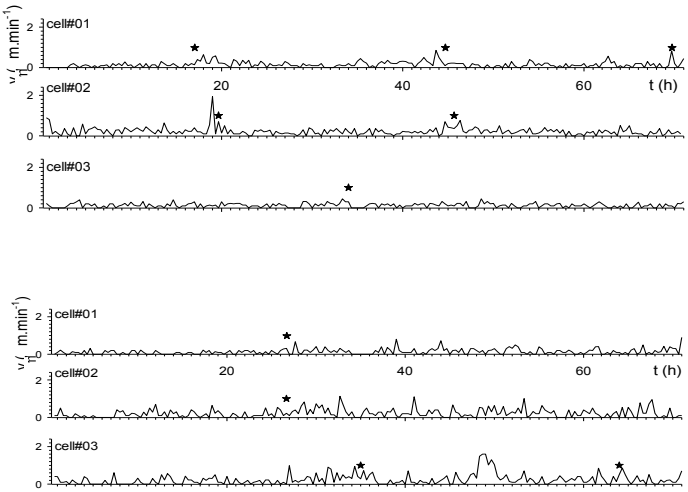

Figure 8.21.a

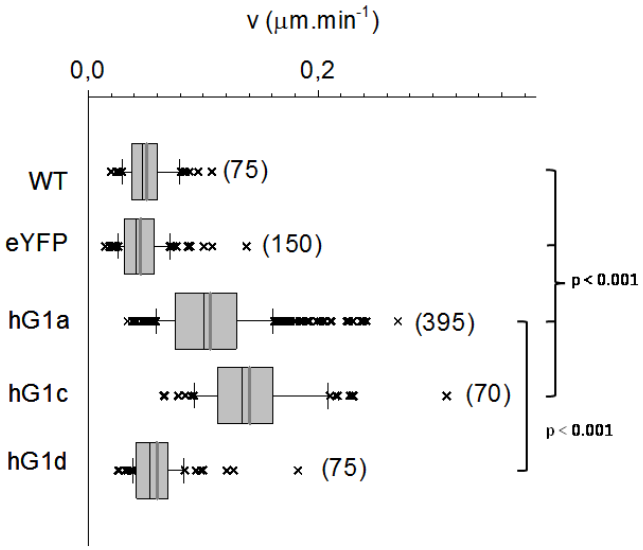

Figure 8.21.b

Figure 8.21: single cell velocity assay. Figure 8.21.a: Cellular velocities for three representative cells during the entire observation interval of 72 hours. Asterisks symbolize cell divisions. *Upper:* control; *lower:* GIRK1a overexpressors. Figure 8.21.b: Graphical representation of mean cellular velocities for different experimental groups. The median value is represented by the black line within the box, box margins represent 75% and 25% percentiles, whiskers indicate 90% and 10% percentiles, values outside the 10%-90% interval are plotted individually as crosses. The grey line represents the mean value. The number of individual cells is given in parenthesis besides each box. Statistical significant differences between groups are indicated. hG1a, as well as hG1c, differ from both WT, as well as from eYFP, statistically significant at the $p < 0.001$ level. hG1d differs from both hG1a, as well as from hG1c, statistically significant at the $p < 0.001$ level. Kruskal-Wallis one way analysis on ranks was used for analysis of statistical significance.

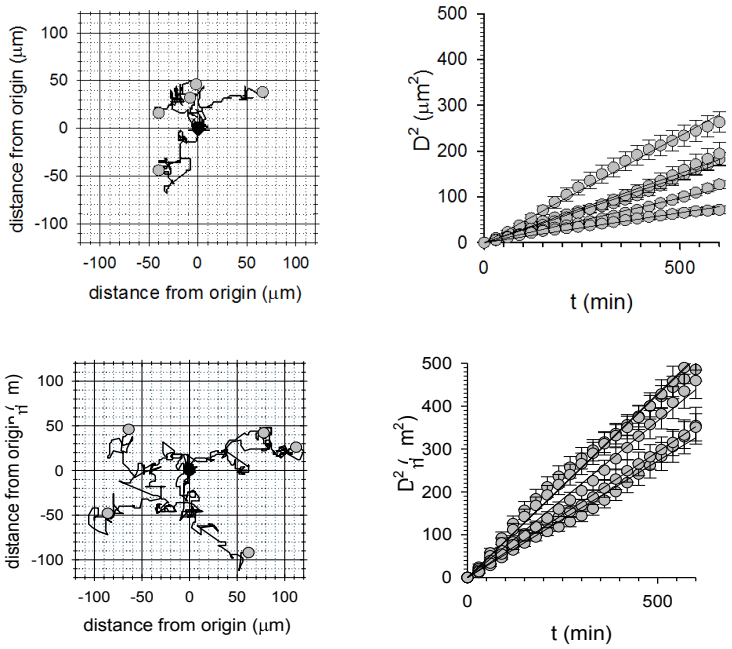

Figure 8.22.a

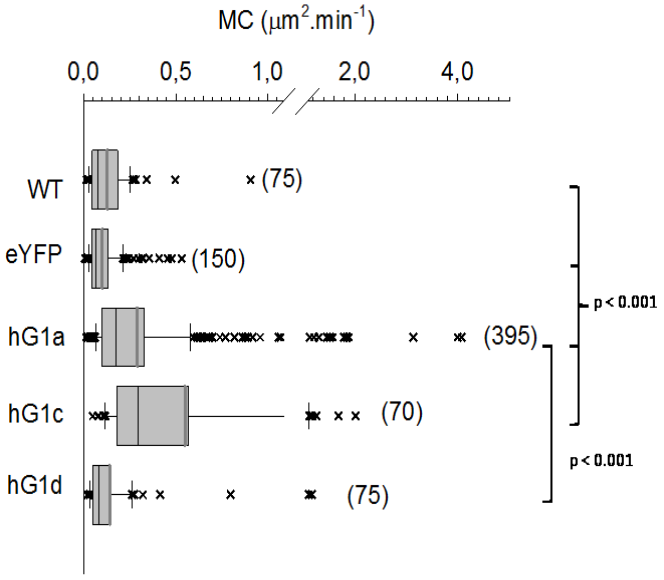

Figure 8.22.b

Figure 8.22: Motility coefficient in MCF-7 overexpressed cells. Figure 3.22.a:Left panel: Flower plots showing the trajectories of 5 representative cells for the entire observation interval of 72 hours (black line). Starting position of each individual cell was set to zero coordinates (black circle). Grey circles indicate the position of an individual cell after 72h. Right panel: Squared distance as a function of time for the five cells shown to the left (circles; bars indicate standard error). Solid lines represent a linear fit through the data, resulting in the motility coefficient (MC). Upper: control; lower: GIRK1a overexpressors. Figure 8.22.b: Graphical representation of cellular motility coefficients for different experimental groups. The median value is

represented by the black line within the box, box margins represent 75% and 25% percentiles, whiskers indicate 90% and 10% percentiles, values outside the 10%-90% interval are plotted individually as crosses. The grey line represents the mean value. The number of individual cells is given in parenthesis besides each box. Statistical significant differences between groups are indicated. hG1a, as well as hG1c, differs from both WT, as well as from eYFP, statistically significant at the $p < 0.001$ level. hG1d differs from both hG1a, as well as from hG1c, statistically significant at the $p < 0.001$ level. Kruskal-Wallis one way analysis on ranks was used for analysis of statistical significance.

8.5.6. Angiogenesis assay:

To gain access to the circulation nutrients cancer cells induce formation of newly synthesized blood vessels, a process that is called angiogenesis. In this regard, CAM assay was done in order to investigate the potential of angiogenesis in MCF-7 based cell lines. Our results showed that despite no significant difference between macroscopic vascularization in MCF-7 ^{GIRK1a} cells and control group, there is a significant reduction of MVs in MCF-7 ^{hGIRK1d} compared to MCF-7 ^{GIRK1a} (Figure 8.23).

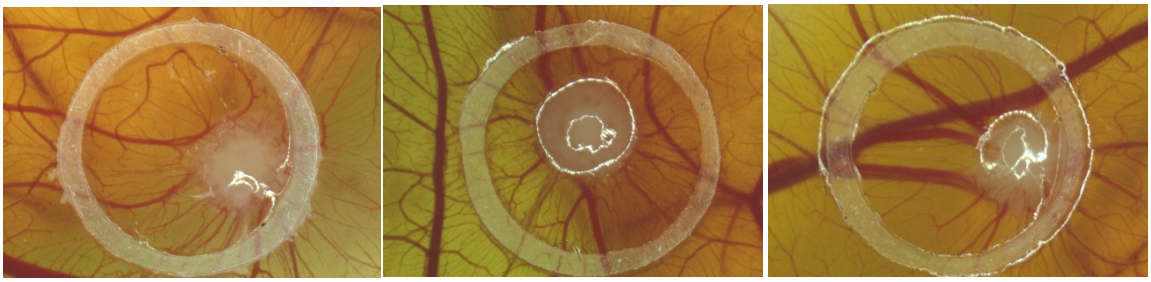

Figure 8.23.a

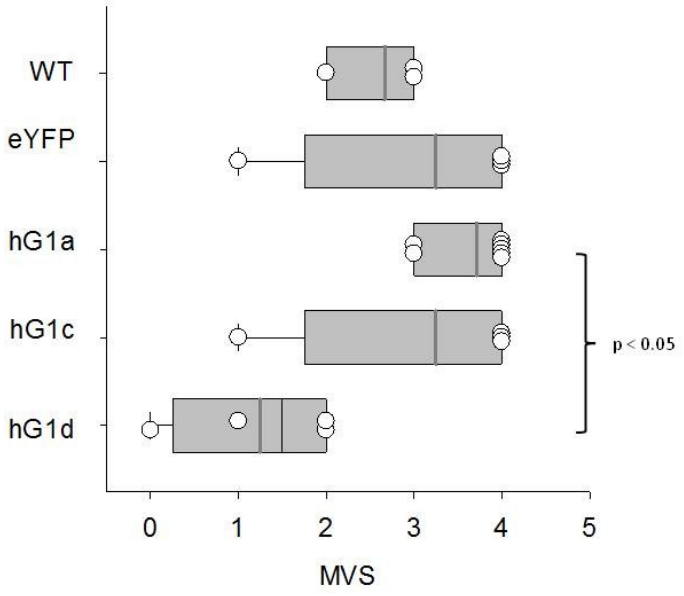

Figure 8.23.b

Figure 8.23. CAM assay (Angiogenesis). Figure 3.22.a: a single view of cellular onplants and vascularization. The silicone ring, used to initially stabilize the onplant is also visible. From left to right: MCF-7 wt, MCF-7^{GIRK1a} and MCF-7^{GIRK1d}. Figure 8.23.b: Macroscopic vascularization scores (MVS) for the different experimental groups. The median value is represented by the black line within the box, box margins represent 75% and 25% percentiles, whiskers indicate 90% and 10% percentiles, values outside the 10%-90% interval are plotted individually as crosses. The grey line represents the mean value. The statistically significant difference between hG1d and hG1a is indicated ($p < 0.05$). Kruskal-Wallis one way analysis on ranks was used for analysis of statistical significance.

9. Discussion:

GIRK channels, which are involved in many cell signaling pathways, are activated by G-protein coupled receptors (GPCRs). The latter bind to cognate ligands such as e.g. γ-amino-butyric-acid (GABA), muscarinic, dopamine, serotonin, opioid, and acetylcholine receptors. When GPCRs are triggered by ligands, dimeric protein Gβγ (formed from inactive heterotrimeric G protein complexes (Gαβγ) associated with pertussistoxin sensitive a subunits; is released and subsequently binds in order to open GIRK channels. The activation of GIRK channels, in turn, results in hyperpolarization of the cell, which is characterized by an increased negative charge caused by the influx of K^+ (10).

While involved in several well-known physiological functions in the central nervous system (CNS) and heartbeat regulation, GIRK channels are also linked to several pathophysiological conditions such as epilepsy and diabetes (3, 10) . Interestingly, recent findings have suggested the GIRK channels are involved in cancer progression. Stringer et al.(20) showed a profound increase (up to 400x) in GIRK1 mRNA expression in primary breast carcinoma as compared to in normal breast tissue. Lymph node metastasis was also correlated with GIRK expression. Later on, Brevet et al. showed that patients with breast (24) and pancreatic carcinomas (35) overexpress GIRK1 at the protein level. Because this evidence support a connection between GIRK expression and cancer development, we tested: 1) the expression of GIRK1a and shorter splice variants of GIRK1 in benign and malignant breast cell lines and 2) the potential effects of GIRK1a, c and d overexpression on vital parameters of breast cancer cells.

Toward this end, we first checked for the expression of the GIRK transcript using qPCR in benign and malignant breast cell lines (see table 9.1 for overview on cell lines).

Table 9.1: Comparison of breast cell lines in terms of gene clusters, hormonal receptors, and tumor types.

Cell line	Gene Cluster	ER	PR	HER2	Tumor Type
MCF10A	BaB	-	-		F
MCF12A	BaB	-	-		F
MCF-7	Lu	+	+		IDC
MDA-MB-231	BaB	-	-		AC
SKBR3	Lu	-	-	+	AC
T47D	Lu	+	+		IDC
KPL-1	Lu	+	-	-	DC
SUM159	BaB	-	-	-	AC
CAL-85-1	Lu	-	-	-	-
DU4475	Ba	-	-	-	

BaB, basal B type; Lu, luminal type; AC, adenocarcinoma; F, fibrocystic disease, IDC, invasive ductal carcinoma.

Our results showed that in contrast to estrogen receptor (ER)-negative breast cancer cells and benign breast cell lines in which GIRK1 mRNA was fairly detectable, ER+ breast cancer cells expressed GIRK1a, among them MCF-7 cells showed the highest expression level. In a recent study by Kammerer et al. (25), samples from 1000 patients with breast cancer were evaluated by in situ hybridization. Significantly higher GIRK mRNA expression was also observed in ER positive patients. This study supported our data, which indicated that GIRK1 mRNA overexpressed in ER-positive cell lines. At present, it is unclear how the expression of ER and GIRK is connected, but it is plausible that ER acts as a check point for the activity of GIRK. Further experiments must be conducted to confirm this hypothesis.

Out of the ER-positive breast cancer cell lines, MCF-7 had the highest level of GIRK1 mRNA expression and was selected for further experiments.

All GIRK1 splice variants, GIRK1a, GIRK1c and GIRK1d were overexpressed in these cells. Overexpression was confirmed using three readout systems i.e. confocal laser scanning microscopy (cLSM), western blotting, and immunocytochemistry.

In qPCR analysis, an up to 300-fold increase in the GIRK1 transcript level was observed in MCF-7^{GIRK1a}, MCF-7^{GIRK1c} and MCF-7^{GIRK1d}, confirming the proper level of overexpression of the molecule. Analysis of the protein expression using western blotting revealed that overexpressing MCF-7 cells produced a protein band of about 85 kD, corresponding to the estimated molecular weight of the GIRK-YFP fusion protein (85.6 kD). It is noteworthy that the epitope recognized by the antibody used in this study was able to react exclusively with the full length GIRK1a. For this reason, it was not possible to monitor the expression of the other variants, GIRK1c/d, at the protein level by either IHC or WB.
Subcellular localization of GIRK in GIRK-overexpressing MCF-7 cells was checked by cLSM using co-transient transfection of the cells with compartment markers, i.e. GPI-eCFP (a marker to detect lipid rafts in the plasma membrane) and Srß-eCFP (a marker for the endoplasmic reticulum). As reported by Wagner et al. (36), we observed that GIRK1a and the shorter splice variants, GIRK1c and GIRK1d, were mostly located in endoplasmic reticulum and to some minor extend in the plasma membrane. No GIRK proteins were detected in nucleus. Interestingly, the arginine-glycine-aspartate (RGD) sequence, located in the extracellular region of the GIRK molecules, is conserved among all identified GIRK subunits and is recognized by integrins. It was observed that the activity and subcellular localization of GIRK was directly regulated by the interaction of GIRKs with integrins as a consequence of the RGD motif. In particular, a mutation of the RGD site to RGE decreased or completely abolished the GIRK current. More importantly, the amount of the mutant channel protein that localized to the plasma membrane was decreased relative to the wild type (37). This observation clearly shows that the level of surface expression of the GIRK molecules is a function of their interaction with extracellular matrixes such as integrins, and that such an interaction is necessary for proper GIRK channel membrane localization and function. Therefore, it is possible that in two-dimensional culture system we used in this study for cell

culture, the absence of integrins lead to the localization of GIRK in the intracellular region of the cells.

Our results on intracellular localization of GIRK1 are in line with those appearing in previous reports about transient transfection of MCF-7 cells with GIRK1 splice variants (36) . Indeed, in studies on GIRK1 synthesis and trafficking, it has frequently been observed that homotetramers of GIRK1 protein are mostly located in intracellular membranes, while upon heteromeric assembly with other GIRK isoforms, the complex tends to move (at least in part) to the plasma membrane (38-40) It has been demonstrated, however, that even in native cells transfected with additional GIRK isoforms as heterooligomerization partners (7, 41) at least 64% of the GIRK1 protein was confined to intracellular membranes (42-44). At present, it is not clear whether intracellular- or plasma membrane-located GIRK protein is responsible for the effects reported here.

Subsequently, residues 375–399 in GIRK4 were identified as being required for its co-assembly with GIRK1 (7). In this regard, a truncation mutant of GIRK4 failed to target GIRK1 in the membrane (38) It seems as though this phenomenon may serve as a quality checkpoint, so that only functional heteromers are processed.

No difference in the expression levels or localization of GIRK were observed in N-terminal- as compared C-terminal-labeled GIRK1a, indicating that localization of GIRK protein is not affected by the position of eYFP.

Despite the high expression level of the GIRK1a transcript, the level of expression at the protein level was found to be below the detection limit of IHC and WB. This finding cannot necessarily be regarded as a proof for the absence of GIRK1 in wild type MCF-7 cells, as signal transduction molecules such as GIRK usually can exert their effects at very low levels of abundance. Although long, noncoding RNAs (lnRNAs) can shift the phenotype of cancer cells towards malignancy without needing the protein to be synthesized (45), the overexpressed mRNAs in this study were devoid of 3’- and 5’-untranslated regions (UTRs), which are presumably crucial for such activities. Thus, we hypothesize that the tumor-promoting effect of GIRK1a/c overexpression is triggered by the corresponding protein(s).

Once we had obtained MCF-7 cells that overexpressed GIRK1a/c/d at both the gene and protein levels, we searched for a potential influence of GIRK overexpression on vital parameters of the breast cancer cell lines including cell

invasion, angiogenesis, and metastasis. We found that overexpression of the GIRK1 protein exerted profound effects on vital parameters of breast cancer cells such as wound healing, chemo invasion, and cellular motility. These findings support the assumption that GIRK complexes are potentially involved in the regulation of breast cancer cell vital parameters. Interestingly, vital parameters affected by either GIRK1a or GIRK1c overexpression were inversely manipulated when compared to MCF-7 cells overexpressing GIRK1d.

MCF-7 cells overexpressing either GIRK1a or GIRK1c showed more malignant phenotypes, while the opposite effects were observed with cells overexpressing GIRK1d (See table 9.2 for the overview).

Table 9.2: Overview of GIRK overexpression on vital parameters of MCF-7 cells. Effects of GIRK1 and splice variants overexpression on vital parameters of MCF-7 cell lines compared to the control group.

	adhesion	invasion	Wound healing	Velocity	Motility	Angiogenesis	proliferation
GIRK1a	NE	+	++	++	++	NE	NE
GIRK1c	NE	+	+	++	++	NE	NE
GIRK1d	NE	- -	-	NE	NE	-	NE

NE: no effects. +: increas but no significant. ++: significantly increased. - : Reduction but not significant. --: Significantly reduced.

Based on these findings, we hypothesize that different GIRK1 variant proteins are responsible for the differential modulation of the cancer phenotype in MCF-7 cells. Detailed information on the putative function of homo- and heterotetrameric K+ channels that contain the full length GIRK1a in physiological responses exist, and links between the abnormal function of GIRK1 and pathophysiology of human diseases have been drawn (10) , Supporting data on the function or potential (patho)physiological role of the smaller GIRK1c and GIRK1d variants, however and especially in cancer is still elusive. In the few studies that have been thus far conducted to study the function of smaller GIRK1 splice variants, it was observed that homotetramers composed of GIRK1c or GIRK1d subunits were inactive as ion channels and hence GIRK1c and GIRK1d exerted a dominant negative effect on heterooligomeric channel function, despite considerable expression at the protein

level (36). Based on these findings and data obtained during this research, we suggest that the opposite effect observed for GIRK1d as compared to that for GIRK1a is mainly due to the dominant negative regulatory effect of this splice variant on the function of GIRK complexes.

The expression of GIRK at both the gene and protein levels and the functional phenotype of this molecule in different breast cancer cell lines, including MCF-7WT, has been reported earlier (36, 46). No information about how the function of the GIRK complex in breast cancer was affected by overexpression of GIRK1d was previously available. Specifically, our findings indicate that GIRK1a-induced invasion and motility were impaired upon overexpression of GIRK1d. These experiments also resulted in a significantly reduced level of angiogenesis in MCF-7 cells, induced by GIRK1d. Indeed, the results of our study revealed for the first time that the functional outcome of GIRK1c overexpression resembles that of overexpression of the GIRK1a subunit. The opposite effect of GIRK1d on the vital parameters of MCF-7 cells as compared to GIRK1a/c may be due to the different composition of the former at both the gene and protein levels. Full length mRNA encoding for GIRK1a is composed of three exons (i.e., exons1-3) (47). GIRK1c shares the first two exons with GIRK1a, while GIRK1d is assembled from exons 1 and 3 (exon 2 is missing) (36). This difference in the transcript composition is also translated at the protein level, so that all variants share amino acid positions 1 – 234 at the N-terminus. Amino acids 235-402 are also shared by GIRK1a and GIRK1c, while this part is missing in GIRK1d. So GIRK1a and GIRK1d have only exon 1 and exon 3 in common, while there is an stop codon after exon 1 in GIRK1d (Figure 9.1). Interestingly, in a study conducted by He et al.(48) , the relative contributions of important residues to the G protein sensitivity of the GIRK4/1 heteromer were tested by expressing mutant subunits and recording the basal current. These experiments revealed that one N-terminal residue, His-64, and one C-terminal residue, Leu-268, were critical for G-protein mediated GIRK4 activity; a single mutation at these sites significantly reduced binding of the channel domains to the G protein. In parallel, mutations in GIRK1 His-57 and Leu-262 residues negatively affected the interactions of the heteromer with G proteins and channel activity. In this context, it is conceivable that the tumor-promoting activity of GIRK1a and GIRK1c is due to the presence of exon two, which contains the critical Leu-262 residue in those splice variants. On the other hand, exon 2

and, consequently, the Leu-262 residue is absent in GIRK1d, which may lead to negative effect on vital parameters of MCF-7 when it is overexpressed.

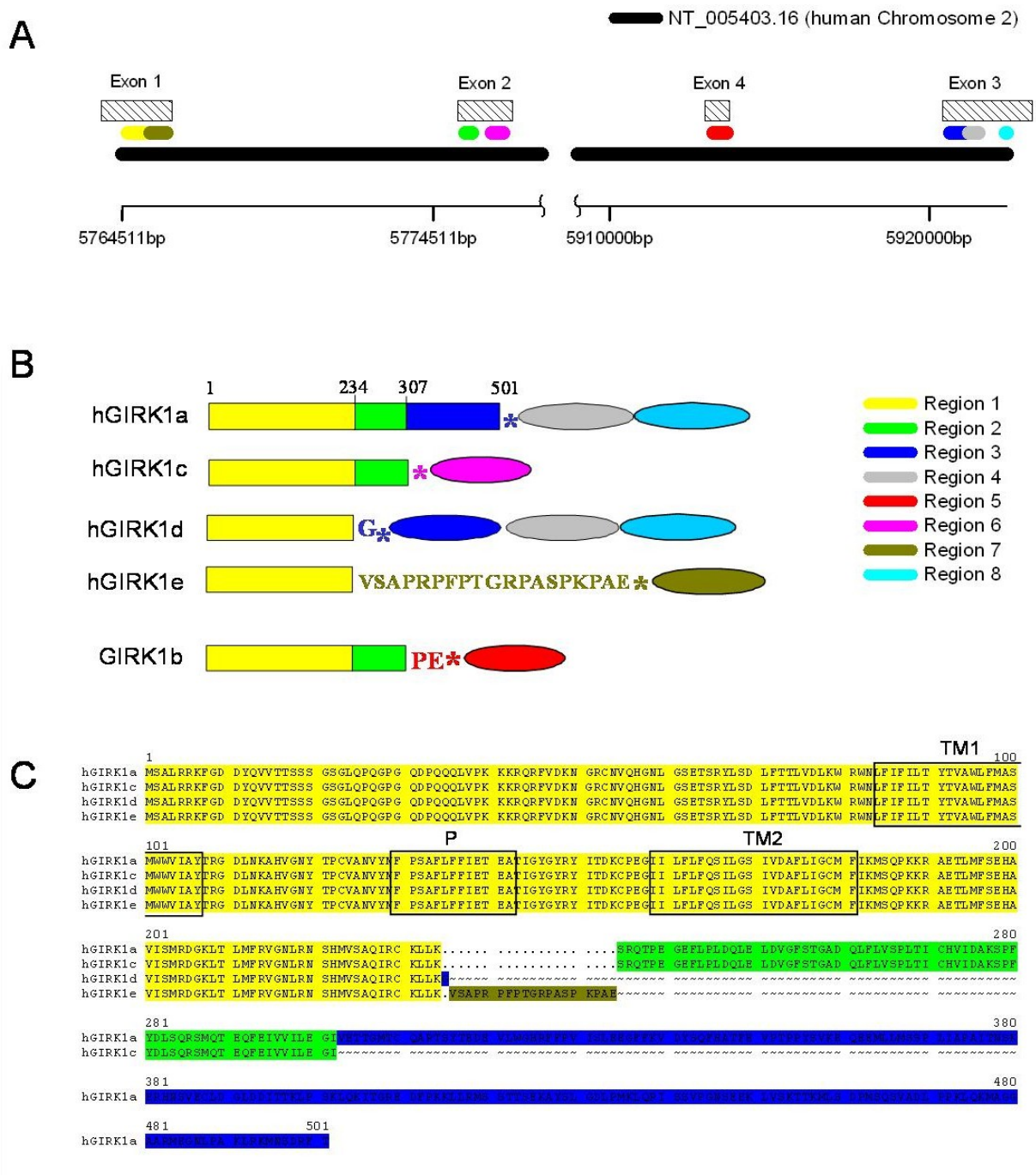

Figure 9.1: Schematic representation of GIRK1 gene splice variants. 9.1.a: Localization of different exons of GIRK1 on chromosome. 9.1.b. Splice variants of GIRK1 gene in MCF-7 cell line. Rectangles represent open reading frames (ORF) of the GIRK1 gene splice variants; ellipsoids, 3´ untranslated regions; and asterisks, stop codons. GIRK1a: Aminoacids 1-501, GIRK1c: Aminoacids 1-308, GIRK1d: Aminoacids 1-235, GIRK1e: Aminoacids 1-253 and GIRK1b: Aminoacids 1-309. 9.1c: Multiple alignment of GRIK1 splice variants. TM1, TM2 and P show the

two transmenbrane regions and the pore region, respectively. (Adapted from: Cloning and characterisation of GIRK1 variants resulting from alternative RNA editing of the KCNJ3 gene transcript in a human breast cancer cell line, Wagner et. al.2010 with permission).

Overexpression of GIRK1d in MCF-7 cells caused prolonged G0/G1, supporting the hypothesis that GIRK1d exerts a dominant negative action on endogenous GIRK complexes by lack or reduce G-protein β/γ subunit binding.

For the first time, we found that the functional consequence of GIRK1c overexpression closely resembles the one produced by overexpression of the GIRK1a subunit. In this regard, the functional activity of this variant seems to be enigmatic, since this finding is contrary to negative properties reported in previous studies. Based on the hypothesis above on the importance of exon 2 and, in particular, Leu-262 for channel formation and G-protein activation, this result may indicate a G-protein dependent action, eventually different to K^+ channel function.

All variants of GIRK1 comprise the integral transmembrane part, including permeation pathway and ion selectivity filter required to catalyze K+ permeation across the plasma membrane. Therefore, it is possible that splice variants of full lemght GIRK1a serve as K+ channels in the cancer cells. Such a phenomenon has, however, never been previously reported.

One important question is that how alteration of GIRK expression affects vital parameters of cancer cells. Some reports indicate that GIRK1 channels in breast cancer cells are actively involved in cellular signaling. Using RNA interference to knockout GIRK, it was observed that beta-adrenergic, MAP kinase, and Akt signaling were significantly reduced (49). Activation of the MAPK/ERK pathway is a critical and frequent event in tumorigenesis. MAPKs have been shown to be involved in proteinase induction, cell migration, angiogenesis, and regulation of apoptosis, all events that are directly related to successful completion of metastasis (50). Agonist stimulation of GPCR is reported to trigger cell proliferation via activation of differnt signaling pathways, including MAPK/ERK cascade(51, 52) It was found that stimulation of MCF-7 cells with carbachol (Cch), a muscarinic acetylcholine receptor (mAChR) agonist, caused a significant increase in protein synthesis and cell proliferation, and these effects were blocked by specific inhibitor of MAPK kinase, PD098059 indicating that MAPK/ERK are involved in the regulation of growth and proliferation of MCF-7 cells (53). In paralel, there was a

considerable reduction in MMP 9 and MMP 2 expression in MCF-7 cells after siRNA inhibition of ERK (54). In this context, the reinforcement of vital parameters of MCF-7 cells following overexpression of GIRK1a/c might be related to the activation of the MAPK/ERK signaling pathways.

Several reports demonstrate that K^+ channel proteins could reinforce the malignant growth of cancer cells (55-58). Enhancement of cell proliferation has been attributed to K^+ channels, while in other reports, reinforcement of angiogenesis and cellular motility, as described in the present study, have been observed (59). K^+ permeation, but also other hitherto unknown functions of K^+ channel proteins (called “moonlighting” functions) has been found to promote the malignant phenotype as well (60-63).

Whether the effects observed in this study are related to K+ permeation itself or another, still unknown biological function still remains unclear at present. Given that the GIRK1c subunit has not been previously reported to act as an ion channel, and that it has biologically similar functions to GIRK1a, the latter hypothesis that “moonlighting” functions are responsible, is favored. Nonetheless, we cannot exclude the possibility that the GIRK1c subunit acts as an ion channel in MCF-7 cells.

In summary, this thesis project, for the first time ever, allowed us to provide insight into functional aspects of GIRK1 overexpression in breast cancer cells for the first time. GIRK1 overexpression was shown to exert opposing effects on vital parameters of MCF-7 cells depending on the variant that was overexpressed. GIRK1a and GIRK1c reinforced the malignant phenotype of breast cancer cells, while GIRK1d overexpression counteracted these effects. We conclude that the differences in biological activity are due to the structural differences between GIRK1a/c and GIRK1d, in particular the region encoded by exon 2, which is absent in GIRK1d. More detailed research is needed to elucidate the molecular events that lead to enhancement of the malignant phenotype by GIRK1a/c. Further research on the clinical application of GIRK1a/c as a potential target for breast cancer immunotherapy is warranted.

10.References:

1. Frank HY, Catterall WA. The VGL-chanome: a protein superfamily specialized for electrical signaling and ionic homeostasis. Science Signaling. 2004;2004(253):re15.
2. Hibino H, Inanobe A, Furutani K, Murakami S, Findlay I, Kurachi Y. Inwardly rectifying potassium channels: their structure, function, and physiological roles. Physiological reviews. 2010;90(1):291-366.
3. Luján R, de Velasco EMF, Aguado C, Wickman K. New insights into the therapeutic potential of Girk channels. Trends in neurosciences. 2014;37(1):20-9.
4. Kubo Y, Reuveny E, Slesinger PA, Jan YN, Jan LY. Primary structure and functional expression of a rat G-protein-coupled muscarinic potassium channel. 1993.
5. Nelson CS, Marino JL, Allen CN. Cloning and characterization of Kir3. 1 (GIRK1) C-terminal alternative splice variants. Molecular brain research. 1997;46(1):185-96.
6. Stoffel M, Espinosa R, Powell KL, Philipson LH, Le Beau MM, Bell GI. Human G-protein-coupled inwardly rectifying potassium channel (GIRK1) gene (KCNJ3): localization to chromosome 2 and identification of a simple tandem repeat polymorphism. Genomics. 1994;21(1):254-6.
7. Kennedy ME, Nemec J, Corey S, Wickman K, Clapham DE. GIRK4 confers appropriate processing and cell surface localization to G-protein-gated potassium channels. Journal of Biological Chemistry. 1999;274(4):2571-82.
8. Jelacic TM, Kennedy ME, Wickman K, Clapham DE. Functional and biochemical evidence for G-protein-gated inwardly rectifying K+ (GIRK) channels composed of GIRK2 and GIRK3. Journal of Biological Chemistry. 2000;275(46):36211-6.
9. Lesage F, Guillemare E, Fink M, Duprat F, Heurteaux C, Fosset M, et al. Molecular properties of neuronal G-protein-activated inwardly rectifying K+ channels. Journal of Biological Chemistry. 1995;270(48):28660-7.
10. Lüscher C, Slesinger PA. Emerging roles for G protein-gated inwardly rectifying potassium (GIRK) channels in health and disease. Nature Reviews Neuroscience. 2010;11(5):301-15.
11. Pfaffinger PJ, Martin JM, Hunter DD, Nathanson NM, Hille B. GTP-binding proteins couple cardiac muscarinic receptors to a K channel. Nature. 1984;317(6037):536-8.
12. Dascal N. Signalling via the G protein-activated K+ channels. Cellular signalling. 1997;9(8):551-73.
13. Smith PA, Sellers LA, Humphrey P. Somatostatin activates two types of inwardly rectifying K+ channels in MIN-6 cells. The Journal of physiology. 2001;532(1):127-42.
14. Shankar H, Murugappan S, Kim S, Jin J, Ding Z, Wickman K, et al. Role of G protein–gated inwardly rectifying potassium channels in P2Y12 receptor–mediated platelet functional responses. Blood. 2004;104(5):1335-43.
15. Perry CA, Pravetoni M, Teske JA, Aguado C, Erickson DJ, Medrano JF, et al. Predisposition to late-onset obesity in GIRK4 knockout mice. Proceedings of the National Academy of Sciences. 2008;105(23):8148-53.
16. Kaneko S, Okada M, Iwasa H, Yamakawa K, Hirose S. Genetics of epilepsy: current status and perspectives. Neuroscience research. 2002;44(1):11-30.
17. Reeves RH, Irving NG, Moran TH, Wohn A, Kitt C, Sisodia SS, et al. A mouse model for Down syndrome exhibits learning and behaviour. Nat Genet. 1995;11:177-84.
18. Patil N, Cox DR, Bhat D, Faham M, Myers RM, Peterson AS. A potassium channel mutation in weaver mice implicates membrane excitability in granule cell differentiation. Nature genetics. 1995;11(2):126-9.
19. Pardo LA, Stühmer W. The roles of K+ channels in cancer. Nature Reviews Cancer. 2014;14(1):39-48.

20. Stringer BK, Cooper AG, Shepard SB. Overexpression of the G-protein inwardly rectifying potassium channel 1 (GIRK1) in primary breast carcinomas correlates with axillary lymph node metastasis. Cancer research. 2001;61(2):582-8.
21. Takanami I, Inoue Y, Gika M. G-protein inwardly rectifying potassium channel 1 (GIRK 1) gene expression correlates with tumor progression in non-small cell lung cancer. BMC cancer. 2004;4(1):1.
22. Plummer HK, Yu Q, Cakir Y, Schuller HM. Expression of inwardly rectifying potassium channels (GIRKs) and beta-adrenergic regulation of breast cancer cell lines. BMC cancer. 2004;4(1):1.
23. Plummer HK, Dhar MS, Cekanova M, Schuller HM. Expression of G-protein inwardly rectifying potassium channels (GIRKs) in lung cancer cell lines. BMC cancer. 2005;5(1):104.
24. Brevet M, Ahidouch A, Sevestre H, Merviel P, El Hiani Y, Robbe M, et al. Expression of K+ channels in normal and cancerous human breast. 2008.
25. Kammerer S, Sokolowski A, Hackl H, Jahn S, Asslaber M, Symmans F, et al. 40POVEREXPRESSION OF G PROTEIN-ACTIVATED INWARD RECTIFIER POTASSIUM CHANNEL 1 (GIRK1) IS ASSOCIATED WITH LYMPH NODE METASTASIS AND POOR PROGNOSIS IN BREAST CANCER. Annals of Oncology. 2014;25(suppl 1):i13-i4.
26. Coleman MP, Quaresma M, Berrino F, Lutz J-M, De Angelis R, Capocaccia R, et al. Cancer survival in five continents: a worldwide population-based study (CONCORD). The lancet oncology. 2008;9(8):730-56.
27. Buijs JT, van der Pluijm G. Osteotropic cancers: from primary tumor to bone. Cancer letters. 2009;273(2):177-93.
28. Li C, Rezania S, Kammerer S, Sokolowski A, Devaney T, Gorischek A, et al. Piezo1 forms mechanosensitive ion channels in the human MCF-7 breast cancer cell line. Scientific reports. 2015;5.
29. Livak KJ, Schmittgen TD. Analysis of relative gene expression data using real-time quantitative PCR and the 2− ΔΔCT method. methods. 2001;25(4):402-8.
30. Liang C-C, Park AY, Guan J-L. In vitro scratch assay: a convenient and inexpensive method for analysis of cell migration in vitro. Nature protocols. 2007;2(2):329-33.
31. Cahalan MD, Parker I. Choreography of cell motility and interaction dynamics imaged by two-photon microscopy in lymphoid organs. Annual review of immunology. 2008;26:585.
32. Ribatti D, Nico B, Vacca A, Presta M. The gelatin sponge–chorioallantoic membrane assay. NATURE PROTOCOLS-ELECTRONIC EDITION-. 2006;1(1):85.
33. Hanahan D, Weinberg RA. Hallmarks of cancer: the next generation. cell. 2011;144(5):646-74.
34. Cohen MB, Griebling TL, Ahaghotu CA, Rokhlin OW, Ross JS. Cellular adhesion molecules in urologic malignancies. American journal of clinical pathology. 1997;107(1):56-63.
35. Brevet M, Fucks D, Chatelain D, Regimbeau J-M, Delcenserie R, Sevestre H, et al. Deregulation of 2 potassium channels in pancreas adenocarcinomas: implication of KV1. 3 gene promoter methylation. Pancreas. 2009;38(6):649-54.
36. Wagner V, Stadelmeyer E, Riederer M, Regitnig P, Gorischek A, DeVaney T, et al. Cloning and characterisation of GIRK1 variants resulting from alternative RNA editing of the KCNJ3 gene transcript in a human breast cancer cell line. Journal of cellular biochemistry. 2010;110(3):598-608.
37. McPhee JC, Dang YL, Davidson N, Lester HA. Evidence for a functional interaction between integrins and G protein-activated inward rectifier K+ channels. Journal of Biological Chemistry. 1998;273(52):34696-702.
38. Mirshahi T, Logothetis DE. Molecular determinants responsible for differential cellular distribution of G protein-gated inwardly rectifying K+ channels. Journal of Biological Chemistry. 2004;279(12):11890-7.

39. Kubo Y, Iizuka M. Identification of domains of the cardiac inward rectifying K+ channel, CIR, involved in the heteromultimer formation and in the G-protein gating. Biochemical and biophysical research communications. 1996;227(1):240-7.
40. Kennedy M, Nemec J, Clapham D. Localization and interaction of epitope-tagged GIRK1 and CIR inward rectifier K+ channel subunits. Neuropharmacology. 1996;35(7):831-9.
41. Fernández-Alacid L, Aguado C, Ciruela F, Martín R, Colón J, Cabañero MJ, et al. Subcellular compartment-specific molecular diversity of pre-and post-synaptic GABAB-activated GIRK channels in Purkinje cells. Journal of neurochemistry. 2009;110(4):1363-76.
42. Chung HJ, Qian X, Ehlers M, Jan YN, Jan LY. Neuronal activity regulates phosphorylation-dependent surface delivery of G protein-activated inwardly rectifying potassium channels. Proceedings of the National Academy of Sciences. 2009;106(2):629-34.
43. Balana B, Bahima L, Bodhinathan K, Taura JJ, Taylor NM, Nettleton MY, et al. Ras-association domain of sorting Nexin 27 is critical for regulating expression of GIRK potassium channels. PloS one. 2013;8(3):e59800.
44. Chung HJ, Ge W-P, Qian X, Wiser O, Jan YN, Jan LY. G protein-activated inwardly rectifying potassium channels mediate depotentiation of long-term potentiation. Proceedings of the National Academy of Sciences. 2009;106(2):635-40.
45. Karapetyan AR, Buiting C, Kuiper RA, Coolen MW. Regulatory roles for long ncRNA and mRNA. Cancers. 2013;5(2):462-90.
46. Dhar MS, Plummer HK. Protein expression of G-protein inwardly rectifying potassium channels (GIRK) in breast cancer cells. BMC physiology. 2006;6(1):8.
47. Schoots O, Voskoglou T, Van Tol HH. Genomic organization and promoter analysis of the human G-protein-coupled K+ channel Kir3. 1 (KCNJ3/HGIRK1). Genomics. 1997;39(3):279-88.
48. He C, Yan X, Zhang H, Mirshahi T, Jin T, Huang A, et al. Identification of critical residues controlling G protein-gated inwardly rectifying K+ channel activity through interactions with the βγ subunits of G proteins. Journal of Biological Chemistry. 2002;277(8):6088-96.
49. Hance MW, Dhar MS, Plummer III HK. G-protein inwardly rectifying potassium channel 1 (GIRK1) knockdown decreases beta-adrenergic, MAP kinase and Akt signaling in the MDA-MB-453 breast cancer cell line. Breast cancer: basic and clinical research. 2008;1:25.
50. Reddy KB, Nabha SM, Atanaskova N. Role of MAP kinase in tumor progression and invasion. Cancer and Metastasis Reviews. 2003;22(4):395-403.
51. Wilkinson MG, MILLAR JB. Control of the eukaryotic cell cycle by MAP kinase signaling pathways. The FASEB Journal. 2000;14(14):2147-57.
52. Zhao WQ, Alkon DL, Ma W. c-Src protein tyrosine kinase activity is required for muscarinic receptor-mediated DNA synthesis and neurogenesis via ERK1/2 and c-AMP-responsive element-binding protein signaling in neural precursor cells. Journal of neuroscience research. 2003;72(3):334-42.
53. Jiménez E, Montiel M. Activation of MAP kinase by muscarinic cholinergic receptors induces cell proliferation and protein synthesis in human breast cancer cells. Journal of cellular physiology. 2005;204(2):678-86.
54. Moulik S, Pal S, Biswas J, Chatterjee A. Role of ERK in modulating MMP 2 and MMP 9 with respect to tumour invasiveness in human cancer cell line MCF-7 and MDA-MB-231. Journal of Tumor. 2014;2(2).
55. Shen Z, Yang Q, You Q. Researches toward potassium channels on tumor progressions. Current topics in medicinal chemistry. 2009;9(4):322-9.
56. Wulff H, Castle NA, Pardo LA. Voltage-gated potassium channels as therapeutic targets. Nature reviews Drug discovery. 2009;8(12):982-1001.
57. Pardo LA, Stühmer W. Eag1: an emerging oncological target. Cancer research. 2008;68(6):1611-3.
58. Yang M, Brackenbury WJ. Membrane potential and cancer progression. Frontiers in physiology. 2013;4:185.

59. Prevarskaya N, Skryma R, Shuba Y. Ion channels and the hallmarks of cancer. Trends in molecular medicine. 2010;16(3):107-21.
60. Downie BR, Sánchez A, Knötgen H, Contreras-Jurado C, Gymnopoulos M, Weber C, et al. Eag1 expression interferes with hypoxia homeostasis and induces angiogenesis in tumors. Journal of Biological Chemistry. 2008;283(52):36234-40.
61. Afrasiabi E, Hietamäki M, Viitanen T, Sukumaran P, Bergelin N, Törnquist K. Expression and significance of HERG (KCNH2) potassium channels in the regulation of MDA-MB-435S melanoma cell proliferation and migration. Cellular signalling. 2010;22(1):57-64.
62. Pei L, Wiser O, Slavin A, Mu D, Powers S, Jan LY, et al. Oncogenic potential of TASK3 (Kcnk9) depends on K+ channel function. Proceedings of the National Academy of Sciences. 2003;100(13):7803-7.
63. Voloshyna I, Besana A, Castillo M, Matos T, Weinstein IB, Mansukhani M, et al. TREK-1 is a novel molecular target in prostate cancer. Cancer research. 2008;68(4):1197-203.